UNIVERSITY OF CALIFORNIA SAN DIEGO

Integrity of Crustacean Predator Defenses Under Ocean Acidification and Warming Conditions

A dissertation submitted in partial satisfaction of the requirements for the degree Doctor of Philosophy

in

Marine Biology with a specialization in Interdisciplinary Environmental Research

by

Kaitlyn B. Lowder

Committee in charge:

Jennifer Taylor, Chair
Andreas Andersson
Dimitri Deheyn
Lisa Levin
Joanna McKittrick

2019

The Dissertation of Kaitlyn B. Lowder is approved, and it is acceptable in quality and form for publication on microfilm and electronically:

_____

_____

_____

_____

_____
Chair

University of California San Diego

2019

DEDICATION

To all the teachers and professors who showed me what we remain to discover

EPIGRAPH

"We'll go where the air is pure, where all sounds are soothing, where, no matter how proud one may be, one feels humble and finds oneself small—in short, we'll go to the sea."

- Alexandre Dumas, *The Count of Monte Cristo*

TABLE OF CONTENTS

LIST OF TABLES

Chapter 2

Chapter 3

Chapter 4

LIST OF FIGURES

Chapter 1

Chapter 2

Chapter 3

Chapter 4

ACKNOWLEDGMENTS

This work was only made possible by a vast number of people, both at Scripps and beyond, to whom I am immensely thankful for their guidance, mentorship, and support.

First, the biggest, deepest thank you to my advisor Jennifer Taylor. I could not imagine having a better advisor. The relative smoothness of my graduate school experience has been because of her constant mentorship and availability. She pushed me to develop my own interests and then fully supported those projects, despite all the speedbumps and potholes along the way. Even when I go into one of our meetings feeling like I have hit a wall in some regard, she has helped me figure out workarounds and improvements with positive encouragement, and I have always come out with a plan and a boost of confidence. She has taught me one of the greatest lessons in science, to rise above failure and try something else. Behind the fellowships, small grants, and manuscripts has been a rare coauthor, a prompt and wonderful editor of both ideas and text, which I know I will greatly miss in the future. As I think back on what I have learned in the past five years, I have much of that to thank Jennifer for, and I am incredibly appreciative of the path she has set me on.

I would also like to thank and acknowledge my other committee members who provided excellent feedback and support throughout the last five years. Thank you to Dimitri Deheyn for the excellent discussions since the very beginning of my PhD. Dimitri has pushed me outside of my comfortable research niche many times and continually encouraged me to explore new techniques and ask new questions. He has been greatly supportive of my career goals, and I very much appreciate how he has gone beyond being a strict mentor of my science to be a mentor of me as a scientist. Thank you to Lisa Levin both for her scientific expertise as well as serving as an excellent model. I greatly admire how Lisa is both highly

accomplished in her field and as an interdisciplinary, policy-minded scientist. She has shown me that these titles are not exclusionary, and I hope to become half as skilled in both regards. She is also a constant reminder that there is always more to learn and that attending seminars, brown bags, and conferences is an integral part of being a well-rounded scientist. Thank you to Andreas Andersson for helping form me into a young, well-trained ocean acidification researcher. I am incredibly appreciative that I have the baseline of broad knowledge in the ocean acidification field, especially in biogeochemistry, that I can draw on to improve my experimental work and critically examine other research as the field continues to expand. It has also been a great experience learning to run my own carbonate chemistry samples in the SCOOBY lab, and I am glad to have trained in a lab that emphasizes high standards of practice. And thank you to Joanna McKittrick for helping me approach my work from an engineering point-of-view. Talking with her always makes me think of biological materials from a new perspective and fully appreciate just how neat it is to be able to study the amazing diversity of animals below the sea's surface.

I could not have done three-fourths of this research without Phil Zerofski, and I cannot thank him enough, as I cannot even begin to count how many times he has done something for me that no one else could help with. Without him, I would not have any research animals nor an experimental system to put them in. He has taught me how to cut and assemble PVC pipe, drill threaded holes, seine-net for grass shrimp, fix a broken glass tank, dock a small boat, build a larval catchment container, and where to buy all those little but necessary experimental odds and ends in San Diego, among many other lessons. Also, thank you Phil for putting up with my somewhat leaky aforementioned PVC pipes and continual mounds of

supplies in the aquarium rooms. We at Scripps are incredibly lucky to have someone in his position that is so kind, willing to teach, and professional.

The boating and diving personnel at Scripps are unparalleled and have provided a whole new facet to the skills I've acquired in graduate school. Thank you especially to Richard Walsh, Christian McDonald, Brett Pickering, and Melissa Torres for teaching me how to be safe in and above the water while I made some of my favorite memories in graduate school. I am grateful to have these skills to not only help advance my science but also to enjoy the ocean as a place for relaxation and rejuvenation outside of work.

The staff at Scripps has made my graduate experience both easier and more vibrant. Thank you to Gilbert Bretado for ensuring all of us students get situated comfortably into life here in San Diego and for supporting our progress year after year. I truly enjoyed the experiences of the mentorship program, both as a mentee and a mentor. I would also like to thank Maureen McGreevy, Shelley Weisel, and other members of the graduate office as well as James Pollock, Gregory Jackson, Marty Tullar, and Yvonne Bohan for handling so many administrative tasks over the years. I appreciate the time and effort Rob Monroe puts into organizing the contingent for COPs and ensuring Scripps students are able to experience what international climate negotiations look like. We are very lucky to be at an institution where this goes on. I would also like to thank the Communications office, including Chase Martin, for helping spread the amazing science at Scripps, including some of my own. Finally, Penny Dockry does unparalleled work in helping run the Center for Marine Biodiversity and Conservation and the interdisciplinary PhD program PIER. I cannot count the number of things Penny has helped me with, and her constant support over the last five years has meant a lot. Additionally, my experience at UCSD has been deeply enriched by the PIER program,

and I am very grateful for the educational opportunities it provided, particularly because it has helped make me a more-rounded natural scientist.

The undergraduate volunteers I have had the pleasure of working with and mentoring have been a special part of my time here at UCSD. I have been continually impressed with the drive and interest of the students that make time in their schedule and step away from other commitments to join me in the lab. I deeply appreciate their assistance—three chapters heavily relied on their work. It is a neat aspect of the sciences that we get to take on the challenge of mentoring as students ourselves, and I have really enjoyed being a small part of the path that each student has set out for themselves.

My friends and cohort have been an irreplaceable well of support and stress relief and a research-related sounding board. I cannot imagine the toil that graduate school would have been without them. Thank you to Jennifer Le for her continual camaraderie and for dragging me to some of the best food experiences in San Diego, Beverly French for being an unending source of wisdom and for listening to me when I'm stressed and could use a talk, and Bethany Kolody for showing me what it looks like to balance science and art, commit to New Year's resolutions, and for assembling the best housing situation ever. Thank you to Georgie Zelanak for never letting me doubt myself, Alyssa Griffin for modeling what a leader and advocate looks like, and Garfield Kwan for the graduate school commiseration and demonstrating how to succeed in both science and in pursuing passions. Thank you to Natalya Gallo for the continual inspiration as an amazing woman in science that not only effectively communicates that science but also speaks up about a wide range of issues. I am very excited to have so many wonderful colleagues in what is sure to be many diverse locations and positions in the coming years.

Before I started the first fall of my PhD, I met a wonderful man that has put up with an incredibly-weird work schedule on my end, numerous trips to conferences in amazing places without him, and quite a few science-y rants, and he has taken it all in stride. Graduate school would have been a whole other beast without his support and would have taken eons longer without his frequent encouragement. Thank you Alex Hill for providing balance in my life.

And finally, I owe so much to my parents. I am incredibly lucky to have parents that have been able to provide so much for my education and have sheltered me from a lot of excess stress along the way. They took my dream to become a marine biologist as a child seriously and helped set me on that path to get there, even though that meant sending me 800 miles away for my undergraduate work (we know the distance well from the long hauls back and forth!) and burdening all of the anxiety that entails. I am so very happy to show them the results of these many years of education now.

Chapter 1, in part, is in preparation for submission for publication. Lowder, K.B., Hattingh, R., Day, J.M, McKittrick, J. and Taylor, J.R.A. The dissertation author was the primary investigator and author of this material.

Chapter 2, in part, is in preparation for submission for publication. Lowder, K. B., Allen, M.C., Deheyn, D., Andersson, A.J., Hattingh, R., Webb, S.J., Day, J.M.D., Taylor, J.R.A. The dissertation author was the primary investigator and author of this material.

Chapter 3, in part, is in preparation for submission for publication. Lowder, K.B., deVries, M.S., Kelly, C.B., Andersson, A.J., Hattingh, R., Day, J.M, and Taylor, J.R.A. The dissertation author was the primary investigator and author of this material.

Chapter 4, in full, is a reprint of the material as it appears in Lowder, K.B., Allen, M.C., Day, J.M., Deheyn, D.D. and Taylor, J.R.A., 2017. Assessment of ocean acidification

and warming on the growth, calcification, and biophotonics of a California grass shrimp. *ICES Journal of Marine Science*, *74*(4), pp.1150-1158. The dissertation author was the primary investigator and author of this material. The material is used by permission of Oxford University Press.

VITA

2014	Bachelor of Science, Biology, Western Washington University
2014	Bachelor of Arts, English, Western Washington University
2016	Master of Science, Biological Oceanography, Scripps Institution of Oceanography, University of California San Diego
2019	Doctor of Philosophy, Marine Biology with a specialization in Interdisciplinary Environmental Research, Scripps Institution of Oceanography, University of California San Diego

PUBLICATIONS

Lowder, K.B., Allen, M.C., Day, J.M., Deheyn, D.D. and Taylor, J.R.A., 2017. Assessment of ocean acidification and warming on the growth, calcification, and biophotonics of a California grass shrimp. *ICES Journal of Marine Science*, *74*(4), pp.1150-1158.

ABSTRACT OF THE DISSERTATION

Integrity of Crustacean Predator Defenses Under Ocean Acidification and Warming Conditions

By

Kaitlyn B. Lowder

Doctor of Philosophy in Marine Biology with a Specialization in Interdisciplinary Environmental Research

University of California San Diego, 2019

Professor Jennifer R. A. Taylor, Chair

Crustaceans are a diverse group of species, but all rely on an exoskeleton that is shed and formed anew throughout their lifetime. Exoskeletons perform a wide range of functions,

sometimes acting as armor, a means to produce sound, a tool to crush hard prey, or even a window to facilitate transparency. The exoskeleton and its functions, however, are likely vulnerable to ocean acidification and ocean warming, which may alter its composition and the energy allocated towards its production. I investigated the effects of these future ocean conditions on two southern Californian crustaceans, the California spiny lobster *Panulirus interruptus* and the grass shrimp *Hippolyte californiensis*, which rely on their exoskeleton for different predator defenses. *P. interruptus* is an iconic feature of southern California's kelp forest ecosystem but also a potential prey item for many of its large predators. Spiny lobsters use their antennae, mandibles, carapace, and horns to avoid predation. Each of these structures is specialized for a certain defense, displaying differences in composition, structure, and material properties that allow the antennae, for example, to remain flexible to avoid breaking when pushing predators away while imbuing hardness in crushing structures like the mandible (Chapter 1). Juvenile lobsters exposed to ocean acidification-like conditions largely maintained their predator defenses, displaying some differences in the composition across the exoskeleton but no strong effects to defense functionality, including the non-exoskeletal defenses of detecting chemical cues and the tail-flip escape response (Chapter 3). Additionally, larval *P. interruptus*, exposed to both ocean acidification and warming conditions, grew slightly smaller in reduced pH but maintained their transparency in both conditions (Chapter 2). In contrast, *H. californiensis* resides in eelgrass meadows where a primary defense strategy is cryptic colouration, accomplished via a transparent exoskeleton with underlying pigment. When exposed to both ocean acidification and ocean warming-like conditions, shrimp maintained their transparency and did not respond negatively to either condition (Chapter 4). Together, this work on both species demonstrates that a diversity of predator defenses in temperate crustaceans, included those afforded by the exoskeleton, appear to be relatively resilient to both future ocean acidification and ocean warming conditions.

Introduction

Anthropogenic activities affect coastal marine ecosystems at small local scales through point-source pollution and overfishing as well as globally via increased carbon dioxide emissions. The oceans account for 90% of the Earth's warming since 1955 (Levitus et al., 2012) and have taken up roughly 30% of the CO_2 emitted in recent decades (Gruber et al., 2019, Le Quéré et al., 2012). As a result, the ongoing processes of ocean warming and ocean acidification, a suite of changes in the seawater carbonate chemistry as CO_2 dissolves into the oceans, are predicted to increase temperature and decrease pH in the open ocean by 3-4°C and 0.3-0.5 units within this century (Caldeira and Wickett, 2005; Solomon, 2007; IPCC, 2014), although changes to coastal areas on a regional and local scale are influenced by existing oceanographical conditions. For example, the California Current, due to frequent upwelling, already has waters with relatively lower pH and buffering capacity, making it especially susceptible to greater decreases in the future (Gruber et al., 2012; Hauri et al., 2013). Additionally, the waters off southern California have experienced numerous bouts of high temperature in the last few years, correlating with unusual population dynamics of zooplankton, benthic invertebrates, and fish (Cavole et al., 2016; Sakuma et al., 2016).

The potential impacts of future ocean acidification (OA) and ocean warming (OW) have been studied across the globe on a diversity of marine organisms. Early ocean acidification research largely focused on corals and shellfish, as high pCO_2 reduces the availability of carbonate ions used for calcification, but many researchers began noting the scant information on the effects of high CO_2 on another group of calcifying organisms, the crustaceans (Kleypas et al., 2005; Doney et al., 2009; Melzner et al., 2009). In 2009, 5.9

million tons of crustaceans were harvested from marine environments, underlining the importance of crustaceans as sources of protein across the globe and as a means to generate revenue through production and trade (Bondad-Reantaso et al., 2012) that may be threatened by OA and OW.

As the OA field has grown in the last few years and crustaceans have gained more research attention, it has been found that adult crustaceans are largely tolerant of the decreased pH conditions expected by the end of the century (Kroeker et al., 2013). However, our current understanding of how crustaceans respond to OA conditions may underestimate the impacts by overlooking key areas of study: the effect of OA and OW together, early life stage responses, and sublethal effects that manifest in increased vulnerability to predation. The goal of this dissertation was to identify the methods crustaceans use to specialize their exoskeleton for various defenses, which may make these structures differentially vulnerable to OA (Chapter 1), and examine these three knowledge gaps through a series of experiments to more fully understand the response of crustaceans to OA, especially in terms of the integrity of their predator defenses (Chapters 2-4) across multiple life stages (Chapters 2 and 3) in combination with OW (Chapters 2 and 4).

This research was performed with two decapod crustacean species living in the coastal ecosystems of the California Current that differ in life history and predator defenses. The first, the California spiny lobster (*Panulirus interruptus*, Randall), is an iconic feature of southern California's coastal waters, both as an important link in coastal ecosystem food webs and as a popular recreational and commercial fishery species, making it an important species for study under future ocean conditions. Spiny lobster have been shown to be a main predator of two species of top snails (*Tegula aureotincta* and *T. eiseni*), are prominent predators on wave-

swept mussel patches and help maintain understory algae otherwise outcompeted by these mussels, and consume large red sea urchins (S*trongylocentrotus franciscanus***)** (Schmitt, 1982; Tegner and Levin, 1983; Robles, 1987; Schmitt, 1987). The commercial fishery in California had an ex-vessel value of ~$13 million in 2011, making it the state's fourth most valuable fishery (Porzio et al., 2012), while the recreational fishery supports over 30,000 participants annually that spend an estimated $37 million—most of it locally—on gear, boat rental or maintenance, lodging, and other costs to support their hobby (Neilson, 2011; California Department of Fish and Wildlife, 2016).

To survive to recruit into the fishery, however, California spiny lobsters must rely on a suite of exoskeletal defenses to avoid predation. They can spar with fish using their sword-like antennae, use their carapace as armor against crunching California sheephead (*Semicossyphus pulcher*), and employ their horns to lock themselves into protective rock crevices. This species is an excellent candidate for studying the functional morphology of predator defenses and the nature of exoskeleton versatility within a single species. To withstand the different force loadings during attack, the spiny lobster may potentially modify the construction of exoskeletal regions, particularly by altering the composition and structure to produce a range of material properties. Chapter 1 explores five structures of the spiny lobster exoskeleton to demonstrate the range of potential modifications crustaceans may make to different regions, delving into the relationship between construction and function of a biomaterial. Additionally, this work informs the selection of structures to be studied under OA-like conditions in Chapter 3.

The diversity of exoskeletal architecture and the array of defenses make the California spiny lobster interesting to explore functional effects of OA. However, there are currently no

medium-to-long term studies examining the effects of pH on any of the 60-plus rock lobster species, highlighting the importance of turning focus to this group. Fishery managers recognize that they are unable to incorporate any information on climate change's potentially significant impact into lobster management plans (Pecl et al., 2009; California Department of Fish and Wildlife, 2016). Chapter 3 provides this first set of information about the responses of a spiny lobster species to ocean acidification-like conditions. In addition to reporting commonly-studied metrics such as survival and growth, it also addresses the resilience of a set of exoskeletal and behavioral predator defenses under three reduced-pH conditions.

In contrast to juvenile and adult spiny lobsters, the early life stage is pelagic and possesses a very different form—that of a flat, leaf-like phyllosoma larva. As larvae, *P. interruptus* spends 7-9 months offshore, completing 11 larval phases before returning inshore and settling (Johnson 1960). Females release larvae in July and August, and small (<10 mm carapace length) settled juveniles are found in seagrass meadows from June to November, although peak settlement is believed to occur in August (Engle, 1979). Relatively little is known about larval behavior and where individuals travel in relation to their release location. While offshore, many species of spiny lobster larvae vertically migrate (exact depths are unknown, although Johnson 1960 notes that not many more are captured in nets towed deeper than 70 m than at shallower depths). Early stages (phyllosoma) are predominately found at night in offshore currents whereas later stages (phyllosoma and post-larval pueruli) spend more time in water just below the surface layer that is primarily moving onshore (Rimmer and Phillips, 1979). This behavior, with the combination of active swimming, brings post-larvae inshore to preferred settling habitats (Butler, 2008). As such, their mortality is tied to the water conditions and currents as well as their ability to swim and avoid visual predators.

Larval marine organisms are believed to be more vulnerable to changing ocean conditions than adults (Kroeker et al. 2013) due to relatively underdeveloped acid-base regulation strategies and smaller energy stores available for other basic processes (Melzner, et al. 2009). As such, in Chapter 2, their survival, development, and growth are studied in response to both ocean acidification and ocean warming conditions. Because mortality is influenced by maintenance of their transparency in the pelagic environment, which can be influenced by the mineral composition of their exoskeleton, those responses are examined in particular.

In comparison, *Hippolyte californiensis*, a Californian grass shrimp less than 3 cm in total length, resides in eelgrass meadows where a primary defense strategy is cryptic coloration. The exoskeleton acts not so much as a wall against a predator's attack but as a window to the underlying chromatophores that enables crypsis, so transparency must be maintained for an effective defense. Because this species relies on its exoskeleton to function in a very different manner than the California spiny lobster, its response to high pCO_2 and increased temperature conditions, studied in Chapter 4, helps elucidate the potential diversity of exoskeleton changes as a result of these conditions. Furthermore, these grass shrimp are prey for many visually-predating fish, including the surf perch *Cymatogaster aggregatus*, the giant kelpfish *Heterostichus rostratus*, and the kelp pipefish *Syngnathus californiensis* (Young and Fox, 1936; Allen et al., 2002; Allen and Horn, 2006), and the persistence of these shrimp as an available food source will aid in maintaining healthy eelgrass habitats in future oceans.

References

Allen, L. G., Findlay, A. M., and Phalen, C. M. 2002. Structure and standing stock of the fish assemblages of San Diego Bay, California from 1994 to 1999. Bulletin-Southern California Academy of Sciences, 101: 49-85.

Allen, L. G., and Horn, M. H. 2006. The ecology of marine fishes: California and adjacent waters, Univ of California Press.

Bondad-Reantaso, M. G., Subasinghe, R. P., Josupeit, H., Cai, J., and Zhou, X. 2012. The role of crustacean fisheries and aquaculture in global food security: past, present and future. Journal of Invertebrate Pathology, 110: 158-165.

Butler, M. J., and Herrnkind, W. F. 2008. Puerulus and Juvenile Ecology. *In* Spiny lobsters: fisheries and culture, pp. 276--301.

Caldeira, K., and Wickett, M. E. 2005. Ocean model predictions of chemistry changes from carbon dioxide emissions to the atmosphere and ocean. Journal of Geophysical Research: Oceans (1978–2012), 110: 365.

California Department of Fish and Wildlife. 2016. California Spiny Lobster Fishery Management Plan. 1-228.

Cavole, L. M., Demko, A. M., Diner, R. E., Giddings, A., Koester, I., Pagniello, C. M., Paulsen, M.-L., Ramirez-Valdez, A., Schwenck, S. M., Yen, N.K. 2016. Biological impacts of the 2013–2015 warm-water anomaly in the Northeast Pacific: Winners, losers, and the future. Oceanography, 29: 273-285.

Doney, S. C., Fabry, V. J., Feely, R., and Kleypas, J. 2009. Ocean acidification: the other CO_2 problem. Annual review of marine science, 1: 169-192.

Engle, J. M. 1979. Ecology and growth of juvenile California spiny lobster, *Panulirus interruptus* (Randall). p. 298. Unpublished doctoral thesis, University of Southern California, Los Angeles, California, United States.

Gruber, N., Hauri, C., Lachkar, Z., Loher, D., Frölicher, T. L., and Plattner, G.-K. 2012. Rapid progression of ocean acidification in the California Current System. Science, 337: 220-223.

Gruber, N., Clement, D., Carter, B. R., Feely, R. A., van Heuven, S., Hoppema, M., Ishii, M., Key, R.M., Kozyr, A., Lauvset, S.K., Lo Monaco, C., Mathis, J.T., Murata, A., Olsen, A., Perez, F.F., Sabine, C.L., Tanhua, T., and Wanninkhof, R.. 2019. The oceanic sink for anthropogenic CO_2 from 1994 to 2007. Science, 363: 1193-1199.

Hauri, C., Gruber, N., Vogt, M., Doney, S. C., Feely, R. A., Lachkar, Z., Leinweber, A., McDonnell, A.M.P., Munnich, M., and Plattner, G. 2013. Spatiotemporal variability and long-term trends of ocean acidification in the California Current System, Biogeosciences: 10, 193-216.

IPCC. 2014. Climate Change 2014: Synthesis Report. Contribution of Working Groups I, II and III to the Fifth Assessment Report of the Intergovernmental Panel on Climate Change [Core Writing Team, R.K. Pachauri and L.A. Meyer (eds.)]. 151 pp.

Kleypas, J. A., Feely, R. A., Fabry, V. J., Langdon, C., Sabine, C. L., and Robbins, L. L. 2005. Impacts of ocean acidification on coral reefs and other marine calcifiers: a guide for future research. *In* report of a workshop held 18–20 April 2005, St. Petersburg, FL, sponsored by NSF, NOAA, and the U.S. Geological Survey, p. 88.

Kroeker, K. J., Kordas, R. L., Crim, R., Hendriks, I. E., Ramajo, L., Singh, G. S., Duarte, C. M., and Gattuso, J. 2013. Impacts of ocean acidification on marine organisms: quantifying sensitivities and interaction with warming. Global Change Biology, 19: 1884-1896.

Le Quéré, C., Andres, R. J., Boden, T., Conway, T., Houghton, R. A., House, J. I., Marland, G., Peters, G.P., Van der Werf, G., and Ahlström, A. 2012. The global carbon budget 1959–2011. Earth System Science Data Discussions, 5: 1107-1157.

Levitus, S., Antonov, J. I., Boyer, T. P., Baranova, O. K., Garcia, H. E., Locarnini, R. A., Mishonov, A. V., Reagan, J.R., Seidov, D., and Yarosh, E.S. 2012. World ocean heat content and thermosteric sea level change (0–2000 m), 1955–2010. Geophysical Research Letters, 39.

Melzner, F., Gutowska, M., Langenbuch, M., Dupont, S., Lucassen, M., Thorndyke, M. C., Bleich, M., Pörtner, H-O. 2009. Physiological basis for high CO_2 tolerance in marine ectothermic animals: pre-adaptation through lifestyle and ontogeny? Biogeosciences, 6: 2313-2331.

Neilson, D. J. 2011. Assessment of the California Spiny Lobster (*Panulirus interruptus*), California Department of Fish and Game. 1-138.

Pecl, G., Frusher, S., Gardner, C., Haward, M., Hobday, A. J., Jennings, S., Nursey-Bray, M., Punt, A.E., Revill, H., Van Putten, I.E. 2009. The east coast Tasmanian rock lobster fishery–vulnerability to climate change impacts and adaptation response options.

Porzio, D., Phillips, J., Loke, K., Tanaka, T., McKnight, C., Neilson, D., Juhasz, C., Mason, T., and Lewis, M. 2012. Review of selected California fisheries for 2011: ocean salmon, California sheephead, California halibut, longnose skate, petrale sole, California spiny lobster, Dungeness crab, garibaldi, white shark, and algal blooms. California Cooperative Oceanic Fisheries Investigations Reports, 53: 15-40.

Rimmer, D. W., and Phillips, B. F. 1979. Diurnal migration and vertical distribution of phyllosoma larvae of the western rock lobster *Panulirus cygnus*. Marine Biology, 54: 109-124.

Robles, C. 1987. Predator foraging characteristics and prey population structure on a sheltered shore. Ecology, 68: 1502-1514.

Sakuma, K. M., Field, J. C., Mantua, N. J., Ralston, S., Marinovic, B. B., and Carrion, C. N. 2016. Anomalous epipelagic micronekton assemblage patterns in the neritic waters of the California Current in spring 2015 during a period of extreme ocean conditions. CalCOFI Rep, 57: 163-183.

Schmitt, R. J. 1982. Consequences of dissimilar defenses against predation in a subtidal marine community. Ecology: 1588-1601.

Schmitt, R. J. 1987. Indirect interactions between prey: apparent competition, predator aggregation, and habitat segregation. Ecology: 1887-1897.

Solomon, S. 2007. Climate change 2007-the physical science basis: Working group I contribution to the fourth assessment report of the IPCC, Cambridge University Press.

Tegner, M., and Levin, L. 1983. Spiny lobsters and sea urchins: analysis of a predator-prey interaction. Journal of Experimental Marine Biology and Ecology, 73: 125-150.

Young, R. T., and Fox, D. L. 1936. The structure and function of the gut in surf perches (Embiotocidae) with reference to their carotenoid metabolism. Biological Bulletin: 217-237.

Chapter 1: An exoskeletal arsenal against predation in the California spiny lobster (*Panulirus interruptus*)

Kaitlyn B. Lowder, Ruan Hattingh, James M.D. Day, Joanna McKittrick, Jennifer R.A. Taylor

Abstract

The decapod crustacean exoskeleton is a complex material that differs in properties such as mineralization, structure, and material properties across species. To better understand how these attributes are altered within a single species and for particular uses, we focused on *Panulirus interruptus*, a large decapod whose exoskeleton carries out a number of functions that may benefit from specialized construction, including predator defense and prey acquisition. We studied the mineralization (% wt and concentration of Ca and Mg), ultrastructure (thickness), and mechanics (hardness and elastic modulus) of five structures: the carapace, abdomen, mandibles, antenna, and rostral horn tips. While the antenna, abdomen, and carapace were similar in composition and material properties, differences in thickness may be important to overall structural integrity. Two structures demonstrated very different properties. The mandibles, which break open prey, were 20x harder and 1.3x thicker than other structures. The horn tips were covered in poorly-mineralized, bromine-rich material over a mineralized core, both of which matched or exceeded the material properties of the mineralized non-mandibular structures. These results demonstrate the incredible diversity of architecture possible within a single species and have implications for region selection for

further exoskeletal characterization and studying responses to a variety of experimental conditions.

Introduction

Crustaceans have evolved a diverse and spectacular array of predator defenses, exemplified by the cavitation-producing snap of snapping shrimp, the complete transparency of ghost shrimp, and the sea-urchin-like armor of spiny king crabs. It is particularly remarkable that all of these specialized defenses are built upon a single material- the cuticular exoskeleton. Across the decapods, exoskeleton construction is notably conserved: an exoskeleton that transmits almost all light and an exoskeleton that can sustain incredibly high forces have the same fundamental pattern of construction. As a source of bioinspiration, the versatility of the crustacean cuticle has been an important aspect of biomaterials research (Naleway et al., 2016; Wu et al., 2019). It is also important for understanding the functional morphology underlying the evolution of ecologically-important behaviors in Crustacea.

Exoskeletons are complex, hierarchical materials that are generated anew repeatedly as animals grow via molting. As the exoskeleton develops, the epicuticle forms first. The epicuticle is a thin surface layer that consists largely of lipoproteins as well as calcium carbonate in the inner region (Travis, 1954; Dillaman et al., 2005), thus acting as a barrier to seawater and abrading substrate like sand and rock. Stacks of rotating lamellae form the two largest and mechanically-important layers of the cuticle, the exocuticle and endocuticle. These two layers are differentiated by elemental composition, lamellae stacking density, and thickness (Travis, 1963; Roer and Dillaman, 1984; Raabe et al., 2005). Typically, the exocuticle is harder (more resistant to permanent deformation when a force is applied) and stiffer (more resistant to displacement when a force is applied) than the endocuticle, which is

thicker and less lamellae-dense (Raabe et al., 2005; Sachs et al., 2006; Chen et al., 2008; Wu and Zhou, 2011). Impregnated within the lamellae is calcium carbonate in the form of amorphous calcium carbonate (ACC) or calcite (Travis, 1963; Addadi et al., 2003). Calcium ions may be replaced by magnesium to varying degrees to form magnesian calcite, which is often a small component of cuticles (Huner et al., 1979; Vigh and Dendinger, 1982; Dillaman et al., 2005; Boßelmann et al., 2007), as it increases hardness (Kunitake et al., 2012).

Across *Decapoda*, there are alterations to this general architecture in the form of variations in total cuticle thickness, layer thickness, and degree of mineralization, likely driven by the need for certain functions. For example, California brown shrimp (*Penaeus californiensis)*, which can tail-flip to escape from predators, have carapaces that are 12-14% Ca by weight, whereas crustaceans that rely on their exoskeleton as armor are more mineralized, as evidenced by the 22-28% Ca by weight of the brown crab *Cancer pagarus* and 17-23% of the American lobster *Homarus americanus* (Boßelmann et al., 2007). Other tradeoffs, such as ease of swimming versus stability in bottom currents, may also drive differences in the amount of material built into an exoskeleton. A nektobenthic species of Penaeid shrimp was found to have a cuticle cross section of just 0.13 mm in the branchial cuticle region, while the benthic crab *Carpilius maculatus* is 1.31 mm thick in this area (Amato et al., 2008).

While there are species-specific variations in cuticle construction, an individual can also benefit from specialization in different regions for a variety of exoskeletal functions. The chelipeds of crabs tend to be harder and stiffer than other regions of the body, such as the merus (Chen et al., 2008) and carapace (Dutil et al., 2000), likely due to a higher degree of mineralization (Chen et al., 2008). More material may be allocated to regions that require it

(Boßelmann et al., 2007), such as claws that are typically used for procuring food items by crushing hard prey. Additionally, some crustaceans exhibit unusual exoskeletal composition in particular areas. For example, calcium phosphate is found in many mandibles of Malacostracan crustaceans (Bentov et al., 2016), and is believed to be acting similar to the enamel of vertebrate teeth, providing increased hardness relative to the amorphous mineral underlying it (Bentov et al., 2012). The dark-tipped chelipeds of stone crabs are much harder than the yellow adjacent material, hypothesized to be from additional protein tanning (Melnick et al., 1996). Translucent brown, rubbery material on the leg and cheliped tips of grapsid crabs has been revealed to lack mineralization, instead containing higher amounts of halogens (Schofield, 2005; Cribb et al., 2009). This construction may improve the resistance of the material to wear relative to calcified cuticle (Schofield, 2005), likely an important feature to maintain cuticle integrity as the crab scrapes rock surfaces for algae. Patches of dark chitin with amorphous mineral are sometimes found on the surfaces of mandibles (Bentov et al., 2012), although their specific functionality during prey processing has not yet been tested.

The focus on areas such as the mandibles, for example, is not common. The detailed understanding of the structure and composition of the crustacean exoskeleton has largely come from study of the carapace or cheliped, if present. Determining how construction can differ among multiple regions of cuticle within a species, however, has typically relied on samples from two or perhaps three locations on the body of the animal. This limits the exploration of diversity of construction within an organism as well as a better understanding of how the necessary material properties are achieved, which may be done through large

changes to elemental composition, layer thickness, or mineral content, but may be through fine-tuning smaller changes to each.

The assortment of exoskeleton based-predator defenses in the California spiny lobster *Panulirus interruptus* (Randall; order Decapoda, class Malacostraca), presents a model system for studying both the functional morphology of predator defense and the nature of exoskeleton versatility within a single species. Here, we characterized the morphology, composition, and material properties of four distinct defensive structures in comparison with the non-specialized abdominal segment. Each of these structures are used differently and experience different types of loading during predator interactions, thus potentially benefitting from one or more of the potential methods of modification. We therefore hypothesized that the cuticle of each structure would be modified at one or more levels of scale to confer the appropriate mechanical properties for this function. The rostral horns over the eyes typically do not come in contact with predators, instead helping the animal lock itself deep under rock overhangs, and perhaps are specialized for wear-resistance. When a lobster is out from under a ledge and exposed, the antennae are often the first line of defense in close range predator attacks, holding or even pushing predators away from its body. Antennae must be stiff enough to withstand this force, but must have enough flexibility to avoid breaking and be lightweight enough to quickly swing around. The mandibles may produce a painful bite to would-be predators, but are undoubtedly specialized for breaking the shells of mussels, requiring extensive hardness themselves. If these other defenses are unsuccessful, lobsters must rely on their body armor to protect important internal organs. In spiny lobsters, the carapace is well-dotted with spines, many of them flattened but still possessing a sharp point. Overall, the

structure protects many organs and is the most important structure to preserve relative to other body parts where damage or loss can be non-fatal, such as the legs and antennae.

Methods

Animal collection and maintenance

Adult spiny lobsters (82.5-89.4 mm carapace length, 480-658 g, n=18, approximately equal ratio of sexes) were obtained from the commercial fish market in San Diego, CA and held for 0-9 months in flow-through seawater at the Scripps Institution of Oceanography, UC San Diego, where adult spiny lobsters that frequent the pier pilings are exposed to the same water conditions. Lobsters were fed squid and tilapia to satiation 2-3x per week.

Sample preparation

Prior to analysis, lobsters were anesthetized but not frozen by placement in a -20 °C freezer and then sacrificed by piercing the exoskeleton and tissue between the rostral horns along the midline of the carapace with a ceramic knife. The structures of interest, the antennae, rostral horns, abdominal segment, mandibles and carapace, were immediately dissected after sacrifice (Fig. 1). We cut approximately a 0.75 x 0.75 cm^2 section around a carapace spine located below the cephalothorax line, a 1 cm x 1 cm^2section near the center of the second abdominal spine, and a 0.5 cm x 2 cm section of the antennae 1 cm above the posterior base of the antennae on the dorsal side between the parallel rows of spines. The rostral horns were removed at the base and the excess materials around the mandible surfaces were removed. Except for the mandibles, cuticle samples from contralateral structures were randomly selected for either materials testing or morphological characterization.

Ultrastructure

Cuticle samples from each exoskeletal structure were freeze-fractured with liquid nitrogen, placed in a critical point drier (AutoSamdri 815 Series A, 570 Tousimis, Rockville, MD, USA), secured to a SEM tip to expose the cross-section, and sputter-coated with iridium prior to being analyzed with ultra-high resolution scanning electron microscopes under high vacuum (XL30 SFEG with Sirion column and Apreo LoVac, FEI, Hillsboro, OR, USA with Oxford X-MAX 80 EDS detector, Concord, MA, USA)**.** The total cuticle thickness (epicuticle, exocuticle, and endocuticle) as well as exocuticle and endocuticle thicknesses were measured from SEM images acquired at 10-20 kV.

Elemental composition

Elemental composition of cuticle samples was quantified using both energy-dispersive x-ray spectroscopy (EDX) and inductively-coupled plasma mass spectrometry (ICP-MS). The spatial resolution of EDX enabled elemental sampling of the exocuticle and endocuticle layers separately, whereas ICP-MS provided precise quantification of elements present in the whole cuticle sample. EDX analyses were conducted concurrently with the SEM analysis described above. Large rectangular areas of the exocuticle and endocuticle layers, along with the outer and core regions of the horn, were selected and spectra collected at 20 kV. We focused analysis on the relative percent weights of Ca and Mg, but elements O, Cl, Al, N, C, S, and P were also consistently present and measured.

ICP-MS was performed in the Scripps Isotope Geochemistry Lab (SIGL) for a precise quantification of elements of the whole cuticle sample. Small fractions of the EDX samples were set aside before critical point drying and were air-dried. Samples were weighed and placed in Teflon vials for digestion with 0.5 ml of concentrated Teflon-distilled (TD) nitric acid (HNO_3) on a hotplate at 100°C for >24 h. Samples were dried down and diluted by a factor of 4000 with 2% TD HNO_3 before being transferred to pre-cleaned centrifuge tubes for analysis. Samples were doped with an indium solution to monitor instrumental drift. Measurements were done using a ThermoScientific iCAPq c ICP-MS (Thermo Fisher Scientific GmbH, Bremen, Germany) in standard mode. Masses of Mg and Ca were sequentially measured for 30 ratios, resulting in internal precision of <2% (2 s.d.). Elements were corrected for total mole fraction. Total procedural blanks represented <0.3% of the measurement for Mg and Ca. Raw data were corrected off line for instrument background and drift. Samples were bracketed by internal standards of crab carapace (n=3), which allowed for calculation of absolute values. The standards yielded external precision of better than 1% for Mg and Ca (2 s.d.). We targeted the following isotopes: ^{10}B, ^{25}Mg, ^{26}M, ^{27}Al, ^{29}Si, ^{31}P, ^{43}Ca, ^{48}Ca, ^{54}Fe, ^{57}Fe, ^{65}Cu, ^{66}Zn, ^{86}Sr, ^{111}Cd, ^{137}Ba, ^{208}Pb and ^{238}U. There were no suitable standards for the halogens Br and Cl, so these were not measured. A weighted average based on the natural abundance of isotopes was calculated for Ca and Mg and used in analyses.

Material properties

Cuticle samples from the antenna, carapace, and abdomen were flat and required no additional preparation for materials testing. The mandibles were lightly sanded with 2500 grit sandpaper to produce a flat surface along the bottom ridge, and one horn per lobster was

trimmed and sanded on the medial side so that the lateral side was not angled. The other horn was positioned upright in cube silicon molds, covered with epoxy (EpoxiCure, Buehler, Lake Bluff, IL, USA), and allowed to cure overnight. The next day, embedded samples were sanded down with 2500 grit sandpaper to expose the horn tip cross-section at a standardized plane where the center of the core gave way to the dermis.

Materials testing was performed on most cuticle samples within 12 hours of dissection (two days for embedded horns) and kept hydrated in seawater until testing. With the exception of the horn cross section, samples were affixed to an aluminum block with cyanoacrylate such that indents were made normal to the epicuticle surface. A nanoindentation materials testing machine (Nano Hardness Tester, Nanovea, Irvine, CA, USA) with a Berkovich diamond tip was used to measure hardness and stiffness of each cuticle sample. Loads of 40 mN were applied to the surface of each mounted sample at loading and unloading rates of 80 mN/min and 30 sec of creep. Indents were made on each sample until at last three consistent values were obtained, and these three were used to calculate mean hardness and stiffness per sample. This eliminated tests that resulted in unusually high values for crustacean cuticle that were likely due to methodologic error.

Statistical analysis

Analysis was carried out in R version 3.5.1 (R Core Team, 2018) with associated packages (Wickham, 2007; Graves et al., 2012; Urbanek, 2013; Peters, 2015; Auguie, 2016; Wickham, 2016b; Wickham, 2016a; Wickham et al., 2016; Wickham, 2017). We employed mixed effects models with each structure and structure/layer if applicable as fixed effects and individual lobster as a random effect with random intercepts using Satterthwaite's method. P-

values were calculated using the Kenward-Roger method. Assumptions were evaluated graphically and with the Shapiro-Wilk test for normality of residuals. Cuticle width, hardness, and stiffness were log-transformed to meet assumptions. To compare variation in cuticle thickness data, a Levene's test and post-hoc Tukey's honest significant differences test were run on ANOVA residuals. All data presented as mean ± standard deviation.

Results

Ultrastructure

Cuticle from the abdomen, carapace and antenna were similar and conformed with typical crustacean cuticle in organization, with a thin epicuticle and distinct exocuticle and endocuticle layers (Fig. 1.1), which were separated by the ecdysial line. The horn had only two layers: an inner region, which we will refer to as the core, and an outer layer that we will refer to as the outer ring (Fig. 1.1). The core had a lamellar construction typical of exocuticle and endocuticle layers, but the translucent, brown outer layer was not lamellar. In contrast to all other structures, the mandible had no distinct layers, but the lamellae increased in stacking density near the inner surface (Fig. 1.1).

While the entire outer region of the horn tip is covered by the "ring" material, the proportion of the horn cross section that was comprised of the core increased with depth from the horn's point, so thickness of these two layers was not analyzed. Total cuticle thickness, which included the epi-, exo-, and endocuticle layers, was significantly different across regions ($F_{3,39.3}$ =21.03, p<0.001) (Fig. 1.2A). The antenna and abdominal segment were of similar thickness, averaging 738 ± 85 and 747 ± 107 μm respectively (p =0.988). The carapace spine (873 ± 82 μm) was significantly thicker than these two regions ($p \leq 0.016$) and

the mandible (1157 ± 251 µm) was thicker than all regions ($p \leq 0.001$). Mandible total cuticle thickness was significantly more variable than the other regions (Levene's test: $F_{3,51}=7.87$, $p<0.001$; mandible posthoc: $p \leq 0.002$). While the range between the minimum and maximum widths of the other regions was 338 - 484 microns, there was a 930-micron difference among the thickest and thinnest regions of mandible samples, reflecting a complex morphology of the biting surface.

Region and the exocuticle and endocuticle significantly affected the layer thickness (region: $F_{2,72.6}=85.3$, $p<0.001$; layer: $F_{3,69.4}=69.7$, $p<0.001$), and the three analyzed structures each showed a difference in thickness between their two main layers. In the antennae, the endocuticle was larger than the exocuticle (399 ± 108 and 302 ± 40 microns; 1.3x thicker) ($p<0.001$), while the opposite was true for the carapace spine (exocuticle: 516 ± 61 microns; endocuticle: 303 ± 57 microns; 1.7x thicker) ($p<0.001$) and abdominal segment ($p<0.001$) (Fig. 1.2B). In the abdominal segment, the exocuticle (494 ± 51 microns) was approximately 2.5x the thickness of the underlying endocuticle (202 ± 54 microns).

Elemental composition: % wt of mineralizing elements

Structure and the layer of the structure significantly affected the % wt Ca (structure: $F_{4,102.1}=58.43$, $p<0.001$; layer: $F_{5,99.5}=32.73$, $p<0.001$; Fig. 1.3B). There were no differences in % wt Ca between the exocuticle and endocuticle layers of the antenna, carapace spine, and abdominal segment ($p>0.181$). The mandible layers were not significantly different either ($p=0.068$), whereas the outer ring and core layers of the horn differed in their composition ($p<0.001$). The outer ring of the horn had the lowest amount of Ca (2.0 ± 0.9%), significantly less than any other structure ($p \leq 0.001$). The abdominal segment (18.5 ± 6.5 %), antenna (24.8

± 5.8%) had similar percentages of Ca (p=0.300), as did the antenna and carapace (27.0 ± 7.4%; p=0.534). There were no differences in % wt Ca among the carapace spine, horn core (31.9 ± 3.7%), and mandible (27.5 ± 7.0%) ($p \geq 0.606$).

Structure and the layer of the structure significantly affected the % wt Mg (structure: $F_{4,102.0}$=56.16, p<0.001; layer: $F_{5,101.0}$= 16.68, p<0.001; Fig. 1.3B). The % wt Mg differed between the outer ring (0.6 ± 0.2%) and core of the horn (1.9 ± 0.5%) (p<0.001) and between the exo- and endocuticle layers of the antenna (2.0 ± 0.7% and 1.6 ± 0.5%) (p=0.003). For all other structures, the layers were combined for analysis (structure: $F_{4,105.4}$=51.47, p<0.001; horn and antenna layers: $F_{2,104.0}$= 34.06, p<0.001). The abdominal segment (1.4 ± 0.3%), carapace spine (2.1 ± 0.6 %), and antenna exocuticle all had similar percentages of Mg ($p \geq 0.074$). The mandible (1.4 ± 0.3%) was similar to the abdominal segment and the antenna exocuticle ($p \geq 0.056$), and the antenna endocuticle grouped with the abdominal segment, mandible, and horn core ($p \geq 0.357$).

While the percentage of mineralizing elements was much lower in the horn outer ring, the halogen Cl was approximately 10 times higher in this area (8.8%) than in all other cuticular structures (<1%).

Elemental composition: Concentration of mineralizing elements

Structure significantly affected the concentration of Ca ($F_{4,29.7}$=589.0, p<0.001) and Mg ($F_{4,27.8}$=18.43, p<0.001) (Fig. 3C, D). The homogenized horn layers contained significantly less Ca and Mg than all other structures, corresponding to the low values in the outer ring identified by EDX (Ca: 2.27 ± 0.40 µmol/ mg sample, p<0.001; Mg: 0.26 ± 0.06 µmol/ mg sample $p \leq 0.002$). The mandible had almost 2x the amount of Ca (7.85 ± 0.24 µmol/

mg sample) than other structures (4.39-4.78 µmol/ mg sample, $p<0.001$), although it had similar amounts of Mg (0.48 ± 0.07) as the carapace spine and abdominal segment (0.46 ± 0.10 and 0.48 ± 0.03 µmol/ mg sample, $p\geq0.996$). The antenna and abdominal segment were similar in terms of Ca concentration (4.38 ± 0.30 and 4.39 ± 0.48, $p=0.921$), but the antenna had significantly less Mg compared to the abdominal segment, mandible and carapace ($p\leq0.025$), although it was still higher than the horn ($p=0.019$).

Material properties

Indentation depth averaged 2.7 to 4.1 µm per structure, indicating that we primarily tested the epicuticle with the support of the underlying exocuticle. Sanding of the mandible surface to produce a flat indentation surface did not affect the material properties, as there were no patterns from the edges of the sanded portion, which was nearer to the surface, to the area in the center.

Hardness was significantly affected by the structure ($F_{4,62.3}=152.12$, $p\leq0.001$) but not location within the region (only the horn was tested in multiple distinct locations, on the surface and on each layer in the cross section) ($F_{2,58.0}=2.72$, $p=0.074$) (Fig. 4A). The mandible (11.73 ± 7.73 GPa) was significantly harder than all other structures ($p\leq0.001$). The outer ring of the horn cross section (0.40 ± 0.09) and the core of the horn (0.62 ± 0.39) ($p=0.810$) were found to be harder than the abdominal segment (0.12 ± 0.05), antenna (0.22 ± 0.09), and carapace spine (0.16 ± 0.09) ($p\leq0.0103$), but did not differ from the horn surface (0.35 ± 0.19) ($p=0.256$). The antenna did not differ from either the abdominal segment ($p=0.295$) or the carapace spine ($p=0.226$).

Stiffness also was significantly affected by structure ($F_{6,62.8}$=77.54, $p \leq 0.001$) (Fig. 4B). The mandibles (157.51 ± 75.80 GPa) were significantly stiffer than all the other structures tested (abdominal segment: 6.83 ± 1.03 GPa; antenna: 6.04 ± 2.33; carapace spine: 8.84 ± 6.44; horn cross section ring: 6.58 ± 1.56; horn cross section core: 10.92 ± 4.43; horn tip normal to surface: 11.09 ± 7.94) ($p<0.001$). The antennae were also significantly less stiff than the horn core ($p=0.021$), but no other structures differed from one another ($p \geq 0.075$).

Discussion

The crustacean exoskeleton is a heterogenous, hierarchical material that follows a general form, but composition, structure, or both can be altered by a minor or major degree, which can then affect its material properties and function as a predator defense. Here, we found significant differences in cuticle thickness, mineralization, hardness, and stiffness across the cuticle of the California spiny lobster. No two structures were the same across all measured properties, demonstrating distinctive methods of construction for the different functions required of different exoskeletal regions.

Abdominal segment: the least defensive region of cuticle

The abdominal segment is potentially one of the least-critical pieces of the exoskeleton during typical predator interactions. When hiding in a crevice or under a ledge, the lobster orients its posterior to the back wall. When exposed on a sand flat, the abdomen is often held underneath the animal, and while escaping from a predator via tail-flips, this part is

both oriented away from the threat, as lobsters swim backwards, and has the additional component of rotational velocity, potentially making it more difficult to target.

The abdominal segment, along with the carapace spine and antennae, had the lowest values for both measures of material properties, and among these three, had the lowest amounts of Ca. Furthermore, it was the thinnest region studied, especially in the endocuticle. This construction mostly supports our hypothesis that a region that is not needed as armor is not as built as those that are. However, the thinner cuticle may be important in other ways. When threatened, spiny lobsters may perform tail flips and quickly escape via momentary swimming. Nektobenthic decapods tend to have thinner cuticles that are believed to reduce density and make the swimming aspect of their lifestyles easier (Amato et al., 2008). Indeed, thin, light abdominal segments are similarly advantageous by reducing the mass of the abdomen and thus lowering the force required for the abdominal muscles to rapidly accelerate during the tail-flip escape response, potentially allowing for quicker movements away from predators with reduced fatigue.

Antenna: tool to keep predators at bay

The antennae are often the first line of defense in close range predator attacks. When threatened, the lobster positions the segmented and spined antennae over their bodies to hold or even push the attacker away (Spanier and Zimmer-Faust, 1988). Here, we found that the base of the antennae is relatively unremarkable when compared to typical crustacean cuticle, such as the abdominal segment, especially in terms of material properties. The common material properties shared by the antenna, abdominal segment, and carapace indicate that these are likely the basal values that are typical across the cuticle and are altered as needed.

Here, the % wt Ca is similar to other large decapod crustaceans (Boßelmann et al., 2007). An absence of modifications to the mineralization and material properties may be in lieu of other construction considerations. The antenna cuticle had a typical layering structure that was dominated by the endocuticle (Roer and Dillaman, 1984; Raabe et al., 2005), but the cuticle has a unique morphology, being formed into a long, segmented, and tapered tube. Across the length of the antennae, cross sections are ovular, which increases the second moment of area in the direction of loading. This confers greater structural stiffness without requiring any cuticle modifications. By reducing deflection when pushing back against predators, the lobsters may reduce antennal breakage and better maintain their distance.

Carapace spine: body armor over organs

The carapace spine was not as robustly built as expected. While we hypothesized that the degree of mineralization was higher than other structures due to the function of the carapace as a large piece of armor, it shared a relatively lower concentration of both Mg and Ca with the antenna, abdominal segment, and horn core. Both hardness and stiffness were also similar to the abdominal segment and the antenna.

One aspect where the carapace spine differed from other structures, however, was in total thickness. Second only to the mandible in total thickness, the carapace spine was about 20% thicker than the antenna and abdominal segment. This mostly came from the exocuticle, which dominated the bulk of the cross section. In typical cuticle, the endocuticle is larger, as it was true for the antennae, where the exocuticle was just 75% of the thickness of the endocuticle. In contrast, the carapace exocuticle was 1.7x thicker and the abdominal exocuticle 2.5x thicker than their respective endocuticles. This studied spine is one of a few

dozen that are formed into the surface of the carapace, a c-shaped structure that is the largest single piece of the cuticle. Potentially, thickening the exocuticle by adding additional material to these regions prior to molting may help reduce the likelihood of damage to the hydrostatic exoskeleton, which enables mobility and helps the new cuticle maintain its shape until it hardens (Taylor et al., 2003). Testing the toughness and rigidity of structures that differ in exocuticle thickness during the postmolt period may help elucidate the seemingly-targeted allocation of resources prior to molt.

Horns: anchors against rock

While in a den, the rostral horns over the eyes can help prevent the animal from being dislodged by acting as an anchor against an overhanging rock ledge (Lindberg, 1955). Despite this relatively demure defense when compared to the others that spiny lobsters employ, horn structure showed the greatest departure from typical cuticle than any other structure we studied. There was a two-layer construction consisting of a calcified core completely covered by a non-lamellar, poorly-calcified outer material. Despite this major difference, we found the surface of the horn to be no different in hardness and stiffness than the other calcified structures, excepting the mandible and a similar result for the sanded inner core. Of note, the outer ring was tested in two directions approximately 90 deg from one another with no significant differences in material properties, signifying an isotropic construction. Despite the absence of calcium carbonate, the outer layer was just as hard as the inner core, suggesting that other factors are conferring hardness. As this outer layer did not appear to be lamellar, the material properties of the non-mineralized structure may match the mineralized regions by employing additional sclerotization to cross link-proteins and form a uniform hydrogen bond

network, as has been observed as a strategy in non-mineralized jewel beetle jaws (Cribb et al., 2010).

The unusual uncalcified, halogen-rich outer layer of the horns is similar in composition and appearance to crab claw tips that are believed to be specialized for wear-resistance (Cribb et al., 2009). Sharing the translucent brown appearance of outer layers and an inner core that some crab claws and leg tips possess, these horns too must resist wear when scraping against the rough surface of rock ledges. Although not studied here, many of the carapace spines and the antennal knuckle share the appearance of this tip and may therefore be constructed similarly. Dissection of two animals in the D-2 premolt stage revealed that the new cuticle already has rigid spines, so this composition may be important in maintaining hard spines during the vulnerable postmolt period.

Mandibles: built for crushing prey and predators

The mandibles were strikingly different than other structures in terms of structure and material properties. In terms of predator defense, mandibles may be employed to induce a captor to release its hold. Multiple SCUBA divers report being bitten upon grabbing a lobster improperly (personal communication to K. Lowder). What is likely driving this specialization, however, is their primary use in feeding. Hard mandibles allow access to the soft tissue in mussels, a common prey item, by allowing the lobster to chip away at the leading edge of the shell. Mussel shells have a hardness of 2.8-4.0 GPa (Fitzer et al., 2015), much lower than the lobster mandibles, allowing the mandibles to have a safety factor and possibly still enabling prey acquisition until the next molt even if they have sustained some damage.

Structure varied considerably across both mandibles, both at the micro and macro scale. Lobster mandibles are asymmetrical; one features a large knob, which contacts a brown material on the other mandible. The brown material is fibrous and coated with a thin layer of calcification, perhaps similar in construction to the chitinous incisor covers in crayfish (Bentov et al., 2012). Both sides of the mandibles have large mastication surfaces and dramatic differences in thickness. The thicker areas were found at contact surfaces, likely increasing the support in the areas that experience the highest forces while biting prey.

The 20x greater hardness and 15x greater stiffness of the mandibles compared to other structures does not appear to be due to elemental composition alone. EDX revealed the standardized cross section of the left mandible had no more mineral than the carapace spine, antenna, and horn core, although ICP-MS, which was performed on a much larger part of the structure (approximately one-third of the left mandible), revealed the calcium concentration to be about 2x the amount observed in other structures. While hardness increases as more Mg is incorporated in calcite (Kunitake et al., 2012), there was no greater amounts of Mg found in the mandible. In many other Malocostracan crustaceans, mandibles are fortified with calcium phosphate, presumably to improve biting and mastication ability (Bentov et al., 2016). However, Bentov et al. 2016 found that an achelate lobster, the Eastern rock lobster *Sagmariasus verreauxi*, did not contain this mineral, and likewise, there was no evidence of increased phosphate content in *P. interruptus* mandibles (Supplementary Figure 1.1). Potentially, the biomineralization process may take advantage of other hardening pathways, including addition of amino acids to calcite during synthesis (Kim et al., 2016). Alternatively, the mineral that is present may be in a different crystalline form than elsewhere in the cuticle. As there are no cleavage planes in ACC and the material is isotropic, it is less brittle than

crystalline forms (Weiner and Addadi, 1997), but crystallography was not pursued here. Finally, stacking distance of lamellae may be reduced in this area, increasing density and strengthening the material. Exploration of how the mandibles are able to perform so well despite no clear alterations to composition may lead to new, bioinspired materials with extraordinary properties.

Lobster cuticle versatility

Within these spiny lobsters, we have found there is evidence of a high degree of specialized construction across regions of the cuticle, indicating a wide breadth of possible ways to modify the cuticle with the potential for other mechanisms to be identified. These spiny lobsters manipulated all of the potential avenues of specialization we studied, including composition, layer thickness, structure thickness, and material properties, demonstrating a high degree of regional control on cuticle formation and maintenance. The abdominal segment and carapace spine had similar material properties, but they diverged in terms of both layer and overall thickness in a manner that relates to their performances of various defense strategies. On the other hand, the mineralization of the mandibles did not differ from most other regions, yet it exhibited a high amount of hardness and stiffness that allows it to contend with both predators and prey. These patterns of manipulation across the cuticle may reflect tradeoffs in the energy required to lay down more lamellae before or after molting or acquire and transport mineralizing elements to the site of deposition. There may be other additional modifications not studied here, like lamellae stacking density, further sclerotization, or control over the forms of calcium carbonate and the organization of crystalline material that can be fine-tuned across the cuticle.

Conclusions

The crustacean cuticle is a remarkable example of a material that is greater than the sum of its constituent elements, a complex amalgamation that is constructed to take advantage of the alterations to material properties that minute changes to ratios of materials, forms of minerals, and ultrastructure can provide. These results provide insight into how spiny lobsters, and crustaceans in general, modify the cuticle for specific roles, including protecting the animal from a variety of predator approaches. In some instances, the mechanism for the observed properties are unknown, such as the hardness of the unmineralized horn ring and the extreme material properties of the mandibles. Closer examination of the mineral form or role of small constituents, potentially heavy metals, is warranted. This work may also be brought to higher scales, studying how the structure, composition, and material properties of the exoskeleton material then relates to the toughness, flexural stiffness, or strength of entire regions like the carapace or antennae. In total, further examination of the cuticle beyond the traditional study of the carapace and cheliped will likely reveal more instances of unusual composition or construction, which are a ripe source of inspiration for materials engineering.

These data also showcase the variability within organisms of a single species. Some studies sample from just one, two, or three animals, which may lead to a biased characterization of the species. Here, some datasets were not normally-distributed due to one or two animals exhibiting quite different properties from the others, despite using an equal number of each sex, intermolt stage animals, and a small size range. Potentially, these variations across specimens may reflect time since the last molt, differences in wear over time due to specific behaviors (a higher dependence on durophagy, sheltering under abrasive low

rock ledges more often than within algae or seagrass), or microhabitat water parameters (pH, temperature) while molting and reforming the cuticle. Further study may be directed towards examination of these factors, but regardless, reports ascribing values to exoskeletal properties of particular species would benefit from the recognition of the inherent variation among individuals.

Furthermore, this diversity across the cuticle of a single organism also highlights the necessity of careful consideration if one is to choose a single region to either characterize the properties of a yet-unstudied species or to examine changes as a result of experimental treatment conditions. Of the many changes occurring to ocean conditions as a result of anthropogenic actions, ocean acidification is a concern for crustaceans and is often addressed by studying impacts to exoskeleton calcification. Because of the different degrees of mineralization found throughout this species and likely in other species, it is imperative to either select multiple regions or justify why a single structure is a good indicator for overall impact.

Acknowledgements

We appreciate the advice and knowledge of lobsters that Phil Zerofski shared and for facilitating specimen holding. This work was partially supported through access and utilization of the UC San Diego Dept. of NanoEngineering's Materials Research Center (NE-MRC), and we especially appreciate the training and support from Sabine Faulhaber. We would like to thank the Nano3 facility at UC San Diego, Catalina Offshore Products for supplying research specimens for purchase, and Carl Robbins and other San Diego divers for

their accounts of lobster-predator interactions. This material is based upon work supported by the National Science Foundation Graduate Research Fellowship Program and the UC San Diego Frontiers of Innovation Scholars Program.

Chapter 1, in part, is in preparation for submission for publication. Lowder, K.B., Hattingh, R., Day, J.M, McKittrick, J. and Taylor, J.R.A. The dissertation author was the primary investigator and author of this material.

Figures

Figure 1.1. Structures of *Panulirus interruptus* studied: A) antenna, B) mandible, C) horn tip, D) carapace spine, E) abdominal segment in image columns I and II. Cross sections used for thickness and EDX measurements are shown in representative SEM micrographs in column III. The white scale bar is 0.5 mm. The exocuticle is indicated by "Ex" and the endocuticle is "En." Nanoindentation was performed normal to the surface in areas around those indicated by black arrows. The horn tip (C) was indented both on the outer surface shown in IC and on a cross section made at the line in image IC and shown in IIC.

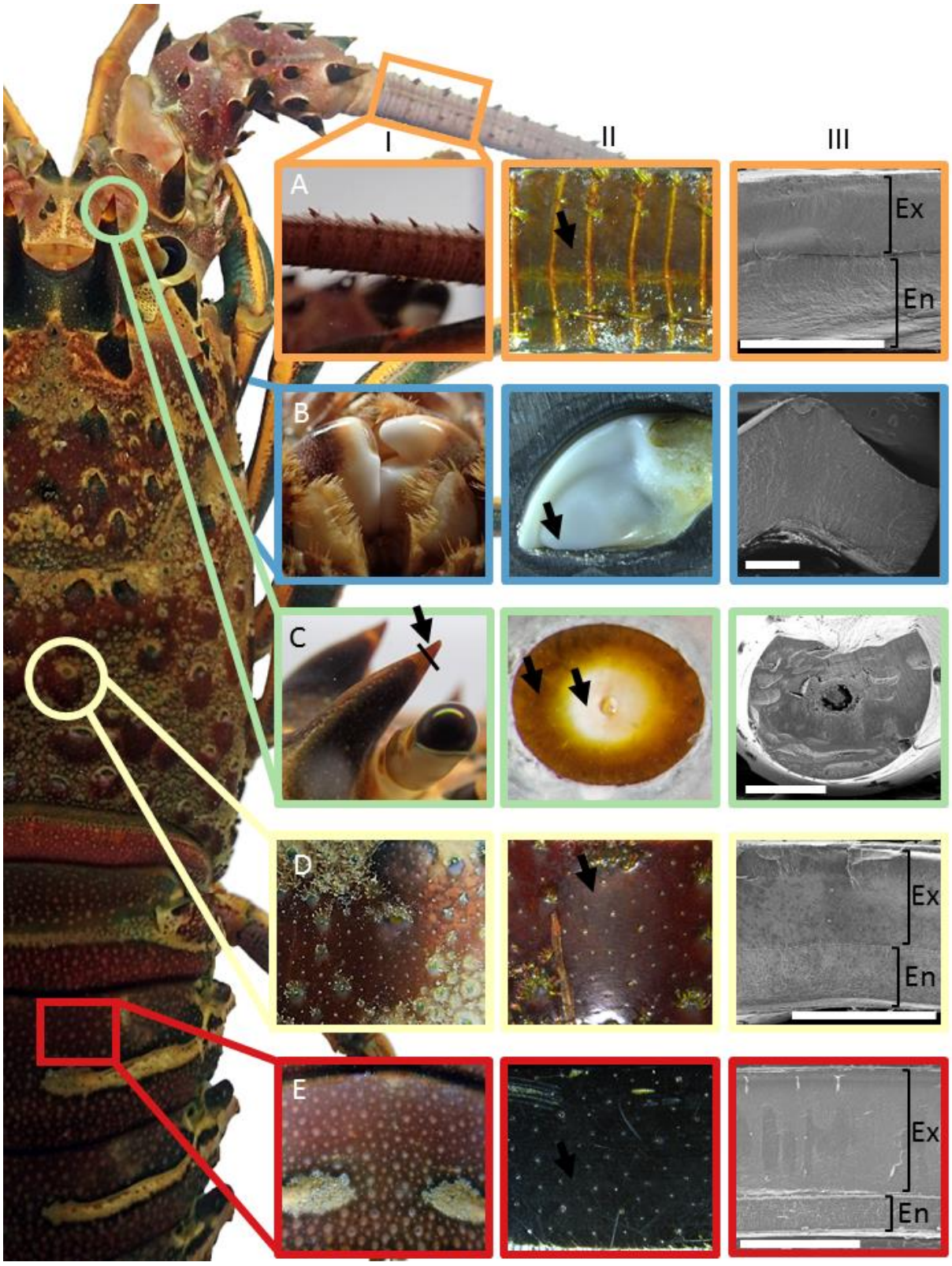
I
II
III
A
B
C
D
E
Ex
En
Ex
En
Ex
En

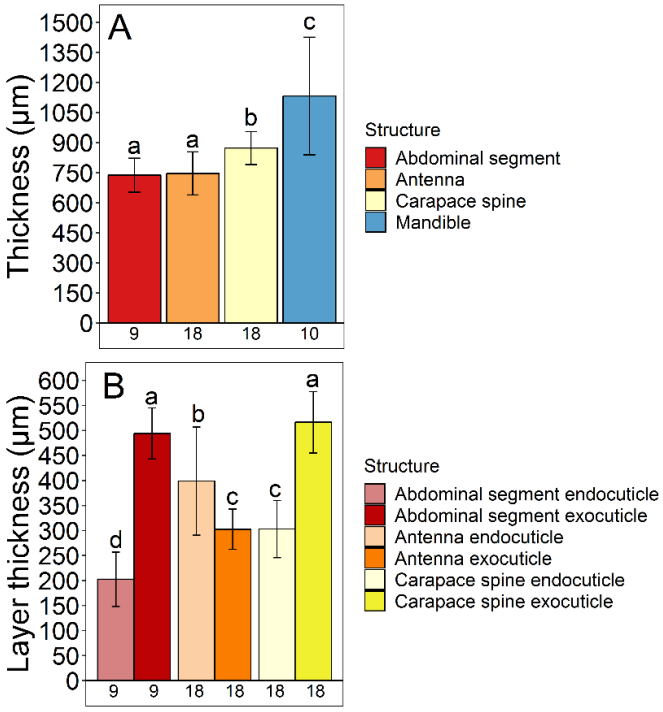

Figure 1.2. Cuticle thickness of exoskeletal structures. (A) Total cuticle thickness and (B) the main two layers of each structure, as measured from SEM images. The mandible was thicker than the carapace spine, and both were significantly thicker than the antenna and abdominal segment. The mandible is much more varied in thickness throughout as well. Within the antenna, the endocuticle comprises more of the structure, while for both the carapace spine and abdominal segment, the exocuticle forms a thicker layer. Plotted as mean ± sd. Statistical differences are represented by letter groupings. Values under the bars indicate sample size.

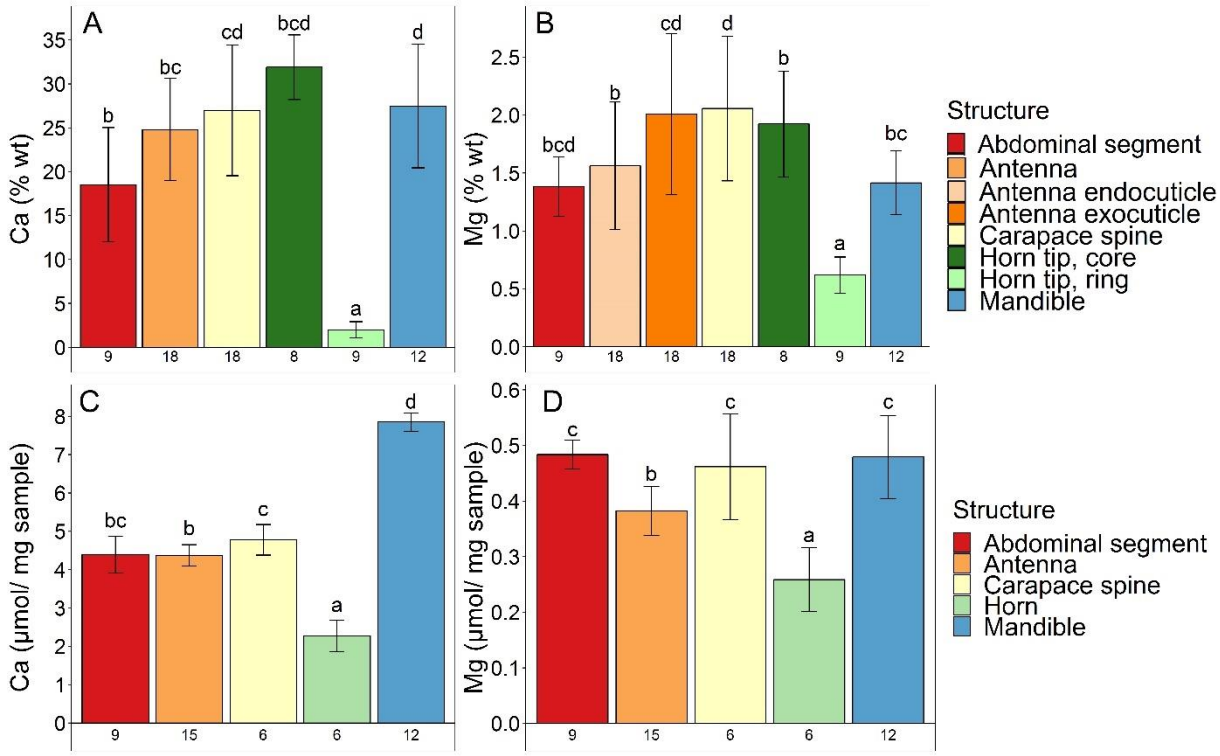

Fig. 1.3. Mineralization of exoskeletal structures measured in both concentration (A, B) and % wt (C, D). The horn was the most unusual structure, demonstrating a minimally-calcified outer ring and an inner core with a high % of Ca. The mandible was also highly calcified, while the antenna and carapace spine demonstrated similar values of mineralization. Plotted as mean ± sd. Statistical differences are represented by letter groupings. Values under the bars indicate sample size.

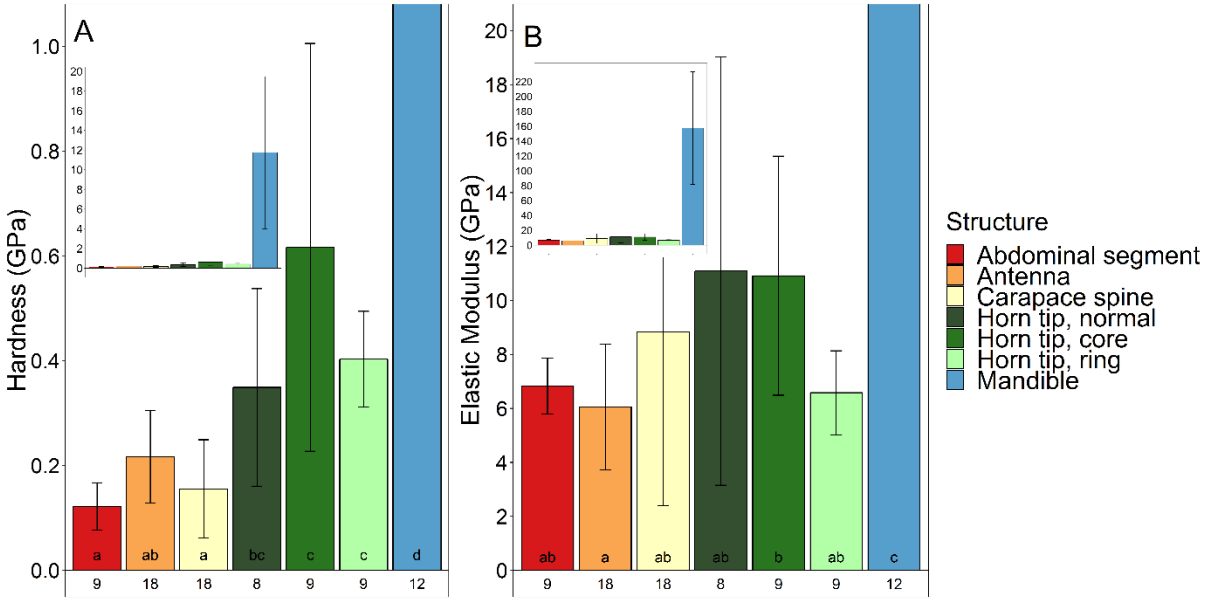

Figure 1.4. Hardness (A) and elastic modulus (B) of the exoskeleton structures. Inset image shows the full scale of the mandible, which was 20x harder than any other tested area and a full order of magnitude stiffer. The tests of three areas of the horn tip revealed no statistical differences among them, although the outer ring of the cross section was significantly harder than the other three structures. Letters indicate statistical groupings. Bars are presented as mean ± sd. Values under the bars are the sample size.

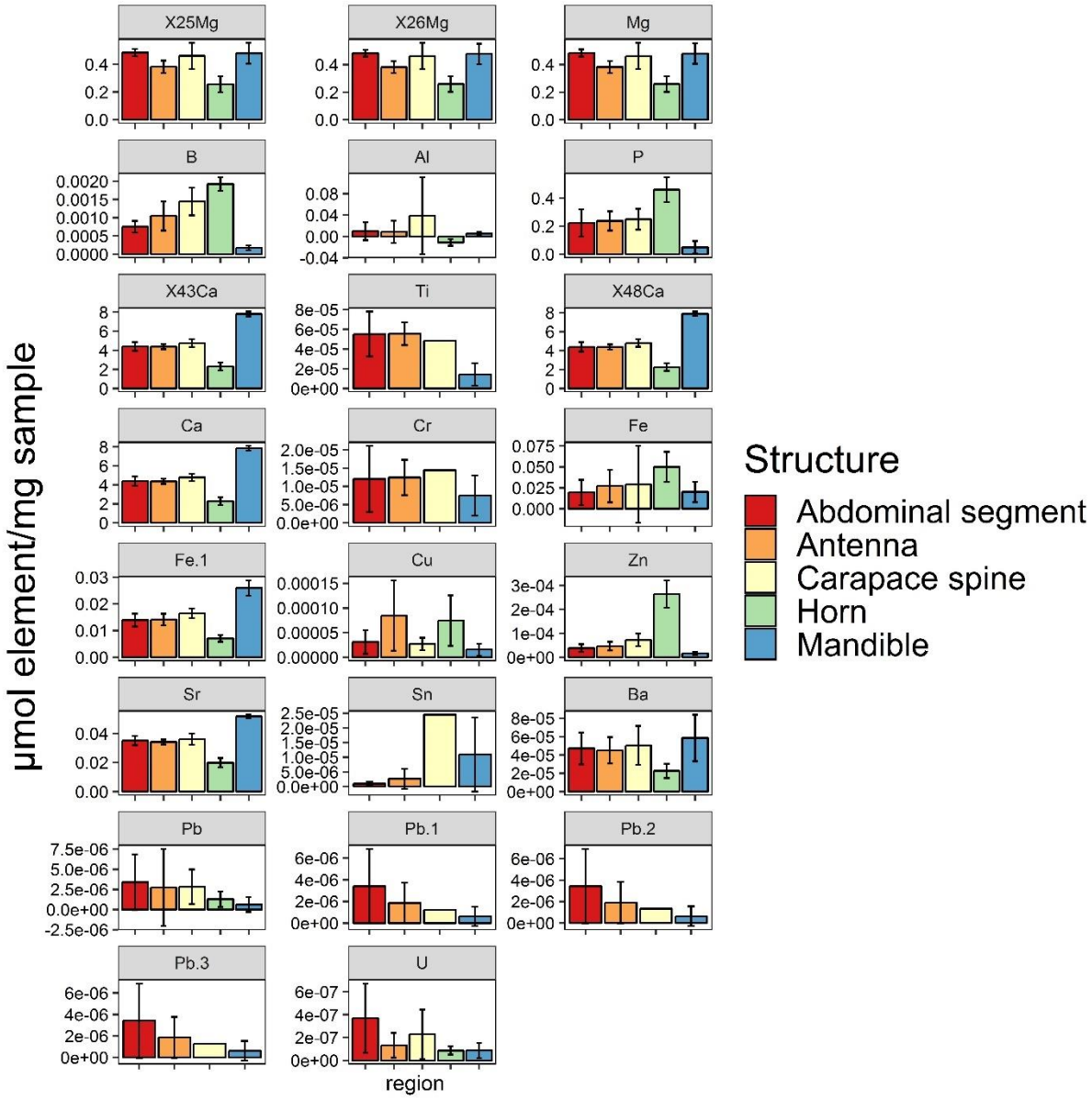

Supplemental Figure 1.1. Concentration of all elements, and multiple isotopes in some instances, measured by ICP-MS.

References

Addadi, L., Raz, S., and Weiner, S. 2003. Taking advantage of disorder: amorphous calcium carbonate and its roles in biomineralization. Advanced Materials, 15: 959-970.

Amato, C. G., Waugh, D. A., Feldmann, R. M., and Schweitzer, C. E. 2008. Effect of calcification on cuticle density in decapods: a key to lifestyle. Journal of Crustacean Biology, 28: 587-595.

Auguie, B. 2016. gridExtra: Miscellaneous functions for "grid" graphics. R package version 2.2. 1. Google Scholar.

Bentov, S., Aflalo, E. D., Tynyakov, J., Glazer, L., and Sagi, A. 2016. Calcium phosphate mineralization is widely applied in crustacean mandibles. Scientific reports, 6.

Bentov, S., Zaslansky, P., Al-Sawalmih, A., Masic, A., Fratzl, P., Sagi, A., Berman, A., and Aichmayer, B. 2012. Enamel-like apatite crown covering amorphous mineral in a crayfish mandible. Nature communications, 3: 839.

Boßelmann, F., Romano, P., Fabritius, H., Raabek, D., and Epple, M. 2007. The composition of the exoskeleton of two crustacea: The American lobster *Homarus americanus* and the edible crab *Cancer pagurus*. Thermochimica Acta, 463: 65--68.

Chen, P.-Y., Lin, A. Y.-M., McKittrick, J., and Meyers, M. A. 2008. Structure and mechanical properties of crab exoskeletons. Acta Biomaterialia, 4: 587--596.

Cribb, B., Lin, C.-L., Rintoul, L., Rasch, R., Hasenpusch, J., and Huang, H. 2010. Hardness in arthropod exoskeletons in the absence of transition metals. Acta Biomaterialia, 6: 3152-3156.

Cribb, B. W., Rathmell, A., Charters, R., Rasch, R., Huang, H., and Tibbetts, I. R. 2009. Structure, composition and properties of naturally occurring non-calcified crustacean cuticle. Arthropod Structure & Development, 38: 173-178.

Dillaman, R., Hequembourg, S., and Gay, M. 2005. Early pattern of calcification in the dorsal carapace of the blue crab, *Callinectes sapidus*. Journal of Morphology, 263: 356-374.

Dutil, J., Rollet, C., Bouchard, R., and Claxton, W. 2000. Shell strength and carapace size in non-adult and adult male snow crab (*Chionoecetes opilio*). Journal of Crustacean Biology, 20: 399-406.

Fitzer, S. C., Zhu, W., Tanner, K. E., Phoenix, V. R., Kamenos, N. A., and Cusack, M. 2015. Ocean acidification alters the material properties of *Mytilus edulis* shells. Journal of the Royal Society Interface, 12: 20141227.

Graves, S., Piepho, H.-P., Selzer, L., and Dorai-Raj, S. 2012. multcompView: visualizations of paired comparisons. R package version 0.1-5, URL http://CRAN. R-project. org/package= multcompView.

Huner, J. V., Colvin, L. B., and Reid, B. 1979. Whole-body calcium, magnesium and phosphorous levels of the California brown shrimp, *Penaeus californiensi*s (Decapoda: Penaeidae) as functions of molt stage. Comparative Biochemistry and Physiology Part A: Physiology, 64: 33-36.

Kim, Y.Y., Carloni, J. D., Demarchi, B., Sparks, D., Reid, D. G., Kunitake, M. E., Tang, C. C., Duer, M.J., Freeman, C.L., and Pokroy, B. 2016. Tuning hardness in calcite by incorporation of amino acids. Nature materials, 15: 903.

Kunitake, M. E., Baker, S. P., and Estroff, L. A. 2012. The effect of magnesium substitution on the hardness of synthetic and biogenic calcite. MRS Communications, 2: 113-116.

Lindberg, R. G. 1955. Growth, population dynamics, and field behavior in the spiny lobster, *Panulirus interruptus* (Randall), University of California Press.

Melnick, C., Chen, Z., and Mecholsky, J. 1996. Hardness and toughness of exoskeleton material in the stone crab, *Menippe mercenaria*. Journal of Materials Research, 11: 2903-2907.

Naleway, S. E., Taylor, J. R., Porter, M. M., Meyers, M. A., and McKittrick, J. 2016. Structure and mechanical properties of selected protective systems in marine organisms. Materials Science and Engineering: C, 59: 1143-1167.

Peters, G. 2015. userfriendlyscience: Quantitative analysis made accessible. R package version 0.3-0.

R Core Team 2018. R: A Language and Environment for Statistical Computing. R Foundation for Statistical Computing, Vienna, Austria.

Raabe, D., Sachs, C., and Romano, P. 2005. The crustacean exoskeleton as an example of a structurally and mechanically graded biological nanocomposite material. Acta Materialia, 53: 4281--4292.

Roer, R., and Dillaman, R. 1984. The Structure and Calcification of the Crustacean Cuticle. Integrative and Comparative Biology, 24: 893--909.

Sachs, C., Fabritius, H., and Raabe, D. 2006. Hardness and elastic properties of dehydrated cuticle from the lobster *Homarus americanus* obtained by nanoindentation. Journal of Materials Research, 21: 1987-1995.

Schofield, R. M. 2005. Metal–halogen biomaterials. American Entomologist, 51: 45-47.

Spanier, E., and Zimmer-Faust, R. K. 1988. Some physical properties of shelter that influence den preference in spiny lobsters. Journal of Experimental Marine Biology and Ecology, 121: 137-149.

Taylor, J. R., Hebrank, J., and Kier, W. M. 2003. Switching skeletons: hydrostatic support in molting crabs. Science, 301: 209-210.

Travis, D. F. 1954. The molting cycle of the spiny lobster, *Panulirus argus* Latreille. I. Molting and growth in laboratory-maintained individuals. The Biological Bulletin, 107: 433-450.

Travis, D. F. 1963. Structural features of mineralization from tissue to macromolecular levels of organization in the decapod Crustacea. Annals of the New York Academy of Sciences, 109: 177-245.

Urbanek, S. 2013. png: Read and write PNG images. R package version 0.1-7.

Vigh, D. A., and Dendinger, J. E. 1982. Temporal relationships of postmolt deposition of calcium, magnesium, chitin and protein in the cuticle of the Atlantic blue crab, *Callinectes sapidus* Rathbun. Comparative Biochemistry and Physiology Part A: Physiology, 72: 365-369.

Weiner, S., and Addadi, L. 1997. Design strategies in mineralized biological materials. Journal of Materials Chemistry, 7: 689-702.

Wickham, H. 2007. Reshaping data with the reshape package. Journal of Statistical Software, 21: 1-20.

Wickham, H. 2016a. ggplot2: elegant graphics for data analysis, Springer.

Wickham, H. 2016b. tidyr: Easily Tidy Data with spread () and gather () Functions. Version 0.6. 0.

Wickham, H. 2017. Forcats: Tools for working with categorical variables (factors). R package version 0.2. 0. URL: https://CRAN. R-project.org/package=forcats.

Wickham, H., Francois, R., Henry, L., and Müller, K. 2016. dplyr: A Grammar of Data Manipulation. R package version 0.5. 0. R Core Development Team Vienna.

Wu, J., Qin, Z., Qu, L., Zhang, H., Deng, F., and Guo, M. 2019. Natural hydrogel in American lobster: A soft armor with high toughness and strength. Acta Biomaterialia.

Wu, Z., and Zhou, F. 2011. Structure and mechanical properties of pincers for freshwater lobster. Science China Technological Sciences, 54: 650-658.

CHAPTER 2: California spiny lobster larvae develop faster in warmer water despite ocean acidification-like decreases in pH

Kaitlyn B. Lowder, Michael C. Allen, Dimitri D. Deheyn, Andreas J. Andersson, Ruan Hattingh, Summer J. Webb, James M.D. Day, Jennifer R.A. Taylor

Abstract

Crustacean larvae are believed to be more vulnerable to the effects of future ocean acidification and warming than adult stages, but estimates of impacts may be understated because critical sources of larval mortality, such as vulnerability to predation, have not been studied. For many larvae that inhabit the water column during development, the ability to maintain a nearly-transparent body is key to avoiding visual predators, but physiological stress and changes to mineralization may render them more opaque. Here, we exposed two hatches of *Panulirus interruptus*, the California spiny lobster, larvae to ambient pH and temperature (8.05 ± 0.04, 18.46 ± 0.58°C), increased temperature (8.05 ± 0.04, 22.23 ± 0.63°C), decreased pH (7.66 ± 0.02, 18.41 ± 0.66°C), and both conditions combined (7.67 ± 0.04), 22.40 ± 0.50°C) for 3.5-5 weeks. We quantified survival, progression to later larval stages, body size, mineralization, and transparency. Survival probability was unaffected by treatments, although larvae in increased temperature conditions increased in size, and even when combined with decreased pH conditions, they reached later stages compared to those in ambient temperature treatments. Additionally, there were no significant impacts to the concentration of Ca^{2+} and Mg^{2+} within larvae, and transparency remained unaffected across

treatments. Early-stage California spiny lobster larvae are comparatively tolerant to changes in pH and temperature expected within the California Current this century.

Introduction

Larval crustaceans have evolved to take on a diversity of forms, ranging from crab zoea and the nauplii of shrimp, copepods, and krill to the phyllosomes of spiny and slipper lobsters, but all must contend with the inherent challenges of growing and developing while avoiding predators, finding prey, and locating an appropriate area to settle. As adults, many of these crustaceans have demonstrated few, if any, effects when exposed to predicted future ocean conditions, such as the high pCO_2/reduced pH of ocean acidification (deVries et al., 2016; Lowder et al., 2017; Ericson et al., 2018; Rankin et al., 2019). As larvae, however, acid-base regulation mechanisms may not be as well-developed (Melzner et al., 2009), and in laboratory experiments, exposure to ocean acidification-like conditions has resulted in negative impacts to survival (Small et al., 2015; McLaskey et al., 2016), linear size or mass (Keppel et al., 2012; Carter et al., 2013; Rato et al., 2017), and development time (Bechmann et al., 2011; Keppel et al., 2012; Arnberg et al., 2013; Schiffer et al., 2014). In other instances, some larvae have demonstrated resilience to reduced pH conditions across one or more of these important aspects of life (Arnold et al., 2009; Bechmann et al., 2011; Schiffer et al., 2014; Small et al., 2015; Rato et al., 2017). The pattern behind these varying responses is not well understood.

Decreases in acidity are occurring at the same time as global increases in ocean temperature, which can have complicated interactions. Moderate increases in temperature

alone may produce negative responses, such as immediate reductions in survival (Small et al., 2015), sustained decreases in survival (Miller et al., 2016), and decreased body size (Arnberg et al., 2013). However, increased temperature conditions may also produce more positive effects, such as increased survival of later stages (Small et al., 2015), increased mineralization (Small et al., 2015), decreased development time (Arnberg et al., 2013; Small et al., 2015), likely because the maximum thermal capacity of the organisms has not been exceeded. In northern shrimp (*Pandalus borealis*) larvae, an increase of 2.8 °C reduced development time while increasing feeding and metabolic rates (Arnberg et al., 2013). American lobster (*Homarus americanus*) larvae also developed faster but experienced reduced survival (Waller et al., 2016). While not as commonly performed as single-stressor experiments, experiments with both reduced pH and increased temperature treatments can reveal the potentially-complex combination of both. Thus far, it appears that the realized effects of temperature are greater than those of pH (Arnberg et al., 2013; Small et al., 2015; Waller et al., 2016).

In addition to direct impacts on survival and growth, ocean acidification and warming may affect aspects of larvae biology that are likely to result in increased mortality in the environment. Larvae that develop in the pelagic environment are vulnerable to a multitude of predators, but they may reduce detection through a variety of strategies. Firstly, many crustacean larvae vertically migrate, both to avoid photodamage and improve access to prey but also to avoid visual predators in the light surface waters during daytime hours (Anger, 2001). Among crustaceans, vertical migration is accomplished primarily through behavioral means (e.g. swimming) (Sulkin, 1984), although physical attributes are also important. For example, exoskeleton calcification affects buoyancy (Sanders and Childress, 1988) by altering density and thus passively aids larvae in vertical movement. Temperature and CO_2-induced

alterations to mineralization (Long et al., 2013; Small et al., 2015) may disrupt larval buoyancy, potentially limiting the depth control that enables vertical migration and eventual settlement.

Changes in exoskeleton composition have another potential consequence for larval predator defenses. Larvae that inhabit the water column are often transparent, which is achieved through precise cuticle organization and composition as well as an extremely-flattened body plan that limits light scattering (Johnsen, 2001). These modifications can be costly, indicating that they have evolved because the benefit of near-invisibility from all viewing angles is greater (Johnsen, 2001). It has been shown that pH-induced changes in calcification can result in reduced transparency in adult shrimp (Taylor et al., 2015), but this is not a commonly-studied metric, despite the diversity of transparent crustacean larvae. Furthermore, changes to internal regulatory processes in response to environmental stressors and other physiological stress can inadvertently induce tissue discoloration by altering fluid dispersion between muscle fibers, impacting overall transparency (Bhandiwad and Johnsen, 2011; Bagge et al., 2017). This is particularly noticeable after the death of transparent crustaceans, as their bodies become an opaque, milky white (Perkins, 1928). Larvae exposed to ocean acidification and ocean warming conditions may become more opaque due to changes in exoskeleton structure, alterations to internal tissue structure, or both, ultimately becoming more easily detected by visual predators.

The functional consequences of observed sublethal responses are rarely studied, though they are critical components of larva survival under ocean acidification and warming conditions. The objectives of this study are to further elucidate the vulnerability of crustacean larvae to OA-like conditions and to better understand the functional impacts on predator

defenses, a potentially unaccounted-for source of mortality. We chose California spiny lobster (*Panulirus interruptus*) larvae for study because they are an ecologically and economically important species to the Southern California Bight, and they emulate key larvae predator defense strategies: their phyllosoma larvae are active swimmers that vertically migrate and have a high degree of transparency. The phyllosoma larval form, which is common to spiny and slipper lobsters, has yet to be studied under ocean acidification-like conditions. Females produce eggs once per year and reach peak hatching in July (Engle, 1979; Lindberg, 1955), As larvae, *P. interruptus* spends 7-9 months offshore, completing 11 larval phases before returning inshore and settling in the spring and summer (Johnson, 1960); this is a relatively long larval duration over which they have to contend with changes in ocean surface conditions.

Analysis of historical California Cooperative Oceanic Fisheries Investigations (CalCOFI) samples have shown that early-stage larvae in US waters are generally in higher abundance in the area between the Channel Islands and the mainland than further offshore and are particularly abundant at stations near Catalina Island and San Diego (Koslow et al., 2012, Johnson, 1960). However, the depth distribution of larval *P. interruptus* has not been well-characterized via sampling at discrete depths. CalCOFI tows are typically carried out with nets open from 0 to 70 m, but deeper tows do have not appreciably higher numbers, indicating that larval vertical migrations are between 0-70 m (Johnson, 1960) but may be shallower. Due to the uncertainty of larval distributions, the dynamic chemistry and other parameters, particularly due to seasonal upwelling, and limited coverage of high-quality carbonate chemistry measurements, characterizing the pH conditions that larvae experience throughout their development is difficult. Based on CalCOFI data from 2011-2012 and 2014-2015

(http://www.calcofi.org/ccdata/dic-data.html) as well as values in Takeshita et al. 2012 and Nam et al. 2011, pH is ~7.7-7.9 at 80-90 m and is higher at 30 m, around 7.9-8.0 in the summer and fall, when early phyllosoma are present.

Here, we exposed early-stage California spiny lobster phyllosoma (Fig. 2.1A) to a combination of reduced pH and increased temperature conditions and addressed the hypotheses that reduced pH decreases survival and growth, slows development time, and alters calcification, which decreases body transparency, and that these effects would be enhanced when combined with increased temperature.

Methods

Animal collection

Adult female lobsters with evidence of successful mating ("plastering") were purchased from a local fisher's market and held in flow-through seawater at the Scripps Institution of Oceanography (SIO), UC San Diego, La Jolla, CA. Two females developed eggs in the spring and carried them to larval release in the summer. After hatching in ambient conditions, phyllosoma were moved to the experimental setup within 1 day (hatch 2) or within 1 to 3 days (hatch 1). Hatch 2 was added to the system five days after hatch 1.

Water chemistry

The experimental ocean acidification and ocean warming system consisted of four header tanks (81 L) that each received filtered, UV-sterilized seawater pumped in from the SIO pier (3-4m depth, 300m offshore) at ambient pH (8.05 ± 0.04), pCO_2 (390.80 ± 20.02 μatm), and salinity (32.8 ± 0.2 PSU) (mean ± sd during the experimental period from

7/8/2018 – 8/13/2019). Phyllosoma were exposed to one of four conditions: 1) ambient pH (8.05 ± 0.04) and ambient temperature (18.46 ± 0.58°C), similar to conditions at approximately 30 m depth when offshore or hatched in shallow coastal waters (Nam et al., 2011; Takeshita et al., 2015) 2) ambient pH (8.05 ± 0.04) and increased temperature (22.23 ± 0.63°C), consistent with a predicted increase of 4 °C by 2100 (IPCC, 2014), 3) decreased pH (7.66 ± 0.02) and ambient temperature (18.41 ± 0.66°C), consistent with a decrease of 0.4 pH units, on the higher range of predicted global change, as the California Current appears to be more vulnerable to acidification (Gruber et al., 2012; Hauri et al., 2013; IPCC, 2014; Feely et al., 2018), and 4) combined decreased pH (7.67 ± 0.04) and increased temperature (22.40 ± 0.50°C) (Table 2.1). Experimental pH conditions were maintained by bubbling 100% CO_2 into three of the four header tanks (as pH is higher at lower temperatures, the ambient pH/ambient temperature header tank was slightly acidified to match the pH of the ambient pH/increased temperature tank), which was controlled by an Apex Lite aquarium controller and Apex Neptune pH and temperature probes (0.01 pH accuracy; temperature accuracy 0.1°C, Neptune Systems, Morgan Hill, CA, USA). Both pH and temperature of the header tanks were continuously controlled by this system, and data were logged every 10 minutes. Apex probes were calibrated at the start of the experiment and showed negligible drift. Temperature conditions were maintained by mixing ambient water with chilled seawater in varying ratios. Aquarium heaters were also placed in the header tanks and controlled by the Apex system, only turning on if needed to maintain a stable temperature. Two 1585 GPH aquarium powerheads were placed in each header tank to provide adequate mixing.

Water samples were collected twice from 12 containers (3 per treatment) over the experimental period in 500 mL Pyrex glass bottles and poisoned with 120 μL of a saturated

solution of $HgCl_2$ in accordance with standard operating procedures (Dickson et al., 2007). Each sampling round corresponded to one calibration period of the portable probe. These were analyzed for total alkalinity (A_T) by potentiometric acid titration using an 876 Dosimat (Metrohm, Riverview, Florida, USA) and pH electrode (Ecotrode Plus, Metrohm, Riverview, Florida, USA) and for dissolved inorganic carbon (DIC) using an AIRICA system (Marianda, Kiel, Germany) with integrated infrared CO_2 analyzer (Li-COR 7000, Li-COR, Lincoln, Nebraska, USA) (Table 2.1). Certified reference material (CRM) batches 171 and 175 provided by the Dickson laboratory at SIO were used to verify the accuracy and precision to ± 1–3 μmol kg^{-1} for both TA and DIC. Other parameters of the carbonate system were calculated using CO2Sys 25.06 (Pierrot et al., 2006) (Table 2.1). For calculations, dissociation constants of K_1, K_2 were from (Mehrbach et al., 1973), refit by (Dickson and Millero, 1987). The HSO_4 constant was from (Dickson, 1990) and the [B]T value was from (Uppström, 1974). pH and temperature were monitored daily in each container using a portable probe (HQ40d, probe PHC201, accuracy 0.01 pH, 0.1 temperature, Hach, Loveland, CO, USA) to characterize variability between bottle samples (Fig. 2.2). This probe was calibrated with NBS buffer solutions (Fisher Scientific, Fair Lawn, NJ, USA) approximately every four weeks based on known probe drift. Calculated pH from water samples were averaged for each sampling period and used to correct daily portable probe values to pH_{total} (Table 2.1). Mean values of DIC and pCO_2 were slightly different (<30 μmol/kg SW and 15 μatm) between ambient and increased temperature treatments.

In rare events (n=5), stability of the pH treatment conditions was interrupted. The pH probe controlling the decreased pH/increased temperature treatment failed within the first week and was replaced. Electrical malfunctions caused the pH in the header tanks to decrease

slightly for 0.2 to 1.5 hours (7.5 hours in one instance). There were also instances (n=6) where the chilled water system failed and the temperature in ambient conditions drifted upwards ~4°C. There were no obvious mortality spikes following any of these events, but the responses of larvae are likely constituted both from long-term stable conditions and exposure to these short-term events. These abnormal pH data are not included in the overall experimental pH average or standard deviation in Table 2.1.

Animal care

Each header tank supplied flow-through seawater to eight 4.2 L experimental containers (replicates) per treatment. Within each container, nine 28 mL polyethylene tubes (Nalgene, Thermo Fisher Scientific, Waltham, MA, USA) were divided between hatches 1 and 2 for tracking of each hatch (hatch 1, n=5; hatch 2, n=4). At the start of the experiment, five phyllosoma were placed in each tube for hatch 2, whereas larger groups of hatch 1 phyllosoma were initially placed in tubes and thinned to 5 larvae per tube on day 3. Survival was calculated from an initial number of 25 larvae for hatch 1 and 20 for hatch 2. Tubes were secured onto egg crate lighting diffusers with Velcro and two large rectangular holes (1.5 cm x 5 cm) were covered with 200-micron mesh to facilitate gentle flow through each tube. Tubes were also fitted with small plastic plugs with Xs cut into them to allow a pipette tip easy entry for food introduction without allowing larval escape (StockCap, St. Louis, MO, USA).

Phyllosoma were fed daily with newly-hatched *Artemia franciscana* nauplii cultured in sterile seawater and enriched for 24 hours with self-emulsifying lipid concentrate (SELCO) to increase lipid concentration (Brine Shrimp Direct, Ogden, UT, USA) (Ritar et al., 2003).

Brine shrimp were decapsulated before hatching to remove capsules that can impede digestion and introduce pathogens. Approximately 50 nauplii were added to each tube daily for a density of 2 nauplii per mL or 10+ per phyllosoma, which is a greater density than what has previously proven successful (Goldstein et al., 2008).

Tubes were checked on a three-day rotation for survival and for cleaning. Live larvae were transferred to a clean tube using a wide-mouthed pipette, whereas dead larvae were preserved in 70% ethanol for later staging and sizing. Occasionally some larvae were lost. In most cases, this was likely due to the degraded state of dead larva and to a limited extent due to researcher error, e.g. an unsuccessful transfer of a larva into the clean tube. It was not feasible to examine the contents of all tubes under a microscope on a regular basis, but subsampling the contents of tubes where larvae could not be initially located revealed indicators of a dead larva, such as the pigmented tissue of a single eye. Under daily visual examination, a dead larva like this would have been characterized as missing. Beginning 2.5 weeks into the experiment, at least three larvae per treatment per day were examined under a dissecting microscope and staged following (Johnson, 1956). Survival and stage data were analyzed in these three-day intervals.

The experiment was run until survival reached critical levels (≤5% in at least one treatment). The duration was 3.5 weeks for hatch 1 and 5 weeks for hatch 2 larvae. When the experiment for each hatch ended, 3 larvae from each treatment were analyzed for spectral properties, and the remaining larvae from each treatment were dried for analysis of elemental composition.

Size

Dead, preserved larvae were sized using an HD digital camera (Leica DFC290, Buffalo Grove, IL, USA) attached to a stereomicroscope (Leica M165 C, Buffalo Grove, IL, USA). Larvae were oriented flat and measurements were taken of the width and length of the cephalic shield and the thoracic width (Fig. 2.1B). The cephalic width was measured at the widest point of the shield and length measured from the most anterior point, between the eyestalks, to the posterior edge of the shield. Thoracic width was measured between the first and second legs. Measurements were not performed if the areas of interest could not be positioned normal to the camera.

Elemental composition

Prior to elemental analysis, larvae were staged, rinsed with DI water, briefly frozen, then air-dried and sealed loosely in aluminum foil envelopes. Elemental analysis was carried out using inductively-coupled plasma mass spectrometry (ICP-MS) in the Scripps Isotope Geochemistry Lab (SIGL). Larvae were pooled in groups of four from the same treatment and hatch due to their small mass (n= 11 total, 1 – 2 per treatment and hatch). Pooled larvae were weighed and placed in Teflon vials for digestion with 0.5 ml of concentrated Teflon-distilled (TD) nitric acid (HNO_3) then placed on a hotplate at 100°C for >24 h. Samples were dried down and diluted by a factor of 4000 with 2% TD HNO_3 before being transferred to pre-cleaned centrifuge tubes for analysis. Samples were doped with an indium solution to monitor instrumental drift. Measurements were done using a ThermoScientific iCAPq c ICP-MS (Thermo Fisher Scientific GmbH, Bremen, Germany) in standard mode. Masses of Mg^{2+} and

Ca^{2+} were sequentially measured for 30 ratios, resulting in internal precision of <2% (2 s.d.). Elements were corrected for total mole fraction. Total procedural blanks represented <0.3% of the measurement for Mg^{2+} and Ca^{2+}. Raw data were corrected offline for instrument background and drift. Samples were bracketed by internal standards of crab carapace (n=3), which allowed for calculation of absolute values. The standards yielded external precision of better than 1% for $Mg^{2+}$and Ca^{2+} (2 s.d.). We targeted the following isotopes: ^{10}B, ^{25}Mg, ^{26}M, ^{27}Al, ^{31}P, ^{43}Ca, ^{48}Ca, ^{54}Fe, ^{57}Fe, ^{65}Cu, ^{66}Zn, ^{86}Sr, ^{111}Cd, ^{137}Ba, ^{208}Pb, and ^{238}U. A weighted average based on the natural abundance of isotopes was calculated for Ca^{2+} and Mg^{2+} and used in analyses.

Transparency

Two to four larvae from each treatment and hatch were indiscriminately selected at 24 and 33 days (hatch 1 and 2, respectively) and anesthetized in a -20°C freezer before being examined for biophotonic properties. Percent transmission (transparency) was quantified using a PARISS© hyperspectral imaging system (LightForm Inc., Asheville, NC, USA) from the region between the mouthparts and eyes, through both the anterior lobe of the hepatopancreas and other tissue (Fig. 2.1C). Measurements were performed on a Nikon 80i microscope at the 10X objective, which was calibrated for spectral accuracy using a mercury-argon calibration lamp (LightForm, Inc., Asheville, NC, USA). Acquisition parameters were performed as previously described in (Taylor et al., 2015). Areas of both the hepatopancreas and adjacent tissue were mapped for spectra if possible, but area was not standardized to allow for data collection from the broadest region possible within individual larvae. Mean and standard deviation were calculated for each nanometer of wavelength across treatment, hatch,

and measurement location. One larva was removed from analysis due to heterogenous and irregular hepatopancreas shape and an additional two were removed due to acquisition irregularities (the region of interest was out-of-focus), leaving n=0-3 per treatment, hatch, and location.

Statistics

Analysis was carried out in R version 3.5.1 (R Core Team, 2018); (Wickham, 2007; Graves et al., 2012; Urbanek, 2013; Peters, 2015; Auguie, 2016; Wickham, 2016b; Wickham, 2016a; Wickham et al., 2016; Wickham, 2017). ANCOVAs were used to test differences in size, and test assumptions were assessed with visualizations of the residual distribution and the Shapiro-Wilk test on residuals. To calculate the probability of survival, we used the Kaplan-Meier method on the survival and missingness of individual larvae within treatments. All other data were tested for normality and homogeneity of variances with the Shapiro-Wilk test and Bartlett's test. If data met these conditions, we used one-way ANOVAs and followed with Tukey's Honest Significant Difference test if appropriate. Otherwise, the Kruskal-Wallis with Dunn's test or Welch's corrected ANOVA with Games-Howell post-hoc test was employed. $\alpha = 0.05$ with the exception of elemental data, where we employed a Bonferroni correction for repeated measures.

Results

Survival

The experiment was ended on day 26 for hatch 1 and day 35 for hatch 2, when survival reached ≤5% in at least one treatment. There was no difference in the overall probability of survival among the treatments for both hatch 1 (χ^2 =4.9, df=3, p=0.18, n=169-201) and hatch 2 (χ^2 =3.6, df=3, p=0.31, n=163-171) (Fig. 2.3), though hatch 2 had a significantly higher survival probability than hatch 1 (χ^2 =184, df=1, p<0.001, n=280-306). On the last experimental day for hatch 1, there were significantly more larvae remaining in the decreased pH/increased temperature treatment (14.8 ± 16.4 %) than all other treatments (ambient: 2.0 ± 1.8 %; increased temperature: 1.8 ± 1.5 %; decreased pH: 3.6 ± 1.8 %) (Kruskal-Wallis, χ^2 =10.99, df=3, p=0.012, n=8; Dunn post hoc, p≤0.007). There was no difference in survival at day 33 among hatch 2 larvae (One-way ANOVA: $F_{3,28}$=0.848, p=0.479). Hatch 2 survival was 10.0 ± 9.3 % in ambient conditions, 5.0 ± 5.3 % in increased temperature conditions, 8.8 ± 8.3 % in decreased pH, and 6.3 ± 3.5 % in decreased pH/increased temperature conditions.

Developmental stage

After 3.5 weeks of exposure, 33% of larvae from hatch 1 and 42% from hatch 2 had reached Stage III in both increased temperature conditions, while 100% of phyllosoma in ambient temperatures were Stage I or II (Fig. 2.4). There was no significant difference in the proportion of Stage II larvae among treatments, however (hatch 1, Kruskal-Wallis: χ^2= 8.822, df = 4, p = 0.066; hatch 2, Kruskal-Wallis rank: χ^2= 7.154, df = 6, p = 0.307). Similarly, there

was no significant difference in the number of days it took for larvae to reach Stage II, although hatch 2 larvae in ambient temperature treatments took approximately four days longer to reach Stage II than those in increased temperature treatments (ambient: 24.0 ± 4.5 days; increased temperature: 20.0 ± 4.0; decreased pH: 23.0 ± 4.5; decreased pH/increased temperature: 19.5 ± 3.5; ANOVA: $F_{3,27} = 1.293$, p=0.297, n=7-8). For larvae in hatch 1, there were also no significant differences in time to Stage II, although reduced pH alone elongated Stage I duration by three to four days (ambient: 20.0 ± 1.5 days; increased temperature: 19.5 ± 3.0; reduced pH: 24.0 ± 2.0; reduced pH/increased temperature: 21.0 ± 3.5; ANOVA: $F_{3,15} = 2.348$, p=0.114, n=3-7).

By 5 weeks, when all hatch 2 larvae were staged at the conclusion of the experiment, phyllosoma showed significant differences in the proportions of Stage II and Stage III phyllosoma (Stage II: Kruskal-Wallis: χ^2= 8.104, df = 2, p = 0.017; Stage III Kruskal-Wallis: χ^2= 8.642, df = 3, p= 0.034). Both increased temperature treatments had similar proportions (Dunn's test, $p \geq 0.412$), as did both ambient temperature treatments (Dunn's test, $p \geq 0.384$), but those in increased temperatures had significantly more Stage III and fewer Stage II larvae (Dunn's test, $p \leq 0.001$).

Size

The results of the full ANCOVAs are reported in Table 2.2. Experimental day significantly affected cephalic length (p= 0.002), cephalic width (p<0.001), and thoracic width (p<0.001) in Stage I larvae (Fig. 2.5), but there were no differences among treatments ($p \geq 0.088$).

Increased temperature, either alone or in combination with decreased pH, affected at least one metric of larval size among Stage II larvae. In the increased temperature treatment, larvae had significantly greater cephalic length ($p<0.001$) and thoracic width ($p= 0.017$). In this treatment, there was a significant effect of experimental day ($p= 0.012$), hatch ($p= 0.031$), and the interaction between experimental day and hatch ($p= 0.026$). There was also an effect of experimental day ($p= 0.049$) on cephalic width and thoracic width day ($p= 0.037$) in the decreased pH/increased temperature treatment. The decreased pH /increased temperature conditions corresponded to increased cephalic width of larvae ($p= 0.010$), and there were significant effects of hatch ($p= 0.034$), experimental day ($p= 0.008$), and the interaction between hatch and experimental day ($p= 0.030$).

Only larvae from the increased temperature and decreased pH/increased temperature treatments reached Stage III, and there was no difference in any measure of size between these treatments ($p\geq0.456$).

Elemental composition

Small sample sizes precluded statistical analyses within hatches; however, in hatch 1, larvae exposed to decreased pH alone had a greater concentration of Ca^{2+} and Mg^{2+}. Within hatch 2, larvae in increased temperature alone had a lower concentration of both elements. When larvae of both hatches were pooled, no significant differences were found among treatments for either [Ca^{2+}] (ANOVA, $F_{3,7}=0.523$, $p=0.680$) or [Mg^{2+}] (Kruskal-Wallis, $\chi^2=2.606$, df=3, $p=0.456$; Fig. 2.6).

Transparency

Percent transmittance was similar across the two locations studied, between 75-85% (Fig. 2.7). There were large differences among individual larvae, resulting in wide standard deviations within treatments, and no clear effect of treatment conditions on transparency. However, hatch 1 larvae exposed to increased temperature were approximately 10% more transparent across all wavelengths through the hepatopancreas region, and larvae in both decreased pH treatments were approximately 5% more transparent at longer wavelengths through the nearby tissue.

Discussion

Larval crustaceans are thought to be the life stage most vulnerable to future ocean acidification and warming conditions because of their less-developed regulatory systems and often limited mobility to find and remain in more favorable conditions geographically or at depth. Yet, the larval California spiny lobsters studied here did not exhibit any significant responses to up to five weeks of decreased pH conditions. Our results suggest that temperature, rather than pH, has a greater effect on early stage California spiny lobster larvae. The combination of both treatments together produced complex effects, such as mitigating measures of size that were sensitive to temperature alone and reducing mortality in one hatch.

Transparency unaffected

Importantly, one of the main predator defenses, transparency, was unaffected in larvae across the treatments and hatches. Transparency through the thickness of the entire body, as

was measured here, is influenced both by the composition of the cuticle as well as the internal physiology. The clarity of the tissue, despite potentially stressful changes in pH and temperature, indicates that larvae were not experiencing regulatory distress and were maintaining the internal structure of both the hepatopancreas and other tissue that allows light to pass through without scattering. This transparency protects larvae from visual predators at depths that receive light, which would otherwise comprise an additional source of mortality under changing ocean conditions.

No changes to mineralization

Alteration to the composition or structure of the cuticle could add more light-scattering discontinuities and reduce transparency as well, but there did not appear to be changes to the structure, and we did not find significant changes, just trends, to the concentration of mineralizing elements. Changes to the concentration of Ca^{2+} and Mg^{2+} could not be fully assessed due to the need to pool the small larvae for accurate measurements, but the trend of increased [Ca^{2+}] in decreased pH conditions, as was seen in hatch 1, has been observed in larval red king crabs (Long et al., 2013) and juvenile blue crabs (Glandon et al., 2018), potentially as a result of increased bicarbonate ions to convert to carbonate ions and use as a substrate for calcification. However, research on larval *Homarus gammarus* has shown an opposite response, that of reduced mineralization after exposure to increased temperature/decreased pH conditions (Small et al., 2015) and decreased pH alone (Arnold et al., 2009; Walther et al., 2011). Additionally, in the spider crab *Hyas araneus,* increased temperature increased calcification, whereas we found that in hatch 2, there was a trend of decreased mineralization in response to increased temperature, in spite of a higher seawater

calcite saturation state. The calcification process in larvae has not been well-studied, and the mechanisms underlying these differing responses across crustacean larvae are not understood.

The difference in responses found between hatches here may be in part because each hatch was sampled after different exposure periods, and there may be some degree of acclimation occurring. But despite this time difference, the hatches were at similar stages at the time of sampling. Both hatches of larvae from the ambient temperature treatments were Stage II at the time of analysis, while most from hatch 1 and all from hatch 2 in the increased temperature conditions were Stage III and had molted an additional time in treatment conditions. The elemental composition measured here was from entire dried bodies, as was true for another study (Walther et al., 2011), because removal of the cuticle alone was not feasible. However, this method may not reflect the concentration of mineral located in the cuticle, as limited research suggests larvae may have relatively unmineralized exoskeletons, but do have Ca^{2+} and Mg^{2+} in their hemolymph (Anger, 2001).

Temperature affects some aspects of larval size

The calcified and tanned cuticle of a crustacean impedes growth in length and width during the intermolt period, but the small or potentially nonexistent mineralization of the larval cuticle may have facilitated an interesting trend of increasing growth across all size measures of intermolt Stage I larvae. As the experiment progressed, larval size increased, indicating either that larvae were growing slightly before molting to Stage II or that larvae that had hatched at a slightly larger size survived longer than larvae that died earlier. Regardless, the size of Stage I larvae did not differ among treatments.

Within Stage II, increased temperature had the greatest effect on larval size, increasing both the cephalic shield length and the thoracic width. Yet, when combined with decreased pH, this effect disappeared, but cephalic shield width increased. These mixed effects on size demonstrate the complexity and unpredictability of independent and combined stressors. Generally, warmer temperatures have positive effects on crustacean growth, but interestingly, increased temperature hindered growth in larvae of both a caridean shrimp and the European lobster (Arnberg et al., 2013; Small et al., 2015). This is hypothesized to occur when temperature has exceeded an optimal range and larval growth cannot keep pace with developmental milestones, like progressing to the next stage (Fitzgibbon and Battaglene, 2012).

We did not find any effect of decreased pH on the size of the larvae across stages, despite decreases in body size being apparent in some other larvae at or below the level of pH decrease implemented here (Walther et al., 2010; Keppel et al., 2012; Rato et al., 2017). Increases in carapace length were observed with similar decreases in pH in larval red king crabs (Long et al., 2013). Instead, California spiny lobster phyllosoma responded similarly to larval *Homarus* that experience no effects on body dimensions under reduced pH conditions (Arnold et al., 2009; Small et al., 2015; Waller et al., 2016). Spiny lobsters diverged from other lobster-like forms 357 Ma (Bracken-Grissom et al., 2014), so these similarities are not likely due to closely-shared genetics.

Here, we used three metrics of larval size, each of which were affected by pH and temperature independently. For example, only cephalic shield width increased under decreased pH/increased temperature conditions. Thus, larvae are potentially vulnerable to disproportionate growth of some regions of their body. As active swimmers, balance and

orientation in the water column may be affected by body shape. Increases in cephalic width without corresponding changes to the thorax, where the swimming legs originate, may hinder mobility and induce greater larval mortality if larvae lose some degree of their depth distribution control.

Increased temperature hastens progression to later stages

Decreased pH and increased temperature often produce contrasting effects on development time. We did not find significant impacts of either pH or temperature in the time it took for larvae to reach Stage II, although the decreased pH tended to slow development in hatch 1 and increased temperature hastened it in hatch 2. Decreased pH commonly hinders normal larval developmental rates, as evidenced in a caridean shrimp (Bechmann et al., 2011; Arnberg et al., 2013), American lobster (Keppel et al., 2012), and krill (McLaskey et al., 2016). California spiny lobster larvae responded more similarly to the European lobster, which did not have any overall pH-induced delay in development (Rato et al., 2017).

Spiny lobster larval development within the two ambient temperature treatments and within the two increased temperature treatments did not differ from one another, despite a difference of 0.4 pH units between them. However, there was undoubtedly an effect of temperature on the progression to Stage III, as just one hatch 2 larva from either ambient temperature treatment reached this stage by the end of the experiment as opposed to 100% in both increased temperature conditions. Moderate increases of temperature are well-documented to increase growth across other life stages of crustaceans (Ponce-Palafox et al., 1997; Crear et al., 2000; Stoner et al., 2010), and that effect has also been documented in larvae as well (Arnberg et al., 2013; Harrington et al., 2019). Faster developmental times and

increased size may be due to higher metabolic rates as temperatures are higher but still within the thermal tolerance of the species (Arnberg et al., 2013; Small et al., 2015). Increased energy requirements, both from acid-base regulation and from higher metabolism may be most apparent in food-limited situations. Larval shrimp that had higher metabolisms at higher temperatures consumed more *Artemia* (Arnberg et al., 2013), which likely allowed them to put more energy into growth . Here, larvae were fed *Artemia* in excess, but we did not measure feeding rates. We therefore could not account for differential metabolism between treatments. Nonetheless, excess food may also have contributed to the faster rates of development, even under the additional condition of reduced pH. In nature, spiny lobster phyllosoma consume diverse prey such as chaetognaths, fish larvae, ctenophores, and hydromedusae (Mitchell, 1971; Anger, 2001), and the availability of this food supply may dictate their ability to contend as positively with increased temperature in the future.

California spiny lobster larvae may benefit from small increases in temperature

Spiny lobster larvae experienced no apparent negative effects of temperature during this experiment, suggesting that the 4°C increase to 22.5°C was within their thermal tolerance. The increased growth and development rates in absence of negative effects indicate that 22.5°C is likely a more preferable temperature than the ambient 18.5°C. The spiny lobster mothers used in this experiment were caught a few hundred miles south of the northern limit of their range, but *P. interruptus* spans down to Bahia Magdalena in Mexico (Vega et al., 1996), and a few populations are found within the Sea of Cortez (Ayala et al., 1988). This 1400-km range includes distinct genetic lobster populations in some areas, but the large genetically-undifferentiated zone across the range suggests mixing of lobsters between the

southern and northern regions (Iacchei, 2013), conferring tolerance to a broad range of temperatures. The natural range of the California spiny lobster, combined with the largely positive effects of warmer temperature found in this study, suggest that moderate increases in temperature above averages in the Southern California Bight may be beneficial to the northern section of the population. Indeed, long-term records correlate higher phyllosoma abundance to warmer years in the US part of the California Current (Koslow et al., 2012), and the warm conditions of 2015 corresponded to a record number of phyllosoma sampled off the California coast (Sakuma et al., 2016). Likely, the larvae at the southern part of the range will be the first to respond to increasing ocean temperature, potentially shifting the population north as conditions continue to change, like in the American lobster that appears to be responding to warming waters in southern New England and the Gulf of Maine (Le Bris et al., 2018).

We hypothesized that reduced pH conditions to negatively affect larvae in a variety of responses, particularly survival and growth. However, there were no pH-induced reductions in survival, in contrast to the response of many other larval crustaceans (Walther et al., 2010; Long et al., 2013; McLaskey et al., 2016; Miller et al., 2016; Tomasetti et al., 2018), *P. interruptus* is similar to *Homarus gammarus* as an apparently-resilient crustacean in terms of larval survival (Arnold et al., 2009; Small et al., 2015; Rato et al., 2017). Additionally, near-future decreases in pH also did not hinder development or size at either temperature. The reasons behind the multifarious responses of larval crustaceans to decreased pH conditions have not been formally studied, but it may be a combination of the range of experimental pH reductions used as well as the mean and variability of pH in their natural environment. Spiny lobster phyllosoma are less commonly found in surface-only tows and tows below 70 m depth than in tows open from 0-70 m depth (Johnson, 1960). However, the exact depth which

California spiny lobster phyllosoma maintain during daylight hours is not known for certain making ascribing exposure to the lower pH conditions at depth difficult. Assuming larvae do regularly reach 70 m, pH at these depths is around 7.7 at certain times of the year (Nam et al., 2011; Takeshita et al., 2015), so larvae may experience short periods of pH conditions slightly higher than they were chronically exposed to in this study. Further exploration of the biology of California spiny lobster phyllosoma may elucidate potential mechanisms for their broad tolerance to ocean conditions. These phyllosoma have a much longer larval duration (7-9 months) (Johnson, 1960) than many other crustaceans, and in the dynamic California Current, they may experience a broad range of environmental conditions that has selected for tolerance throughout their evolution.

Differences in hatch responses may indicate maternal or genetic differences

Rather than combining the two hatches for analyses, we chose to consider them separately. The two hatches used in this experiment differed in their overall survival, but they also had opposing trends of Stage I duration, transparency and Ca^{2+} and Mg^{2+} concentration. These differences may stem from the first three days after initial hatching when larvae from hatch 1 were initially stocked at high densities, potentially leading to food limitation or other stress, before being thinned to five per tube. In contrast, hatch 2 was stocked at this density on the day of hatching. Differences between hatches may also stem from genetic differences or differences in maternal condition or care during egg development. Other research has identified hatch-specific differences in hatching success, survival, and development (McLaskey et al., 2016) as well as metabolism and total protein content (Carter et al., 2013). With the genetic diversity present across their range (Iacchei, 2013) and the high degree of

success observed in two hatches exposed to our experimental treatments, it appears that there is tolerance to reduced (7.67) pH conditions within the California spiny lobster population.

Using a small number of hatches (n=1-5) is not unusual for larval research (Arnold et al., 2009; Walther et al., 2010; Miller et al., 2016; Rato et al., 2017). Yet, including additional hatches in these experiments will aid in gaining a stronger scope of the variability within the species' response to changing ocean conditions. However, this may come at a tradeoff of statistical power as the number of replicates per hatch will likely have to be concomitantly reduced due to limitations of available space and manpower to adequately care for cultures.

Conclusions

California spiny lobster larvae are an example of a larval crustacean resilient to both increased temperature and decreased pH conditions. As this is the first ocean-acidification-like study with spiny lobster phyllosoma, it is unclear if their mechanisms for tolerating reduced pH conditions are present across the genus, which includes 19 species from both tropical and temperate regions (Ptacek et al., 2001), or if the *P. interruptus* life history in the southern region of the California Current has been selected for adaptation to a wide range of ocean conditions. While lobster larvae positively responded to increased temperature conditions alone, growing bigger faster, the combination with decreased pH reset most of these responses to the level of ambient conditions. This demonstrates the importance of performing multistressor experiments, when parameters such as pH and temperature are changing together. While phyllosoma were resilient to temperature and pH conditions expected for the region by the end of the century, the impact of other concurrent changes to abiotic conditions, such as declining oxygen, as well as larger-scale phenomena, such as

eddies and currents that influence settlement, still need to be assessed to fully understand the outlook of California spiny lobster larvae.

Acknowledgements

We thank the numerous volunteers that contributed to this experiment, including Hengyu Zhou, Kellen Eastwood, Zhuoying Lin, Nate Hietala, Kate Riordan, Nina Scott, Lucero Sanchez, Nisha Rao, Jan Hsaio, Hannah Hillman, Brigid McCay, and Angeline Wong, who assisted in maintaining the experiment and collecting survival data. Chrissy Tustison, Jindi Song, Nadia Haghani, Airrell Gaither, Carl Whitesel, Brigid McCay, Angeline Wong, and Ye Jin assisted in measuring and staging preserved larvae. We appreciate the advice and assistance that Phil Zerofski shared and for managing the aquarium space. Thank you to Casey Butler, the aquarists at Birch Aquarium, and Eugenio Diaz Iglesias for sharing their expertise in raising crustacean larvae and to Linsey Sala for sharing her knowledge on phyllosoma distributions. We especially appreciate the assistance of the UC San Diego Facilities staff at the Scripps Institution of Oceanography for their ongoing maintenance of the seawater system. Thank you to Christine Hill, Alicia Hill, and the LE3D group at Ramona High School for their help in consistently and quickly building tubes for larvae. We also appreciate the crews of CalCOFI cruises who have produced an extensive record of carbonate chemistry data in the California Current. This material is based upon work supported by the National Science Foundation Graduate Research Fellowship Program and the generous support of The Crustacean Society and the Mia J. Tegner fellowship.

Chapter 2, in part, is in preparation for submission for publication. Lowder, K. B., Allen, M.C., Deheyn, D., Andersson, A.J., Hattingh, R., Webb, S.J., Day, J.M.D., Taylor, J.R.A. The dissertation author was the primary investigator and author of this material.

Tables

Table 2.1. Water parameters during the experimental period as mean ± sd. Values in brackets indicate the sample size. pH is calculated from the offset from discrete water samples that is applied to daily probe readings. Temperature is from daily probe readings. DIC and TA are directly measured from discrete water samples, while pCO_2, HCO_3^-, and calcite saturation state are calculated from discrete water samples using CO2Sys.

Treatment	pH (total)	Temperature (°C)	DIC (µmol/kg SW)	TA (µmol/kg SW)	$p\,CO_2$ (µatm)	HCO_3^- (µmol/kg SW)	Ω Calcite
Ambient pH, ambient T	8.05 ± 0.04 [303]	18.46 ± 0.58 [303]	1997.54 ± 19.61 [6]	2225.95 ± 11.0 [6]	390.80 ± 20.02 [6]	1819.08 ± 23.82 [6]	4.01 ± 0.11 [6]
Ambient pH, increased T	8.05 ± 0.04 [307]	22.23 ± 0.63 [307]	1967.13 ± 53.28 [6]	2225.28 ± 9.97 [6]	398.48 ± 90.74 [6]	1769.39 ± 77.63 [6]	4.52 ± 0.65 [6]
Decreased pH, ambient T	7.66 ± 0.02 [297]	18.41 ± 0.66 [324]	2149.79 ± 14.39 [6]	2225.59 ± 9.39 [6]	1065.35 ± 36.94 [6]	2037.12 ± 15.28 [6]	1.86 ± 0.05 [6]
Decreased pH, increased T	7.67 ± 0.04 [289]	22.40 ± 0.50 [313]	2129.99 ± 14.78 [6]	2225.99 ± 9.34 [6]	1050.46 ± 44.35 [6]	2009.39 ± 16.27 [6]	2.15 ± 0.08 [6]

Table 2.2. ANCOVA results testing the effect of treatment, hatch, and experimental day on three measurements of larval size across three stages. ***≤ 0.001, **≤0.01, *≤ 0.05.

Stage	Measurement	Source	adj R^2	df	Sum sq	Means Sq	F	*p*	Sig.
1	Cephalic length	Day + Treat + Hatch	0.05	5,196			3.32	0.007	**
		Day		1	0.02	0.02	8.64	0.004	**
		Treatment		3	0.01	0.00	1.70	0.168	
		Hatch		1	0.01	0.01	2.85	0.093	
		Residuals		196	0.52	0.00			
1	Cephalic width	Day * Treat * Hatch	0.19	15,187			4.115	<0.001	***
		Day		1	0.04	0.04	26.43	<0.001	***
		Treatment		3	0.01	0.00	2.21	0.088	
		Hatch		1	0.00	0.00	0.85	0.356	
		Day * Treat		3	0.02	0.01	3.66	0.014	*
		Day * Hatch		1	0.01	0.01	8.37	0.004	**
		Treat * Hatch		3	0.00	0.00	0.75	0.526	
		Day * Treat * Hatch		3	0.01	0.00	2.08	0.105	
		Residuals		187	0.28	0.00			
1	Thoracic width	Day + Treat + Hatch	0.16	5,159			7.06	<0.001	***
		Day		1	0.06	0.06	31.4048	<0.001	***
		Treatment		3	0.01	0.00	1.1917	0.315	
		Hatch		1	0.00	0.00	0.3301	0.566	
		Residuals		159	0.30	0.00			
2	Cephalic length	Day + Treat + Hatch	0.20	5,78			5.13	<0.001	***
		Day		1	0.00	0.00	0.22	0.641	
		Treatment		3	0.14	0.05	8.47	<0.001	***
		Hatch		1	0.00	0.00	0.01	0.909	
		Residuals		78	0.43	0.01			
2	Cephalic width	Day * Treat * Hatch	0.28	14,66			3.17	<0.001	***
		Day		1	0.00	0.00	0.06	0.809	
		Treatment		3	0.07	0.02	6.90	<0.001	***
		Hatch		1	0.02	0.02	5.24	0.025	*
		Day * Treat		3	0.03	0.01	2.44	0.072	
		Day * Hatch		1	0.00	0.00	0.73	0.397	
		Treat * Hatch		3	0.01	0.00	1.41	0.247	
		Day * Treat * Hatch		2	0.02	0.01	3.03	0.055	
		Residuals		66	0.23	0.00			

Table 2.2 continued

Stage	Measurement	Source	adj R^2	df	Sum sq	Means Sq	F	*p*	Sig.
2	Thoracic width	Day * Treat * Hatch	-0.01	14,62			0.95	0.513	
		Day		1	0.00	0.00	0.66	0.418	
		Treatment		3	0.02	0.01	1.40	0.251	
		Hatch		1	0.00	0.00	0.02	0.878	
		Day * Treat		3	0.01	0.00	0.65	0.586	
		Day * Hatch		1	0.00	0.00	0.04	0.845	
		Treat * Hatch		3	0.00	0.00	0.35	0.789	
		Day * Treat * Hatch		2	0.02	0.01	2.68	0.076	
		Residuals		62	0.27	0.00			
3	Cephalic length	Day + Treat + Hatch	-0.32	4,5			0.46	0.765	
		Day		1	0.01	0.01	0.55	0.491	
		Treatment		2	0.00	0.00	0.14	0.873	
		Hatch		1	0.01	0.01	1.00	0.362	
		Residuals		5	0.05	0.01			
3	Cephalic width	Day + Treat + Hatch	0.18	4,5			1.49	0.332	
		Day		1	0.01	0.01	3.72	0.112	
		Treatment		2	0.01	0.00	0.92	0.456	
		Hatch		1	0.00	0.00	0.39	0.562	
		Residuals		5	0.02	0.00			
3	Thoracic width	Day + Treat + Hatch	-0.47	4,5			0.28	0.882	
		Day		1	0.00	0.00	0.13	0.729	
		Treatment		2	0.00	0.00	0.48	0.644	
		Hatch		1	0.00	0.00	0.01	0.927	
		Residuals		5	0.02	0.00			

Figures

Figure 2.1. (A) Stage I *Panulirus interruptus* phyllosoma. (B) Standardized measurements of preserved lobster phyllosoma cephalic shield width (CW), length (CL), and the thoracic width (TW). (C) Locations of transparency measurements on the cephalic shield through both general tissue (T) and the hepatopancreas (Hp).

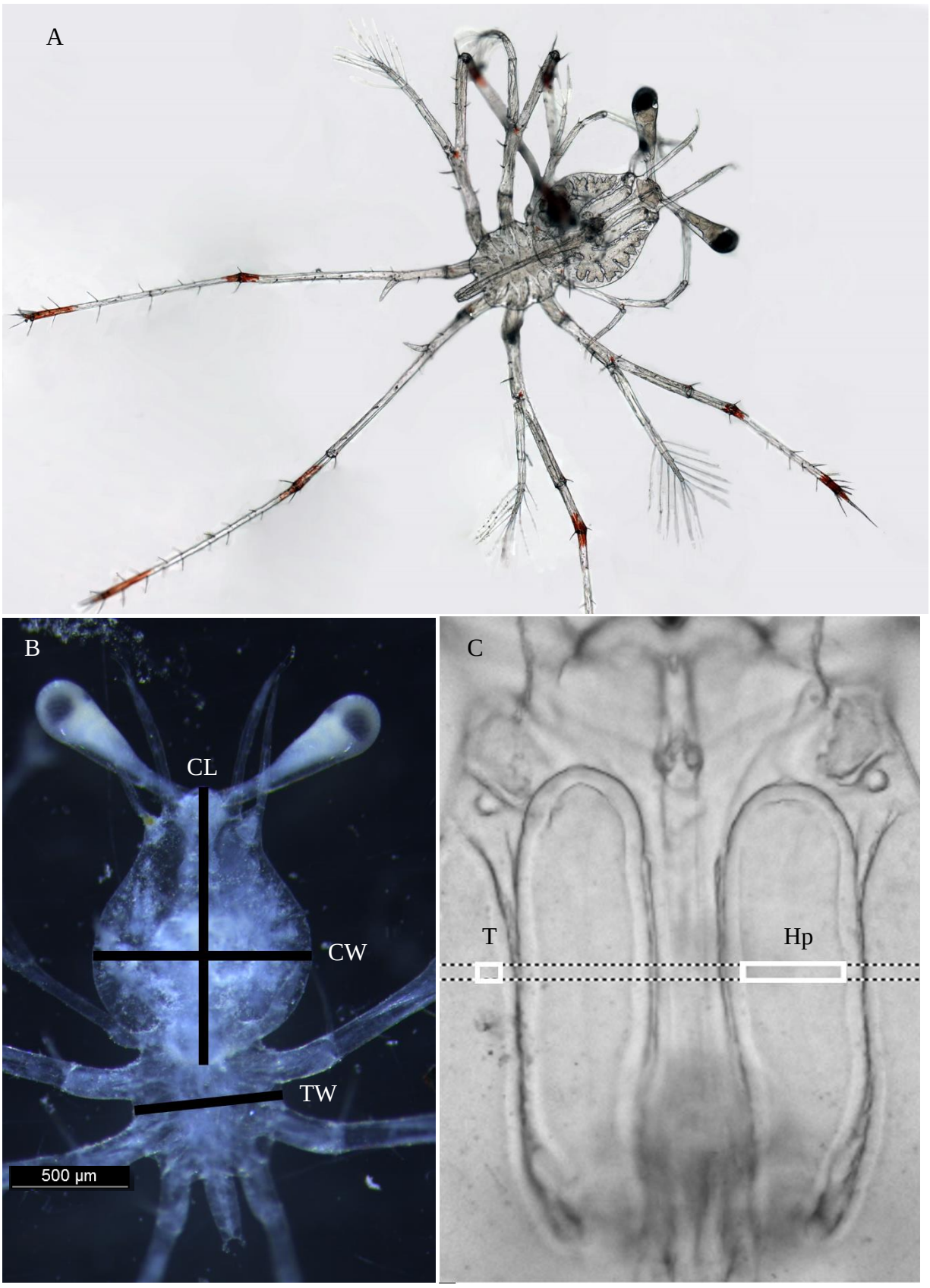
A
B
CL
CW
TW
500 µm
C
T
Hp

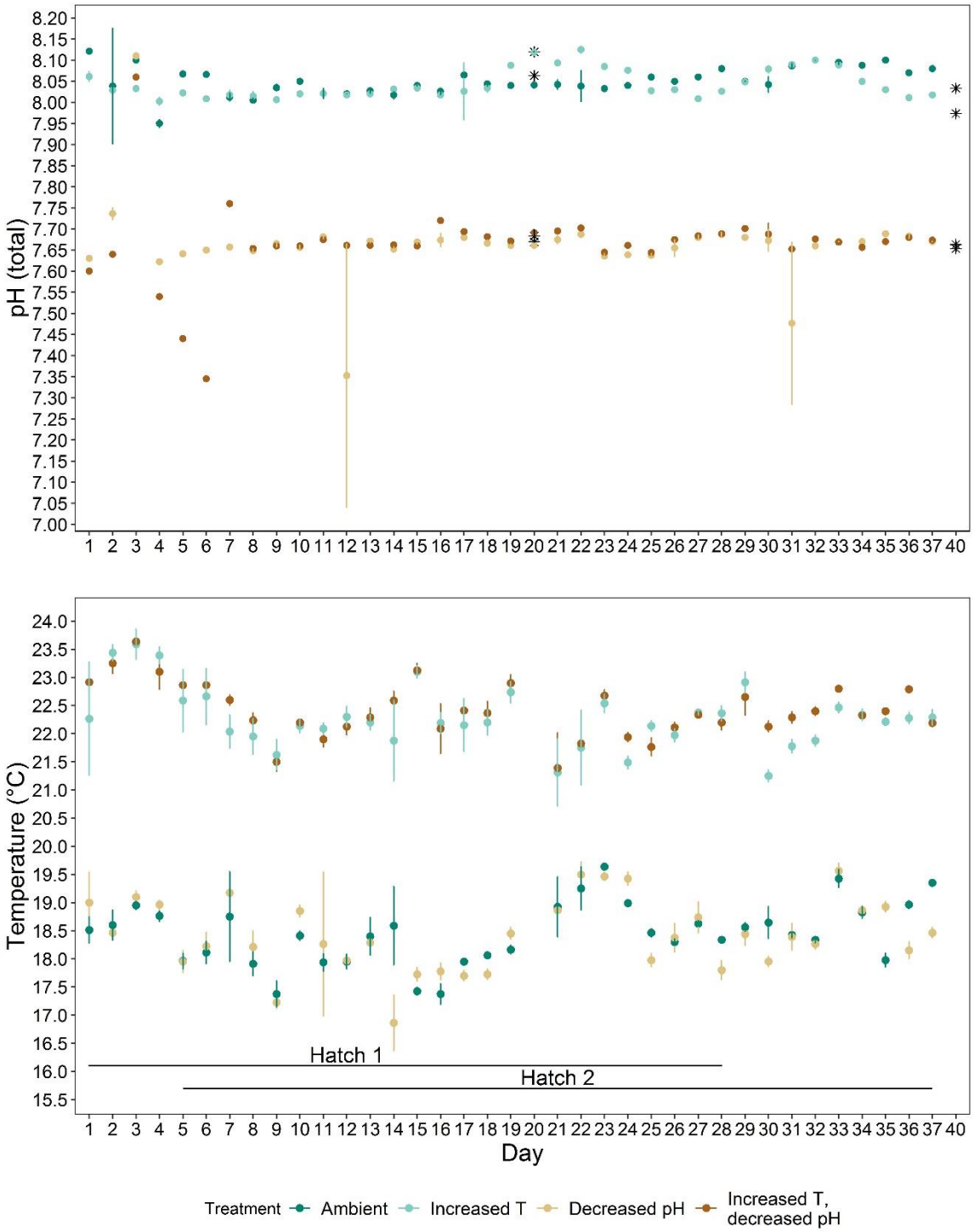

Figure 2.2. Parameters of each treatment across the experimental duration. pH_{NBS} in each replicate was measured daily with a portable pH electrode and corrected to pH_{total} (circles) via two sets of bottle samples (stars). Temperature was measured by the portable electrode. Electrode values are means ± sd.

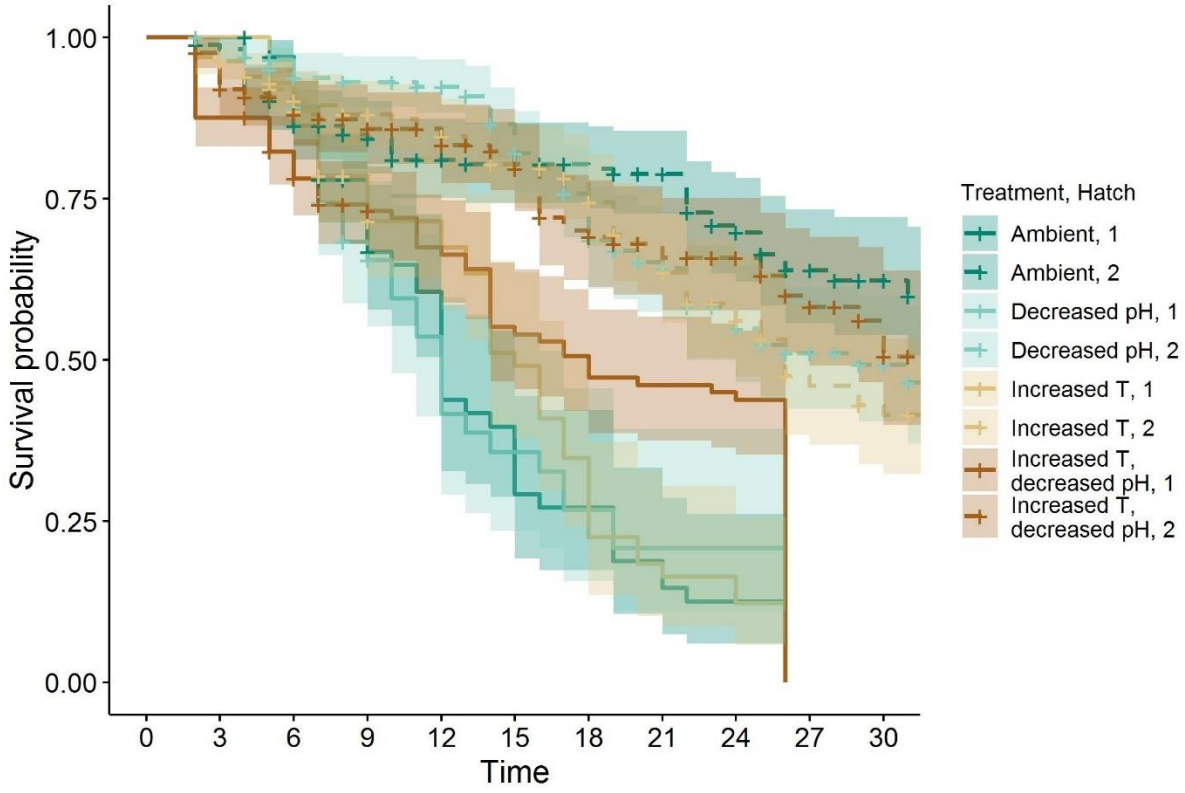

Figure 2.3. Survival probability for both hatches across the experimental duration in days (time). There was no difference in survival probability among treatments, although hatch 1 (solid lines) had a lower survival probability than hatch 2 (dashed lines) and was ended on day 26, rather than day 33 for hatch 2. Events where a larva was lost are indicated by crosses.

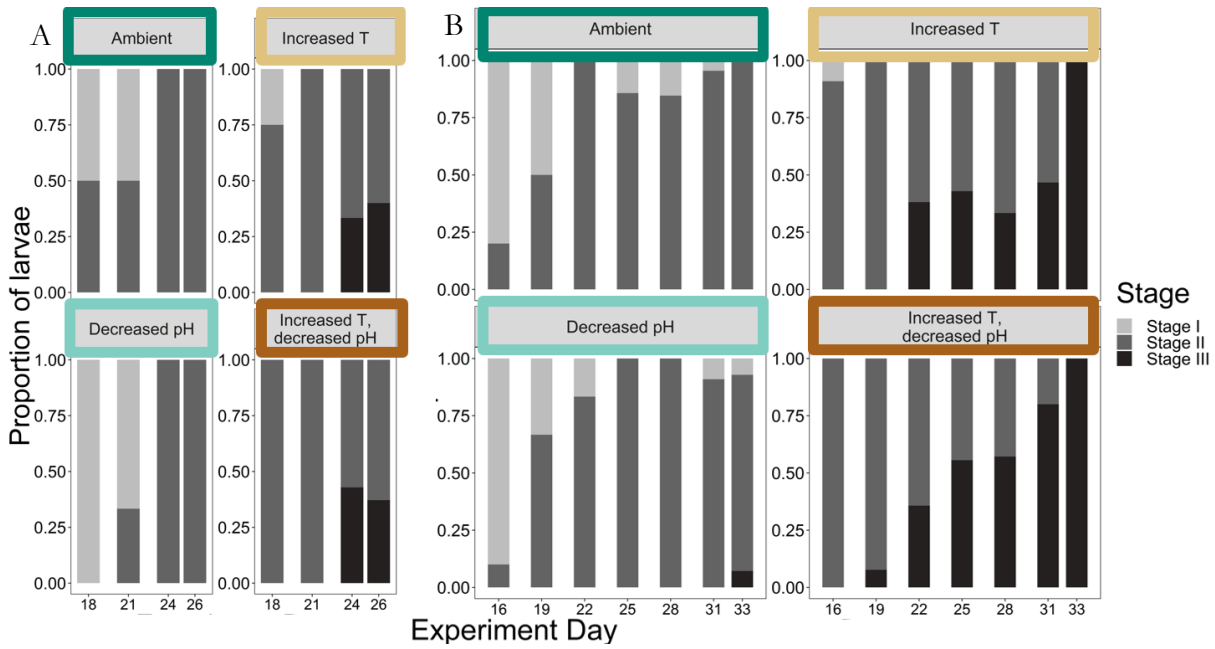

Figure 2.4. Proportion of live larvae in the first three phyllosoma stages during weeks 2.5 to 5. Significantly more hatch 2 larvae reached Stage III in the increased temperature treatments by the end of the experiment. Days 18-24 and 16-31 for hatch 1 and 2, respectively, are subsamples from each treatment, while all remaining larvae were staged on the last day for each hatch (n=1 - 42).

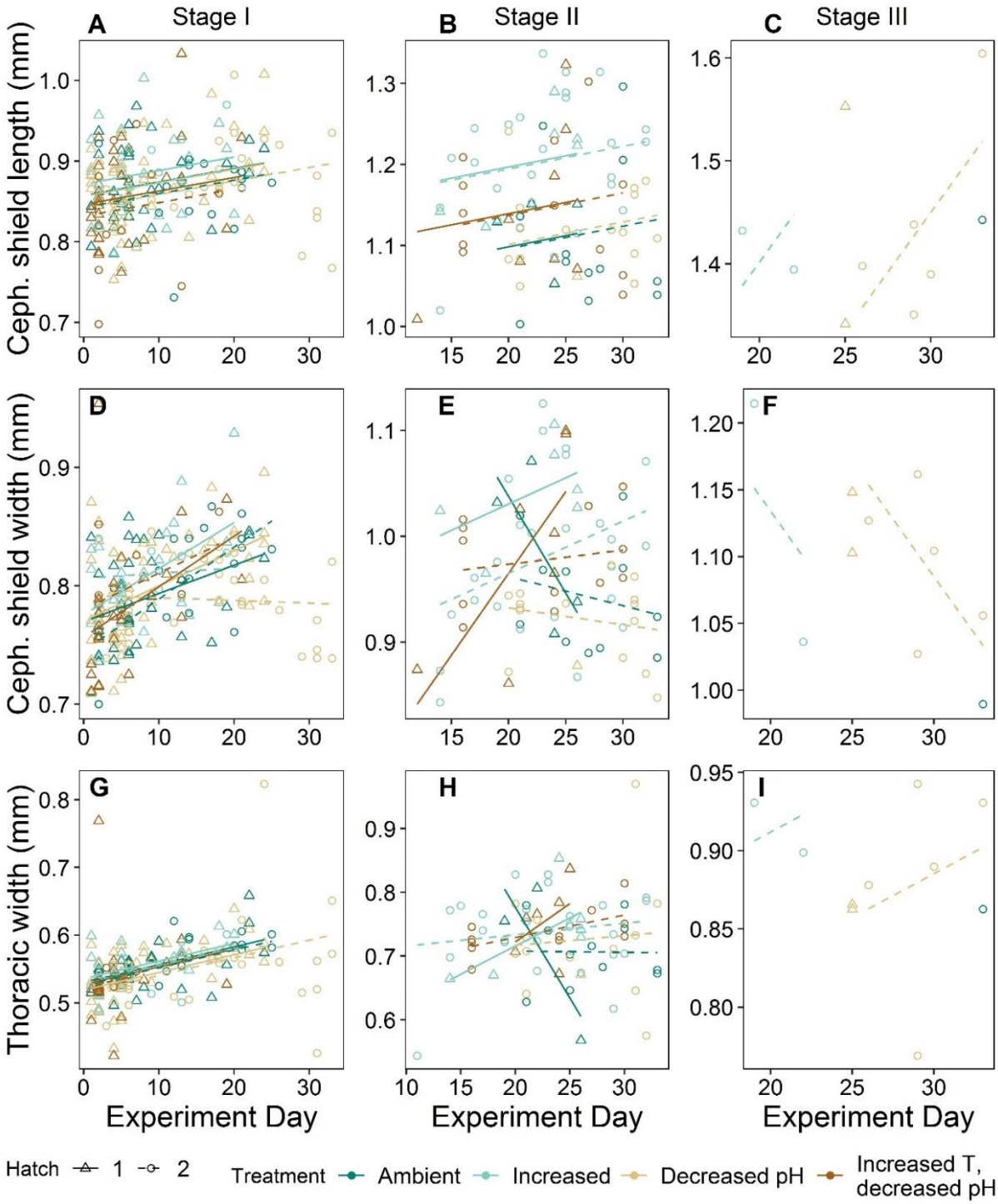

Figure 2.5. The cephalic width (A-C), cephalic length (D-F), and thorax width (G-I) of three stages of California spiny lobster larvae over the experimental period across treatments and hatches. In Stage II, cephalic length and thoracic width increased with increased temperature, while decreased pH/increased temperature conditions increased the cephalic width.

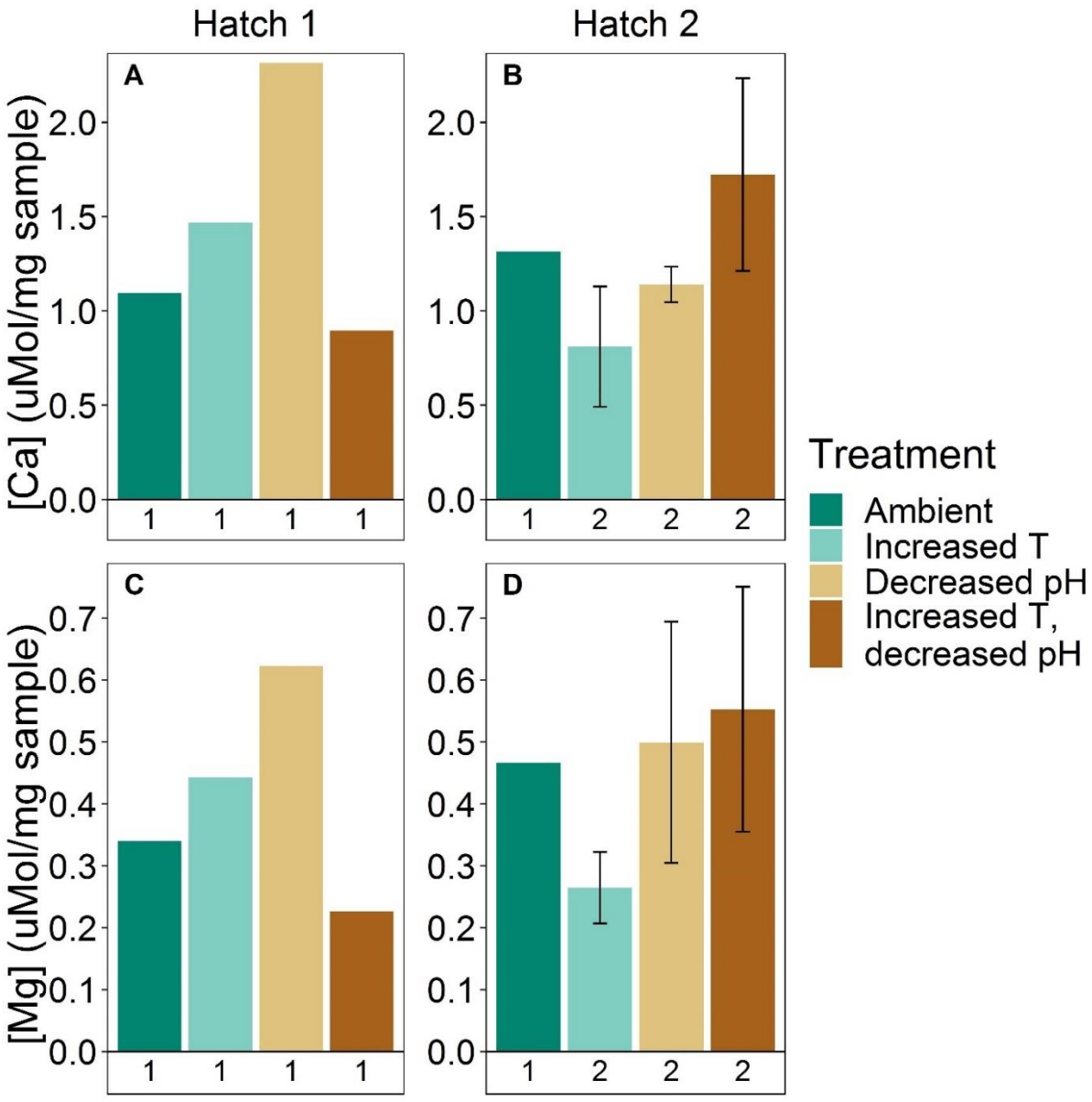

Figure 2.6. Concentrations of Ca^{2+} and Mg^{2+} in the two hatches across treatments. Small sample sizes, listed below each bar, precluded statistical analysis, but each hatch showed different trends: higher mineralization in decreased pH conditions in hatch 1 and lower mineralization in increased temperature conditions in hatch 2.

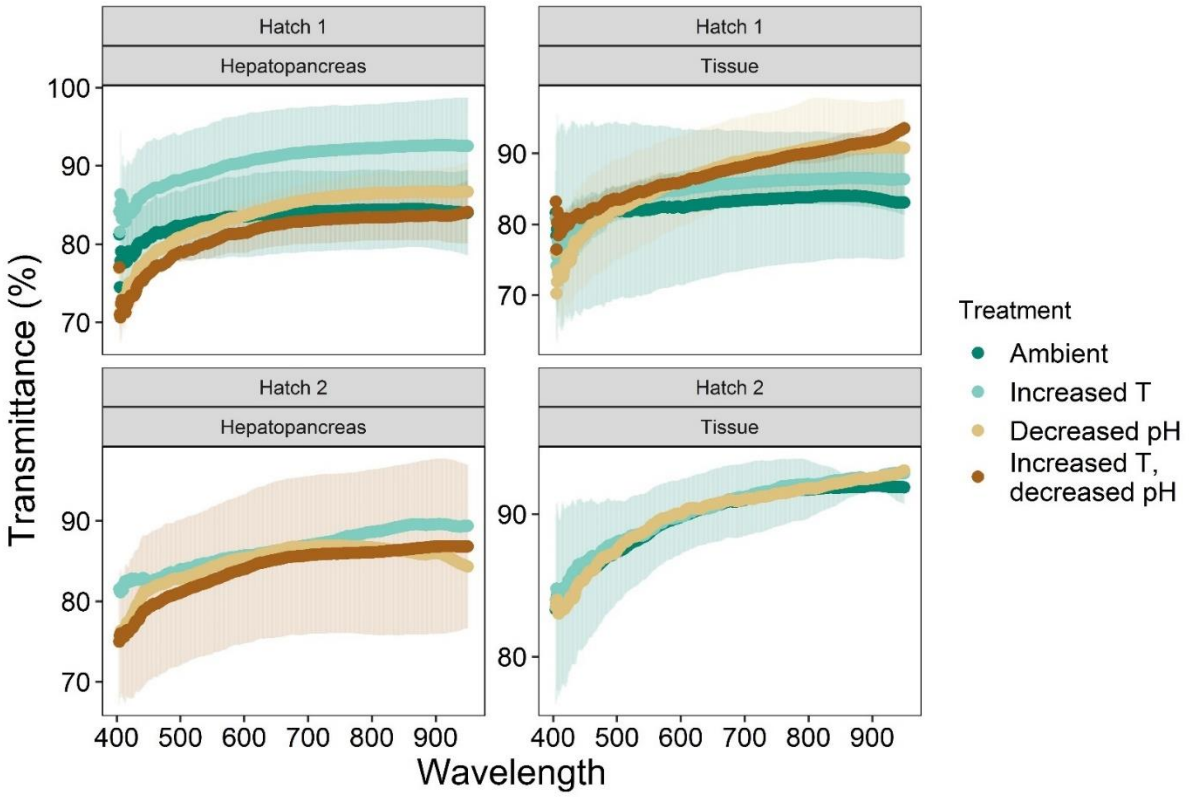

Figure 2.7. Mean percent transmittance through the body of both hatches of larvae in two locations across a spectrum of wavelengths. There were no general effects of treatment on transmittance, although hatch 1 larvae from the increased temperature treatment are slightly more transparent through the region of the hepatopancreas and those from both decreased pH treatments are slightly more transparent at higher wavelengths over general tissue (n= 0 - 3). Ribbons are the standard deviation.

References

Anger, K. 2001. The biology of decapod crustacean larvae, AA Balkema Publishers Lisse.

Arnberg, M., Calosi, P., Spicer, J. I., Tandberg, A. H. S., Nilsen, M., Westerlund, S., and Bechmann, R. K. 2013. Elevated temperature elicits greater effects than decreased pH on the development, feeding and metabolism of northern shrimp (*Pandalus borealis*) larvae. Marine biology, 160: 2037-2048.

Arnold, K., Findlay, H., Spicer, J., Daniels, C., and Boothroyd, D. 2009. Effect of CO 2-related acidification on aspects of the larval development of the European lobster, *Homarus gammarus* (L.). Biogeosciences, 6: 1747-1754.

Auguie, B. 2016. gridExtra: Miscellaneous functions for "grid" graphics. R package version 2.2. 1. Google Scholar.

Ayala, Y., González-Avilés, J., and Espinoza-Castro, G. 1988. Biología y pesca de langosta en el Pacífico Mexicano. Los Recursos Pesqueros del País: 251-286.

Bagge, L. E., Kinsey, S. T., Gladman, J., and Johnsen, S. 2017. Transparent anemone shrimp (*Ancylomenes pedersoni*) become opaque after exercise and physiological stress in correlation with increased hemolymph perfusion. Journal of Experimental Biology, 220: 4225-4233.

Bechmann, R. K., Taban, I. C., Westerlund, S., Godal, B. F., Arnberg, M., Vingen, S., Ingvarsdottir, A., Baussant, T. 2011. Effects of ocean acidification on early life stages of shrimp (*Pandalus borealis*) and mussel (*Mytilus edulis*). Journal of Toxicology and Environmental Health, Part A, 74: 424-438.

Bhandiwad, A., and Johnsen, S. 2011. The effects of salinity and temperature on the transparency of the grass shrimp *Palaemonetes pugio*. The Journal of Experimental Biology, 214: 709-716.

Bracken-Grissom, H. D., Ahyong, S. T., Wilkinson, R. D., Feldmann, R. M., Schweitzer, C. E., Breinholt, J. W., Bendall, M., Palero, F., Chan, T.-Y., and Felder, D.L. 2014. The emergence of lobsters: phylogenetic relationships, morphological evolution and divergence time comparisons of an ancient group (Decapoda: Achelata, Astacidea, Glypheidea, Polychelida). Systematic Biology, 63: 457-479.

Carter, H. A., Ceballos-Osuna, L., Miller, N. A., and Stillman, J. H. 2013. Impact of ocean acidification on metabolism and energetics during early life stages of the intertidal porcelain crab *Petrolisthes cinctipes*. Journal of Experimental Biology, 216: 1412-1422.

Crear, B., Thomas, C., Hart, P., and Carter, C. 2000. Growth of juvenile southern rock lobsters, *Jasus edwardsii*, is influenced by diet and temperature, whilst survival is influenced by diet and tank environment. Aquaculture, 190: 169-182.

deVries, M. S., Webb, S. J., Tu, J., Cory, E., Morgan, V., Sah, R. L., Deheyn, D.D., Taylor, J.R.A. 2016. Stress physiology and weapon integrity of intertidal mantis shrimp under future ocean conditions. Scientific Reports, 6: 38637.

Dickson, A., and Millero, F. J. 1987. A comparison of the equilibrium constants for the dissociation of carbonic acid in seawater media. Deep Sea Research Part A. Oceanographic Research Papers, 34: 1733-1743.

Dickson, A. G. 1990. Standard potential of the reaction: AgCl (s)+ $12H_2$ (g) = Ag (s) + HCl (aq), and and the standard acidity constant of the ion HSO_4^- in synthetic sea water from 273.15 to 318.15 K. The Journal of Chemical Thermodynamics, 22: 113-127.

Dickson, A. G., Sabine, C. L., and Christian, J. R. 2007. Guide to best practices for ocean CO_2 measurements, North Pacific Marine Science Organization, Sidney, BC. 191 pp.

Engle, J. M. 1979. Ecology and growth of juvenile California spiny lobster, *Panulirus interruptus* (Randall). p. 298. Unpublished doctoral thesis, University of Southern California, Los Angeles, California, United States.

Ericson, J. A., Hellessey, N., Kawaguchi, S., Nicol, S., Nichols, P. D., Hoem, N., and Virtue, P. 2018. Adult Antarctic krill proves resilient in a simulated high CO_2 ocean. Communications biology, 1: 190.

Feely, R. A., Okazaki, R. R., Cai, W.-J., Bednaršek, N., Alin, S. R., Byrne, R. H., and Fassbender, A. 2018. The combined effects of acidification and hypoxia on pH and aragonite saturation in the coastal waters of the California current ecosystem and the northern Gulf of Mexico. Continental Shelf Research, 152: 50-60.

Fitzgibbon, Q., and Battaglene, S. 2012. Effect of water temperature on the development and energetics of early, mid and late-stage phyllosoma larvae of spiny lobster *Sagmariasus verreauxi*. Aquaculture, 344: 153-160.

Glandon, H. L., Kilbourne, K. H., Schijf, J., and Miller, T. J. 2018. Counteractive effects of increased temperature and pCO2 on the thickness and chemistry of the carapace of juvenile blue crab, *Callinectes sapidus*, from the Patuxent River, Chesapeake Bay. Journal of Experimental Marine Biology and Ecology, 498: 39-45.

Goldstein, J. S., Matsuda, H., Takenouchi, T., and Butler IV, M. J. 2008. The complete development of larval Caribbean spiny lobster *Panulirus argus* in culture. Journal of Crustacean Biology, 28: 306-327.

Graves, S., Piepho, H.-P., Selzer, L., and Dorai-Raj, S. 2012. multcompView: visualizations of paired comparisons. R package version 0.1-5, URL http://CRAN.R-project.org/package=multcompView.

Gruber, N., Hauri, C., Lachkar, Z., Loher, D., Frölicher, T. L., and Plattner, G.-K. 2012. Rapid progression of ocean acidification in the California Current System. Science, 337: 220-223.

Harrington, A. M., Tudor, M. S., Reese, H. R., Bouchard, D. A., and Hamlin, H. J. 2019. Effects of temperature on larval American lobster (*Homarus americanus*): Is there a trade-off between growth rate and developmental stability? Ecological Indicators, 96: 404-411.

Hauri, C., Gruber, N., Vogt, M., Doney, S. C., Feely, R. A., Lachkar, Z., Leinweber, A., McDonnell, A.M.P., Munnich, M., and Plattner, G. 2013. Spatiotemporal variability and long-term trends of ocean acidification in the California Current System, Biogeosciences: 10, 193-216.

Iacchei, M., Ben-Horin, T., Selkoe, K., Bird, C. E., Garcia-Rodriguez, F. J., and Toonen, R. J. 2013. Combined analyses of kinship and FST suggest potential drivers of chaotic genetic patchiness in high gene-flow populations. Molecular ecology, 22: 3476--3494.

IPCC. 2014. Climate Change 2014: Synthesis Report. Contribution of Working Groups I, II and III to the Fifth Assessment Report of the Intergovernmental Panel on Climate Change [Core Writing Team, R.K. Pachauri and L.A. Meyer (eds.)]. 151 pp.

Johnsen, S. 2001. Hidden in plain sight: the ecology and physiology of organismal transparency. The Biological Bulletin, 201: 301-318.

Johnson, M. W. 1956. The larval development of the California spiny lobster, *Panulirus interruptus* (Randall), with notes on *Panulirus gracilis* Streets. Proceedings of the California Academy of Sciences, 29: 19.

Johnson, M. W. 1960. Production and Distribution of Larvae of the Spiny Lobster *Panulirus interruptus* (Randall) with records on *P. gracilis* Streets. Bulletin of the Scripps Institution of Oceanography, La Jolla, CA, 7: 413-461.

Keppel, E. A., Scrosati, R. A., and Courtenay, S. C. 2012. Ocean acidification decreases growth and development in American lobster (*Homarus americanus*) larvae. Journal of Northwest Atlantic Fishery Science, 44: 61-66.

Koslow, J. A., Rogers-Bennett, L., and Neilson, D. J. 2012. A time series of California spiny lobster (*Panulirus interruptus*) phyllosoma from 1951 to 2008 links abundance to warm oceanographic conditions in southern California. CalCOFI Report, 53: 132-139.

Lindberg, R. G. 1955. Growth, population dynamics, and field behavior in the spiny lobster, *Panulirus interruptus* (Randall), University of California Press.

Le Bris, A., Mills, K. E., Wahle, R. A., Chen, Y., Alexander, M. A., Allyn, A. J., Schuetz, J. G., Scott, J.D., Pershing, A.J. 2018. Climate vulnerability and resilience in the most valuable North American fishery. Proceedings of the National Academy of Sciences: 201711122.

Long, W. C., Swiney, K. M., and Foy, R. J. 2013. Effects of ocean acidification on the embryos and larvae of red king crab, *Paralithodes camtschaticus*. Marine Pollution Bulletin, 69: 38-47.

Lowder, K. B., Allen, M. C., Day, J. M., Deheyn, D. D., Taylor, J. R.A. 2017. Assessment of ocean acidification and warming on the growth, calcification, and biophotonics of a California grass shrimp. ICES Journal of Marine Science, 74: 1150-1158.

McLaskey, A. K., Keister, J. E., McElhany, P., Olson, M. B., Busch, D. S., Maher, M., and Winans, A. K. 2016. Development of *Euphausia pacifica* (krill) larvae is impaired under pCO_2 levels currently observed in the Northeast Pacific. Marine Ecology Progress Series, 555: 65-78.

Mehrbach, C., Culberson, C. H., Hawley, J. E., and Pytkowicz, R. M. 1973. Measurement of the apparent dissociation constants of carbonic acid in seawater at atmospheric pressure. Limnology and Oceanography, 18: 897-907.

Melzner, F., Gutowska, M., Langenbuch, M., Dupont, S., Lucassen, M., Thorndyke, M. C., Bleich, M., Pörtner, H-O. 2009. Physiological basis for high CO_2 tolerance in marine ectothermic animals: pre-adaptation through lifestyle and ontogeny? Biogeosciences, 6: 2313-2331.

Miller, J. J., Maher, M., Bohaboy, E., Friedman, C. S., and McElhany, P. 2016. Exposure to low pH reduces survival and delays development in early life stages of Dungeness crab (*Cancer magister*). Marine Biology, 163: 1-11.

Mitchell, J. R. 1971. Food preferences, feeding mechanisms, and related behavior in phyllosoma larvae of the California spiny lobster, *Panulirus interruptus* (Randall). San Diego State College.

Nam, S., Kim, H. J., and Send, U. 2011. Amplification of hypoxic and acidic events by La Niña conditions on the continental shelf off California. Geophysical Research Letters, 38.

Perkins, E. B. 1928. Color changes in crustaceans, especially in Palaemonetes. Journal of Experimental Zoology, 50: 71-105.

Peters, G. 2015. userfriendlyscience: Quantitative analysis made accessible. R package version 0.3-0.

Pierrot, D., Lewis, E., and Wallace, D. 2006. MS Excel Program Developed for CO2 System Calculations.

Ponce-Palafox, J., Martinez-Palacios, C. A., and Ross, L. G. 1997. The effects of salinity and temperature on the growth and survival rates of juvenile white shrimp, *Penaeus vannamei*, Boone, 1931. Aquaculture, 157: 107-115.

Ptacek, M. B., Sarver, S. K., Childress, M. J., and Herrnkind, W. F. 2001. Molecular phylogeny of the spiny lobster genus *Panulirus* (Decapoda: Palinuridae). Marine and Freshwater Research, 52: 1037-1047.

R Core Team 2018. R: A Language and Environment for Statistical Computing. R Foundation for Statistical Computing, Vienna, Austria.

Rankin, A., Seo, K., Graeve, O. A., and Taylor, J. R. 2019. No compromise between metabolism and behavior of decorator crabs in reduced pH conditions. Scientific reports, 9: 6262.

Rato, L. D., Novais, S. C., Lemos, M. F., Alves, L. M., and Leandro, S. M. 2017. *Homarus gammarus* (Crustacea: Decapoda) larvae under an ocean acidification scenario: responses across different levels of biological organization. Comparative Biochemistry and Physiology Part C: Toxicology & Pharmacology, 203: 29-38.

Ritar, A. J., Dunstan, G. A., Crear, B. J., and Brown, M. R. 2003. Biochemical composition during growth and starvation of early larval stages of cultured spiny lobster (*Jasus edwardsii*) phyllosoma. Comparative Biochemistry and Physiology Part A: Molecular & Integrative Physiology, 136: 353-370.

Sakuma, K. M., Field, J. C., Mantua, N. J., Ralston, S., Marinovic, B. B., and Carrion, C. N. 2016. Anomalous epipelagic micronekton assemblage patterns in the neritic waters of the California Current in spring 2015 during a period of extreme ocean conditions. CalCOFI Rep, 57: 163-183.

Sanders, N., and Childress, J. 1988. Ion replacement as a buoyancy mechanism in a pelagic deep-sea crustacean. Journal of Experimental Biology, 138: 333-343.

Schiffer, M., Harms, L., Pörtner, H. O., Mark, F. C., and Storch, D. 2014. Pre-hatching seawater pCO_2 affects development and survival of zoea stages of Arctic spider crab *Hyas araneus*. Marine Ecology Progress Series, 501: 127-139.

Small, D. P., Calosi, P., Boothroyd, D., Widdicombe, S., and Spicer, J. I. 2015. Stage-specific changes in physiological and life-history responses to elevated temperature and pCO2 during the larval development of the European lobster *Homarus gammarus* (L.). Physiological and Biochemical Zoology, 88: 494-507.

Stoner, A. W., Ottmar, M. L., and Copeman, L. A. 2010. Temperature effects on the molting, growth, and lipid composition of newly-settled red king crab. Journal of Experimental Marine Biology and Ecology, 393: 138-147.

Sulkin, S. D. 1984. Behavioral basis of depth regulation in the larvae of brachyuran crabs. Marine ecology progress series. Oldendorf, 15: 181-205.

Takeshita, Y., Frieder, C., Martz, T., Ballard, J., Feely, R., Kram, S., Nam, S., Navarro, M.O., Price, N.N., Smith, J.E. 2015. Including high-frequency variability in coastal ocean acidification projections. Biogeosciences, 12: 5853-5870.

Taylor, J. R. A., Gilleard, J. M., Allen, M. C., and Deheyn, D. D. 2015. Effects of CO2-induced pH reduction on the exoskeleton structure and biophotonic properties of the shrimp *Lysmata californica*. Scientific Reports, 5: 10608.

Tomasetti, S. J., Morrell, B. K., Merlo, L. R., and Gobler, C. J. 2018. Individual and combined effects of low dissolved oxygen and low pH on survival of early stage larval blue crabs, *Callinectes sapidus*. PLOS ONE, 13: e0208629.

Uppström, L. R. 1974. The boron/chlorinity ratio of deep-sea water from the Pacific Ocean. *In* Deep Sea Research and Oceanographic Abstracts, pp. 161-162. Elsevier.

Urbanek, S. 2013. png: Read and write PNG images. R package version 0.1-7.

Vega, V., Espinoza-Castro, G., and Gómez-Rojo, C. 1996. Pesquería de langosta *Panulirus sp*. Estudio del potencial pesquero y acuícola de Baja California Sur'.(Eds M. Casas-Valdez and G. Ponce-Díaz.) pp: 227-261.

Waller, J. D., Wahle, R. A., McVeigh, H., and Fields, D. M. 2016. Linking rising pCO_2 and temperature to the larval development and physiology of the American lobster (*Homarus americanus*). ICES Journal of Marine Science: Journal du Conseil: fsw154.

Walther, K., Anger, K., and Pörtner, H.-O. 2010. Effects of ocean acidification and warming on the larval development of the spider crab *Hyas araneus* from different latitudes (54 vs. 79 N). Mar Ecol Prog Ser, 417: 159-170.

Walther, K., Sartoris, F. J., and Pörtner, H. O. 2011. Impacts of temperature and acidification on larval calcium incorporation of the spider crab *Hyas araneus* from different latitudes (54 vs. 79 N). Marine Biology, 158: 2043-2053.

Wickham, H. 2007. Reshaping data with the reshape package. Journal of Statistical Software, 21: 1-20.

Wickham, H. 2016a. ggplot2: elegant graphics for data analysis, Springer.

Wickham, H. 2016b. tidyr: Easily Tidy Data with spread () and gather () Functions. Version 0.6. 0.

Wickham, H. 2017. Forcats: Tools for working with categorical variables (factors). R package version 0.2. 0. URL: https://CRAN.R-project.org/package=forcats.

Wickham, H., Francois, R., Henry, L., and Müller, K. 2016. dplyr: A Grammar of Data Manipulation. R package version 0.5. 0. R Core Development Team Vienna.

CHAPTER 3: Mixed responses of California spiny lobster, Panulirus interruptus, predator defenses in reduced and fluctuating pH conditions

Kaitlyn B. Lowder, Maya S. DeVries, Cierra B. Kelly, Andreas J. Andersson, Ruan Hattingh, James M.D. Day, Jennifer R.A. Taylor

Abstract

Crustaceans are believed to be relatively resilient to ocean acidification-like conditions. However, the potential impacts to their predator defenses are not often studied, though they may constitute a large source of mortality in their environment. Here, we exposed juvenile *Panulirus interruptus*, the California spiny lobster, to three months of reduced pH conditions with three levels of daily pH variation (ambient/stable, 7.97; reduced/stable 7.67; reduced with low fluctuations, 7.67 ± 0.05; reduced with high fluctuations, 7.67 ± 0.10) and studied both exoskeletal and behavioral predator defenses. Notably, the carapace was less mineralized in reduced, fluctuating pH treatments but without an effect on material properties, and the rostral horn had lower hardness in reduced/high fluctuating conditions without a corresponding difference in mineralization. There were no significant impacts of reduced pH on antennae flexural stiffness, antennule flick rates in response to a chemical cue, or the kinematics of the tail-flip escape response. These results demonstrate a complex relationship between mineralization and mechanical properties of the exoskeleton under changing ocean chemistry, and that fluctuating reduced pH conditions can induce responses of a different magnitude than the stable reduced pH conditions often used in ocean acidification research. Juvenile California spiny lobsters survive and continue to have a large suite of predator

defenses in their arsenal under ocean acidification-like conditions, suggesting that this life stage will not be a source of greater natural mortality within the population in the coming century.

Introduction

The predator defenses of marine organisms are multifarious, ranging from the chemical secretions of sea hares (Aggio and Derby, 2008) to the dynamic transparency and pigmentation of mesopelagic cephalopods (Zylinski and Johnsen, 2011) and the iron-plated shells of a deep-sea gastropod (Yao et al., 2010). Within Crustacea, the gamut of defense strategies is just as diverse, ranging from the crypsis of skeleton shrimp that mimic filamentous strands of algae to the threatening displays of crab meral spreads and the long, protruding spines of porcelain crab larvae. There is evidence that changes in ocean carbon chemistry associated with ocean acidification can affect the structural (McClintock et al., 2009; McDonald et al., 2009) and behavioral (Dixson et al., 2010; Jarrold et al., 2017) aspects of animals that are at the root of their ability to use defenses successfully against predators. Rarely are predator defense mechanisms studied in experimental ocean acidification research, but they are critical components of mortality at all life stages and are of great ecological importance.

The California spiny lobster, *Panulirus interruptus*, has a suite of structural and behavioral defenses to protect them from a wide range of potential predators, including octopus, eels, and large fish. As their name suggests, one of their most overt defenses is the spiny exoskeleton, or cuticle, that protects against attacks from crushing or smashing predators. Yet, this exoskeleton enables a gamut of strategies that the animal can sequentially

employ to avoid harm. While sheltering in cavities, the rostral horns can lock onto the rock roof, making it difficult for predators to extract them (Lindberg, 1955). Spiny lobsters also have long, spiny antennae that they use to push against predators, keeping the bulk of their body a safe distance away. In addition to the essential exoskeletal armor, some crustaceans use other defenses to detect and quickly move away from predators. Before predators get too close, spiny lobsters may anticipate their approach through chemical signals detected during the flicking of their antennules (Zimmer-Faust and Case, 1983). They may also sense injured conspecifics (Shabani et al., 2008), another warning of predators nearby, and move to a safer location or shelter further. If the predator moves too close, a tail-flip escape strategy may be employed, quickly propelling the animal backwards and away from the threat.

At a fundamental level, this impressive suite of predator defense strategies all depend on the versatile exoskeleton, either to physically perform the defense or to anchor the muscles involved. The exoskeleton has four distinguishable layers: the epicuticle, exocuticle, endocuticle, and membranous layer (Roer and Dillaman, 1984). The two thickest layers, the endocuticle and exocuticle, are largely comprised of proteins and sugars laid down in a lamellar structure embedded with minerals such as calcium carbonate and magnesian calcite (Dillaman et al., 2005). Both layer thickness and mineral composition can be modified to produce a spectrum of material properties to support a range of exoskeletal functions (Raabe et al., 2005; Chen et al., 2008) on a micro or nano material scale, which includes hardness (resistance to permanent deformation) and stiffness (resistance to deformation as force is applied), and to the material properties on the scale of entire structures, such as antennae, that can be analyzed for flexural stiffness.

The exoskeleton may be sensitive to the changing ocean carbonate chemistry system in multiple ways. Energy may be diverted to acid-base regulation and away from the costly activities of molting and reforming the exoskeleton, which could reduce the amount of mineral in the exoskeleton, as is evident in some species after exposure to reduced pH conditions (Findlay et al., 2010; Swiney et al., 2015). Yet, crustaceans may be able to convert bicarbonate at the site of calcification, potentially drawing upon bicarbonate accumulated for acid-base regulation (Truchot, 1979; Pane and Barry, 2007; Spicer et al., 2007; Knapp et al., 2015; Whiteley et al., 2018) and thereby maintaining (Findlay et al., 2010; Rankin et al., 2019) or increasing the degree of calcification (McDonald et al., 2009; Taylor et al., 2015). The mineral composition of the crustacean exoskeleton plays an integral role in its various functions by modulating mechanical properties such as hardness and stiffness (Sachs et al., 2006), so altered mineral concentration can have broad ranging effects. The scope of these potential effects is rarely studied, but research so far has revealed complex results. Although a relationship between reduced mineralization and lower material properties is sometimes clear, as in the mermaid's wineglass and some mussels (Newcomb et al., 2015; Duquette et al., 2017), increased calcification seemed to increase brittleness of barnacle shell wall plates (McDonald et al., 2009). In other organisms, material properties remain the same despite changes to mineralization (deVries et al., 2016; Duquette et al., 2017).

Other defense strategies may be impaired as well, as has been evidenced in some phyla. Responses to predator and other chemical cues seem to be impaired across a broad range of fishes under reduced pH conditions, although the exact mechanisms behind the disfunction are not always totally understood (Leduc et al., 2004; Munday et al., 2009; Dixson et al., 2010; Munday et al., 2016; Williams et al., 2019). Escape responses, such as the tail flip

escape performed by shrimp and lobsters, are complex behaviors that require recognition of a threat, energy invested over time in locomotory means such as muscles, and immediately-available energy to perform the quick movement. In other invertebrates, the escape performance has been found to be reduced in king scallops (Schalkhausser et al., 2013; Schalkhausser et al., 2014) and conch snails (Watson et al., 2014).

Juvenile spiny lobsters spend 2-3 years in shallow eelgrass or kelp environments (Engle, 1979), where they must be able to successfully exercise their full range of predator defense strategies while contending with an environment that has diurnal changes in carbonate chemistry conditions (Frieder et al., 2012). In coastal environments, carbonate chemistry variables fluctuate diurnally, tidally, and seasonally (Johnson et al., 2013), producing variable conditions to which organisms in these habitats are subjected. In environments dominated by a large biomass of photosynthetic organisms, such as kelp forests or seagrass meadows, daily ranges of pH may be as great as the decrease in pH expected over the next century, ~0.35 units (Frieder et al., 2012; Challener et al., 2015), or even greater than 1 unit (Semesi et al., 2009), depending on currents, tides, storms, and community composition (Hofmann, 2011; Page et al., 2016; Silbiger and Sorte, 2018). Seawater buffering capacity will decrease as pCO_2 increases, and consequently the magnitude of pH fluctuations will increase as well (Zeebe and Wolf-Gladrow, 2001).

For organisms that inhabit dynamic environments, the exposure to a range of conditions has potentially led to a degree of adaptation that may be beneficial as ocean carbonate chemistry continues to change. A growing but still limited number of studies have imposed fluctuations around low and high pH setpoints and discovered varied responses. Fluctuating conditions may ameliorate some or all of the negative growth and sensory impacts

observed at stable reduced pH in pink salmon (Ou et al., 2015) and coral reef fish, where it is hypothesized to help prevent physiological changes in the brain (Jarrold et al., 2017). *Mytilus edulis* mussels take advantage of higher pH during the day to increase calcification rates, lessening the overall negative impact to calcification (Wahl et al., 2018). Yet, in some organisms, fluctuating pH conditions either have no discernable effect from stable reduced pH conditions (Clark and Gobler, 2016), or they appear to increase stress, producing more negative responses than stable reduced pH conditions alone (Alenius and Munguia, 2012; Mangan et al., 2017; Onitsuka et al., 2017; Johnson et al., 2019). Thus, to establish realistic impacts on organisms, it is important to incorporate the natural fluctuating conditions of their habitat into ocean acidification experiments (Andersson and Mackenzie, 2012; McElhany and Busch, 2013; Andersson et al., 2015).

Here, we exposed juvenile California spiny lobsters (*Panulirus interruptus)* to stable and fluctuating high pCO_2/reduced pH conditions that mimic their current and future habitat to examine their survival, growth, and predator defenses. Specifically, we examined their exoskeleton defenses by analyzing elemental composition (calcification), structure (layer thickness), and material properties (hardness and stiffness) (Fig. 3.1). We also examined behavioral defenses, including antennule flicking rate as an indicator of chemical sensing and the kinematics of the tail flip escape response. We hypothesized that lobsters under low, stable pH conditions would have relatively greater exoskeleton mineralization resulting in altered mechanical properties as well as impaired defensive behaviors. We also hypothesized that fluctuating reduced pH conditions would mitigate the effects of reduced pH by providing a respite from stable reduced conditions.

Methods

Animal collection

Sixty-four juvenile lobsters were collected from offshore La Jolla, San Diego, CA over the course of 6 days in October 2016. Commercial lobster traps were modified with smaller mesh and set at depths of 8.5 to 15.2 m. Lobsters were transported to the experimental aquarium at Scripps Institution of Oceanography (SIO) within 2.5 hours of collection and placed in flow-through seawater pumped from the Scripps Pier, approximately 2 km from the site of collection.

Experimental design

The experimental ocean acidification system consisted of four 81 L header tanks that each received filtered seawater pumped from the SIO pier (3-4m depth, 300m offshore) at ambient pH (7.97 ± 0.03), pCO_2 (464 ± 39 μatm), and salinity (33.4 ± 0.2 PSU) (mean ± s.d. during the experimental period). A mix of chilled and ambient temperature water was fed into the header tanks, which heaters maintained at 16.5 ± 0.6, so despite incoming fluctuations, temperature could be well-controlled. Two 1585 GPH aquarium powerheads were placed in each header tank to ensure adequate mixing.

One header tank was kept at ambient pH to provide the control treatment while the three others were adjusted for high pCO_2/low pH treatments. One treatment was adjusted to a stable pH of 7.7, congruent with current predictions for decreases in global ocean surface pH values of 0.3 pH units (IPCC, 2014). The two other treatments were set to fluctuate around this reduced pH, but to different degrees. The reduced/low fluctuating pH treatment was set to

7.7 ± 0.05 (7.65-7.75) pH units based on published measurements of southern California kelp forest diurnal pH variations, which depend upon tide, season, and weather conditions, but are approximately 0.1 pH units on average (Frieder et al., 2012; Kapsenberg and Hofmann, 2016). The reduced/high fluctuating pH treatment was set to 7.7 ± 0.10 (7.6-7.8) pH units, which mimics future diurnal fluctuations, calculated in CO_2Sys for decreases in buffering capacity and larger pH swings assuming the same autotrophic forcing of DIC (Pierrot et al., 2006). For both of the fluctuating treatments, high pH values were held stable for approximately 10 hours to match daylight (and photosynthesis) hours at the time of the experiment. Nighttime low pH values were held stable for 12 hours. pH was set at a midpoint value for one hour between each of these highs and lows as a transition period.

Experimental pH conditions were achieved and maintained by bubbling 100% CO_2 into the three treatment header tanks and controlled by an Apex Lite aquarium controller and Apex Neptune pH and temperature probes (0.01 pH accuracy; temperature accuracy 0.1°C, Neptune Systems, Morgan Hill, CA, USA). pH and temperature of the header tanks were logged every 10 minutes throughout the duration of the experiment. The Apex pH probes were calibrated prior to the experimental period, but because stability and not accuracy was desired, they were not calibrated again.

Each header tank supplied flow-through seawater separately to 16 experimental tanks (8.4 L) that each contained a single lobster, for a combined total of 64 individuals. Experimental water parameters were gradually altered over the course of three days to minimize potential acute stress. Once the targeted water parameters were reached, the experiment was run for 102 days (11/14/2016-2/23/2017).

Water chemistry

Daily readings of pH and temperature were taken from each lobster tank using a portable probe (HQ40d, probe PHC201, accuracy 0.01 pH, 0.1 temperature, Hach, Loveland, CO, USA) as a method of high-frequency measurements in between carbonate chemistry bottle sample measurements (Fig. 3.2). This probe was calibrated with NBS buffer solutions (Fisher Scientific, Fair Lawn, NJ, USA) approximately every three weeks to control its slow drift. Daily readings were taken at consistent times during the daytime to capture the high value in the fluctuating treatments. Calculated pH from bottle samples (see below) was averaged for each sampling period and used to correct these values to pH_{total}. Each bottle sampling round corresponded to one calibration period of the portable probe.

Nighttime pH was checked using two methods to confirm that stable treatments were indeed constant and that target fluctuations were achieved and consistent. In addition to four probes constantly monitoring and logging header tank pH, two additional Neptune Apex electrodes were rotated between random lobster tanks once per day and recorded pH every 10 minutes over the course of each 24-hour period. Nighttime pH in the fluctuating treatments was recorded to be 0.11 ± 0.02 (n = 54) and 0.21 ± 0.03 (n = 46) pH units lower than daytime pH, consistent with our targeted values. Periodic measurements of nighttime pH with the handheld probe (n=8) were in agreement with the readings of the Apex probes.

In infrequent events (n=7), the pH control system malfunctioned, dropping pH 0.15-1 unit from one to four hours. In these instances, two reduced pH treatments experienced these effects nearly equally, although the reduced/high fluctuating treatment tended to drop 0.1-0.3 pH units lower. In five instances, the power was lost to the system, returning values to ambient conditions for one to fifteen hours. These temporary pH excursions did not appear to

induce animal stress nor were they likely to affect responses that are a function of long-term conditions, e.g. the exoskeleton. Behavioral measurements were not performed during these times. These events are included in treatment averages if they occurred during the time of day when pH was checked. Additionally, for a period of 10 days, a borrowed and old handheld pH probe was used that, despite calibration, was recording consistently high pH values, including in ambient seawater. Because a bottle sample was not taken during its use, these values were not used for calculation of treatment averages. However, treatments were in all likelihood maintained by the control system during this time, evidenced by the stability both before and after this period.

Bottle samples were collected four times from three lobster tanks per treatment over the experimental period in 500 mL Pyrex glass bottles and poisoned with 120 μL of a saturated solution of $HgCl_2$ in accordance with standard operating procedures (Dickson et al., 2007) (Fig. 3.2). These were analyzed for total alkalinity (A_T) by potentiometric acid titration using an 876 Dosimat (Metrohm, Riverview, Florida, USA) and pH electrode (Ecotrode Plus, Metrohm, Riverview, Florida, USA) and for dissolved inorganic carbon (DIC) using an AIRICA system (Marianda, Kiel, Germany) with integrated infrared CO_2 analyzer (Li-COR 7000, Li-COR, Lincoln, Nebraska, USA) (Table 3.1). Certified reference material (CRM) batches 151, 155, and 159 provided by the Dickson laboratory at SIO were used to verify the accuracy and precision to ± 1–4 μmol kg^{-1} for both. Other parameters of the carbonate system were calculated using CO_2Sys 25.06 (Pierrot et al., 2006) (Table 3.1). For calculations, dissociation constants of K_1, K_2 were from (Mehrbach et al., 1973), refit by (Dickson and Millero, 1987). The HSO_4^- constant was from (Dickson, 1990) and the [B]T value was from (Uppström, 1974).

Survival, molting, and growth

Lobsters were fed equal amounts of squid five days per week in excess, with remaining food removed daily. Tanks were checked daily for deaths and molting events; exuviae were promptly removed to prevent fouling and consumption. Growth was recorded at the start and end of the experiment by weighing damp lobsters in air. Carapace length was measured from the notch at the base of the rostral horns to the posterior edge of the carapace at the dorsal midline. Initial size ranged from 43.5 to 58.5 mm carapace length (CL) and 75.4 to 198.2 g. Of the 64 lobsters, 20 were male and 44 were female, and 30% showed at least some physical indications of sexual maturity (e.g., softened sternal plates and enlarged testes identified during dissection). Individuals were assigned to each treatment so that body size and sex were evenly distributed.

Exoskeleton defenses

Cuticle structure and elemental composition

Immediately after the end of the experiment, lobsters were anesthetized but not frozen by placement in a -20°C freezer and then sacrificed by piercing the exoskeleton and tissue between the rostral horns along the midline of the carapace with a ceramic knife. Samples of cuticle were dissected by cutting ~ 0.75 x 0.75 cm^2 around a carapace spine located below the cephalothorax line, 0.5 x 1.5 cm^2 section of the antennae 1 cm above the posterior base of the antennae on the dorsal side, and around the base of the rostral horn. Each cuticle sample was rinsed with DI water and allowed to air dry. Samples were then freeze-fractured with liquid

nitrogen and critical-point dried (AutoSamdri 815 Series A, Tousimis, Rockville, MD, USA) before being mounted on a 90-degree SEM tip and sputter-coated with iridium.

Cross-sections of these cuticle samples were examined with ultra-high-resolution scanning electron microscopy under high vacuum (XL30 SFEG with Sirion column and Apreo LoVac, FEI, Hillsboro, OR, USA with Oxford X-MAX 80 EDS detector, Concord, MA, USA) at 10 or 20 kV. One to two samples each of the carapace spine and antenna from individual lobsters were imaged and measured for the total cuticle thickness (epicuticle, exocuticle, and endocuticle), as well as thickness of the exo- and endocuticle layers. The rostral horn has an unusual structure, consisting of only two layers: an inner region, which we will refer to as the core, and an outer layer that we will refer to as the outer ring (Lowder, unpublished data).

Elemental composition of cuticle samples was measured using energy dispersive x-ray spectroscopy (EDX) with two machines (XL30 SFEG with Sirion column and Apreo LoVac, FEI, Hillsboro, OR, USA with Oxford X-MAX 80 EDS detector, Concord, MA, USA) at 20 kV acceleration voltage. Spectra were taken on the cross- sectional surface of the exocuticle and the endocuticle layers of the carapace spine and antenna base and the core and outer ring of the horn tip. Eleven elements were consistently present in varying amounts: C, N, O, Ca, Mg, Na, Al, P, Si, S, and Cl. The amount of Ca and Mg were expressed as weight percent relative to the other nine elements.

Inductively-coupled plasma mass spectrometry (ICP-MS) was performed in the Scripps Isotope Geochemistry Lab (SIGL) for a precise quantification of elements. The carapace spine was used for nanoindentation tests (below), air-dried, and then trimmed so only the spine remained with no setae, and the abdominal segment was cut as a 1 x 1 cm^2

from the center of the second abdominal segment and air-dried. Samples were weighed and placed in Teflon vials for digestion with 0.5 ml of concentrated Teflon-distilled (TD) nitric acid (HNO_3) on a hotplate at 100°C for >24 h. Samples were dried down and diluted by a factor of 4000 with 2% TD HNO_3 before being transferred to pre-cleaned centrifuge tubes for analysis. Samples were doped with an indium solution to monitor instrumental drift. Measurements were done using a ThermoScientific iCAPq c ICP-MS (Thermo Fisher Scientific GmbH, Bremen, Germany) in standard mode. Masses of Mg and Ca were sequentially measured for 30 ratios, resulting in internal precision of <2% (2 s.d.). Elements were corrected for total mole fraction. Total procedural blanks represented <0.3% of the measurement for Mg and Ca. Raw data were corrected offline for instrument background and drift. Samples were bracketed by internal standards of crab carapace (n=3), which allowed for calculation of absolute values. The standards yielded external precision of better than 1% for Mg and Ca (2 s.d.).We targeted the following isotopes: ^{10}B, ^{25}Mg, ^{26}M, ^{27}Al, ^{29}Si, ^{31}P, ^{43}Ca, ^{48}Ca, ^{54}Fe, ^{57}Fe, ^{65}Cu, ^{66}Zn, ^{86}Sr, ^{111}Cd, ^{137}Ba, ^{208}Pb, and ^{238}U. A weighted average based on the natural abundance of isotopes was calculated for Ca and Mg and used in analyses.

Material properties

The carapace spine and rostral horn tip were tested for hardness and stiffness using a nanoindentation materials testing machine (Nano Hardness Tester, Nanovea, Irvine, CA, USA) equipped with a Berkovich tip. Fresh samples (<12 hours, except for two samples tested within 24 hours) were kept hydrated in seawater until testing. Samples were secured to an aluminum block with cyanoacrylate glue such that the outer surface was facing up. Indentations were performed by applying a load of 40 mN to the outer surface of the sample

at loading and unloading rates of 80 mN/min, and 30 sec hold for creep. At least three indents were taken per sample.

Antenna stiffness

One antenna was removed from each lobster at the base (first segment above the antennae knuckle). The proximal 5 mm of the antennal base was embedded in epoxy (EpoxiCure, Buehler, Lake Bluff, IL, USA) and allowed to cure overnight. Antennae were covered with seawater-soaked paper towels to remain hydrated until testing. The embedded ends of the antennae were clamped in a universal materials testing machine (E1000, 250N load cell, Instron, Norwood, MA, USA) such that the antennae extended laterally. A force was applied at a rate of 20 mm/min to two locations on the antennae, one at 1/3 of the total antenna length ("proximal") and one at 2/3 of the total antenna length ("distal"), until a displacement of 10% of total antenna length was reached. The stiffer proximal region of the antenna has a thicker ovular cross section than the distal location, and it lies directly over the carapace when the lobster raises its antennae in a defensive position, so it is believed to be the primary location where force is applied by predators. The distal end appears to be more flexible to avoid breakage. Flexural stiffness, *EI*, in N was calculated as:

$$EI = \frac{F_{max} \times antennal\ length^3}{3 \times deflection_{max} \times 0.001}$$

Chemical sensing

Prior to the end of the experiment, on experimental days 86-87, the chemical sensing ability of lobsters from each treatment was tested. California spiny lobsters modify their behavior in response to cues from food, live conspecifics, and dead conspecifics in part by the flicking of their antennules (Zimmer-Faust and Case, 1983; Zimmer-Faust et al., 1985). To measure the detection of a chemical cue introduced to their environment, lobsters were exposed to mussel tissue, a common prey item. To control for the possibility of increased response due to a sudden influx of water, lobsters were also exposed to a dose of their treatment water administered in the same manner as the mussel cue. These cues were given to lobsters on separate days and in randomized order. Lobsters were not fed for 48 hours prior to the introduction of the mussel cue to ensure food cues were not already present.

Just prior to each test, flow was halted to a lobster's tank and a 0.25" diameter tube with a funnel used to introduce the water or mussel cue was secured into the tank approximately 5-10 cm from the antennules in front of the lobster. Using a video camera mounted above the tanks (Handicam HDR-CX405, Sony, New York, NY, USA), lobsters were filmed for one minute to establish a baseline of antennal flicking and movements. After this period, half of the lobsters from each treatment received a control dose of water (44 mL of their respective treatment water) and half received a dose of mussel cue (4 mL of fresh, homogenized mussel tissue washed down immediately by 40 mL of treatment water). This dose of cue resulted in a concentration of 0.5 g/L, which is 50,000,000x the concentration known to illicit increased antennule flicking in this species and 500,000x the concentration sufficient to stimulate leg movements that are as indication of prey searching behavior in this

species (Zimmer-Faust and Case, 1983). Lobsters were filmed for a subsequent three minutes following administration of the cue. Lobsters were tested again the following day with the cue treatments reversed; lobsters that received the water cue on the first day received the mussel cue on the second day and vice versa. Antennule flicks, defined as a rapid downstroke of either antennule, were counted from the recorded videos by three people. Specifically, the number of antennule flicks were counted for one minute just prior to the addition of a cue and for one minute beginning ten seconds after entire cue was administered.

Escape response

The kinematics of the tail-flip escape response were measured from each lobster prior to the end of the experiment, on experimental days 89-90. Individual lobsters were placed at one end of a clear acrylic tank (91 x 31.5 x 31.5 cm) filled with their respective treatment water. The escape response, known as a tail-flip, was stimulated by startling it with a quick opening hand gesture approximately 10 cm away from their eyes. A high-speed video camera (Phantom Miro M310, Vision Research AMETEK, Wayne, NJ, USA) was positioned so that it captured the lateral view of the first 1-2 tail flips at 1000 frames per second. Each lobster was startled three to seven times consecutively, and water was replaced after four animals from the same treatment were run. Only escape responses where lobsters were not off-axis, did not push from the tank floor, and did not break the water surface were used for analysis. One high-speed video sequence of the escape response was analyzed for each lobster using high speed camera software (Phantom Video Player, v2.8.761.0, Vision Research, Wayne, NJ, USA). Three consistent landmark points were digitized on each lobster. The first point was a small spine on the carapace, near the lateral midpoint and adjacent to the posterior end of the

carapace. The second point was the abdominal pleurite spine of the fifth segment. The third digitized point was on the prominent eyespot located below the eyes. The initiation of a tail flip was defined as the start of the decrease in distance between the abdominal point and the carapace point. A tail flexion began at the initiation point and ended when the distance between the abdominal and carapace points reached a minimum, and this period was used to calculate both distance and duration of the flip. The point of maximum tail flexion was considered as the end of the tail flip. Lobsters may either glide in this position of maximum tail flexion or immediately unfurl the abdomen for a subsequent tail flip.

The carapace point was used to calculate the velocity and acceleration of the lobster through at least one, but up to three, subsequent tail flips. Velocity and acceleration data were smoothed with a running average using a subset of 15 frames before and 15 frames after the value (each parameter at each point is from an average of 31 milliseconds). We recorded the maximum velocity achieved over each tail flip as well as the distance and duration of each flip from the initiation of the tail flip until maximum flexion.

Abdominal muscle

The tail flip movement is primarily carried out by flexion of the abdominal muscle mass. We examined the abdominal muscle after the end of the experiment to determine if any significant changes in mass occurred that might affect the escape response. First, the abdomen was cut transversely between the third and fourth segments, which is in the middle of the abdomen at the widest section. The tail section was unflexed and measurements of the height and width of the cross section of this muscle were taken using calipers from the edges of the

epidermis under the cuticle. The muscle is ovular in cross-section; therefore, we estimated muscle cross-sectional area as an oval. The entire wet abdominal muscle was carefully dissected from the exoskeleton and weighed on a balance accurate to 0.01 grams.

Statistics

All analyses were carried out in R version 3.5.1 (Kassambara, 2018; R Core Team, 2018) and associated packages (Wickham, 2007; Graves et al., 2012; Auguie, 2016; Wickham, 2016a; Wickham et al., 2016; Wickham, 2017). The small number of animals that had molted during the experiment were excluded from analyses of exoskeletal characteristics. We tested survival, growth, elemental, thickness, material properties, flexural stiffness, and kinematic data for normality and homogeneity of variances with the Shapiro-Wilk test and Bartlett's test. If data met these conditions, we compared metrics across treatments using one-way ANOVAs and followed with Tukey's Honest Significant Difference test if appropriate. Otherwise, the Kruskal-Wallis with Dunn's test or Welch's corrected ANOVA with Games-Howell post-hoc test was employed. Abdominal muscle mass and carapace length ANOVA residuals were checked for test assumptions visually and with the Shapiro-Wilks test, then log-transformed to meet assumptions. $\alpha = 0.05$ with the exception of elemental data, where we employed a Bonferroni correction for repeated measures.

Some cuticle samples had one or two material properties tests that resulted in unusually high values for crustacean cuticle and were likely due to methodologic error. As such, material property outliers of each treatment were calculated and removed via the Tukey "fence" or "boxplot rules" method of $Q_3 + 1.5 \times IQR$, where Q_3 is the third quartile and IQR is

the interquartile range from the first to the third quartile (Tukey, 1977). The lower "fence" was also calculated, but was always below zero. This method identified outliers ≥ 13.4 GPA in stiffness for the horn and ≥13.1 GPa for the carapace spine. Hardness outliers were ≥ 0.49 GPa for the horn and ≥ 0.52 GPa for the carapace spine.

The number of antennule flicks before and after cue addition was analyzed as a repeated measures ANCOVA through the framework of a linear mixed effects model (lme4 package) (Bates et al., 2007). Treatment and liquid added were fixed factors, flicking rate prior to liquid addition was a covariate and individual lobster was a random effect, as each lobster was tested with each cue. The model was fit with maximum likelihood tests and the significance of fixed factors was evaluated with a type II ANOVA using Satterthwaite's method. Significant differences between factor levels were determined with Tukey's post hoc tests using the Kenward-Roger method for degrees of freedom through package emmeans (Lenth, 2018). Test assumptions were evaluated visually through plots of residuals.

Results

Survival, molting, and growth

All lobsters survived the experimental period and appeared healthy at its conclusion. Molting only occurred in nine out of the sixty-four animals (n=4 in ambient/stable; n=1 in reduced/stable pH; n=3 in reduced/low fluctuating; n=1 in reduced/high fluctuating treatment).

Lobsters that molted grew an average of 4.18 ± 3.99% or 5.88 ± 3.11 g, which did not differ between lobsters in ambient/stable and reduced/low fluctuating treatments (the only

treatments where more than one animal molted) (Student's t-test, t =-0.427, df=3.684, p=0.693). Lobsters that molted increased in carapace length by 2.00 ± 1.31% (~1 mm) and this increase did not differ between lobsters in ambient/stable and reduced/low fluctuating treatments (t =-0.204, df=2.938, p=0.852). Animals that did not molt showed no differences in percent change in mass (ANOVA, $F_{3,49}$=0.267, p=0.849), and lost an average of 0.71 ± 0.99% of their mass, or 0.06 ± 0.37 g.

Cuticle structure

There were no significant differences in total cuticle thickness of the carapace (664 ± 90 µm) (ANOVA: $F_{3,48}$=0.870, p=0.463) and antennae (517 ± 59 µm) (ANOVA: $F_{3,51}$=2.006, p =0.125) among treatments (Fig. 3.3). Lobsters that molted tended to have thicker exoskeletons (carapace: 851 ± 108 µm; antenna: 617 ± 43 µm), although no statistical analyses were performed due to low sample size.

Cuticle elemental composition

Elemental data from the XL30 SFEG EDX were inconsistent with that of the other instrument used as well as with previous data on lobster cuticle (Lowder et al, unpublished), and so were excluded from analysis. The remaining data revealed no significant differences in % wt Ca in either of the carapace layers (Fig. 3.4A; exocuticle: Kruskal-Wallis, χ^2 = 1.355, df=3, p = 0.716; endocuticle: ANOVA, $F_{3,25}$ = 1.081, p = 0.375), horn layers (Fig. 3.4B; outer ring: Kruskal-Wallis, χ^2 = 0.453, df=3, p = 0.929; core: ANOVA, $F_{3,21}$ = 0.04, p = 0.989), and antenna layers (Fig. 3.4C; exocuticle: Kruskal-Wallis, χ^2 = 3.494, df=3, p = 0.322;

endocuticle: ANOVA, $F_{3,25} = 0.658$, $p = 0.585$). Ca % wt averaged over both cuticle layers for the antenna was 23.1 ± 8.5% in the ambient/stable, 18.4 ± 7.8% in the reduced/stable, 22.7 ± 10.9% in the reduced/low fluctuating, and 25.4 ± 9.2% in the reduced/high fluctuating treatments. They were 22.9 ± 8.9% in the ambient/stable, 27.6 ± 9.6% in the reduced/stable, 22.3 ± 7.1% in the reduced/low fluctuating, and 23.0 ± 6.4% in the reduced/high fluctuating treatments for the carapace.

There were also no significant differences in % wt Mg in either of the carapace layers (Fig. 3.4D; exocuticle: Welch's ANOVA, $F_{3,11.83} = 2.103$, $p = 0.154$; endocuticle: Kruskal-Wallis, $\chi^2 = 1.266$, df=3, $p = 0.737$), horn layers (Fig. 3.3E; outer ring: Kruskal-Wallis, $\chi^2 = 0.754$, df=3, $p = 0.861$; core: Kruskal-Wallis, $\chi^2 = 2.559$, df=3, $p = 0.465$), and antenna layers (Fig. 3.3F; exocuticle: Kruskal-Wallis, $\chi^2 = 5.986$, df=3, $p = 0.112$; endocuticle: Kruskal-Wallis, $\chi^2 = 0.968$, df=3, $p = 0.809$). Mg % wt in the antenna was 1.3 ± 0.4% in the ambient/stable, 1.1 ± 0.2% reduced/stable, 1.3 ± 0.3% in the reduced/low fluctuating, and 1.3 ± 0.3% in the reduced/high fluctuating treatments and 1.5 ± 0.4% in the ambient/stable, 1.6 ± 0.3% reduced/stable, 1.7 ± 0.2% in the reduced/low fluctuating, and 1.3 ± 0.3% in the reduced/high fluctuating treatments in the carapace.

Elemental analysis of the carapace using ICP-MS contrasted with the results obtained from the EDX analysis. There were significant differences in calcium and magnesium in the carapace across treatments (calcium: ANOVA, $F_{3,51} = 4.313$, $p = 0.009$; magnesium: Kruskal-Wallis, $\chi^2 = 15.184$, df=3, $p = 0.002$; Fig. 3.5A,C). Calcium was slightly lower in the reduced/high fluctuating (5.62 ± 0.25 μmol /mg sample) than the reduced/stable (5.95 ± 0.39 μmol /mg sample) (Tukey HSD, $p = 0.043$) treatment. The reduced/high fluctuating treatment

was significantly decreased by 7% compared to the ambient/stable conditions (6.04 ± 0.36 μmol /mg sample) (Tukey HSD, $p = 0.010$). Reduced/low fluctuating conditions averaged 5.78 ± 0.31 μmol /mg sample.

Carapace magnesium was significantly lower in the reduced/high fluctuating treatment (0.41 ± 0.02 μmol /mg sample) in comparison to both ambient/stable (0.47 ± 0.04 μmol /mg sample) and the reduced/stable treatments (0.44 ± 0.04 μmol /mg sample) (Tukey HSD, $p \leq 0.006$; Fig. 3.5C). The reduced/low fluctuating treatment (0.43 ± 0.04 μmol /mg sample) was also significantly decreased by 8% compared to the ambient/stable treatment (Dunn's test, $p = 0.011$). Magnesium tended to be lower in the reduced/stable treatment than in ambient/stable (Dunn's test, $p = 0.047$), and the two fluctuating treatments showed slightly different concentrations (Dunn's test, $p = 0.042$), although these trends were not statistically significant, as the Bonferroni correction for repeated measures was applied.

In the abdominal segment, there were no significant differences in the calcium (ANOVA: $F_{3,51}=2.21$, p=0.098; Fig. 3.5B), and magnesium (ANOVA: $F_{3,51}=1.36$, p=0.266; Fig 3.5D) concentrations between treatments (in the order of ambient/stable, reduced/stable, reduced/low fluctuating, and reduced/high fluctuating treatments: calcium: 4.65 ± 0.13, 4.57 ± 0.18, 4.48 ± 0.10, 4.59 ± 0.21 μmol /mg sample; magnesium: 0.44 ± 0.02, 0.42 ± 0.03, 0.44 ± 0.03, 0.42 ± 0.03 μmol /mg sample).

Cuticle material properties

The carapace spine and rostral horn responded differently to treatment conditions. The carapace spine did not show a significant difference in hardness (ANOVA: $F_{3,37}$ =2.708,

p=0.06; Fig. 3.6A) or stiffness (ANOVA: $F_{3,37} = 1.376$, $p = 0.27$; Fig. 3.6B) across treatments. In general, lobsters exposed to both reduced fluctuating pH treatments (reduced/low fluctuating: 0.23 ± 0.11 GPa hardness, 11.37 ± 5.26 GPa stiffness; reduced/high fluctuating: 0.24 ± 0.09 GPa, 11.45 ± 3.96 GPa) had a 28% lower hardness when compared to lobsters in stable pH treatments, which had slightly higher hardness and stiffness (ambient/stable: 0.32 ± 0.11 GPa hardness, 15.60 ± 5.25 GPa stiffness; reduced/stable: 0.32 ± 0.13 GPa, 13.89 ± 6.07 GPa).

The horns differed significantly in hardness among treatments (ANOVA: $F_{3,36} = 7.307$, $p<0.001$) (Fig. 3.6B). Horns from lobsters exposed to both of the stable pH treatments were statistically the same (ambient/stable: 0.33 ± 0.04 GPa; reduced/stable: 0.36 ± 0.05; $p=0.738$), as were those exposed to both of the fluctuating conditions (reduced/low fluctuating: 0.30 ± 0.04 GPa; reduced/high fluctuating: 0.28 ± 0.06 GPa, $p = 0.999$). However, horn samples from the reduced/high fluctuating treatment were significantly less hard than those from either of the stable pH treatments by 15 - 22% ($p \leq 0.045$). The reduced/low fluctuating treatment horns were lower but not significantly different from those in the ambient/stable pH treatment ($p=0.050$), although they were significantly lower than those in reduced/stable pH treatment ($p=0.004$). There were no significant differences in horn stiffness among the treatments (ANOVA: $F_{3,36} = 0.077$, $p = 0.972$) (Fig. 3.6D). Stiffness was 6.49 ± 2.22 GPa in the ambient/stable, 7.44 ± 1.88 GPa in the reduced/stable, 7.37 ± 2.23 GPa in the reduced/low fluctuating, and 7.14 ± 1.93 GPa in the reduced/high fluctuating treatments.

Antenna stiffness

Mean antennal flexural stiffness (*EI*) at the distal location did not differ among lobsters in any treatments (Kruskal-Wallis rank sum test, χ^2 =3.52, df=3, p=0.318) (mean ± sd: ambient/stable: 0.004 ± 0.002 Nm^2; reduced/stable: 0.003 ± 0.002 Nm^2; reduced/low fluctuating: 0.003 ± 0.001 Nm^2; reduced/high fluctuating: 0.004 ± 0.002 Nm^2) (Fig. 3.7). At the proximal location, *EI* was significantly lower in lobsters exposed to reduced/stable pH treatments than lobsters exposed to reduced/high fluctuating pH (Welch's ANOVA: $F_{3,22.55}$= 3.15, p = 0.045; Games-Howell posthoc p = 0.035). There were no significant differences among the other treatments ($p \geq 0.20$), although *EI* was slightly lower in antennae from the reduced/stable and reduced/low fluctuating treatment than those in ambient conditions (mean ± sd: ambient/stable: 0.023 ± 0.012 Nm^2; reduced/stable: 0.018 ± 0.004 Nm^2; reduced/low fluctuating: 0.020 ± 0.004 Nm^2; reduced/high fluctuating: 0.026 ± 0.010 Nm^2).

Chemical sensing

The best-fit model of antennule flicking did not include any interactions between factors. There was a significant effect of the type of liquid introduced on the antennule flicking rate ($F_{1,50.2}$ = 18.25, p<0.001) (Fig. 3.8). Mussel cue stimulated an increased flicking rate of 47 flicks min^{-1}, demonstrating that lobsters across all treatments responded to the prey cue. The rate of flicking prior to the addition of any liquid also significantly influenced flicking rate after liquid was added ($F_{1,80.1}$ = 48.05, p<0.001). There was no significant effect of treatment on flicking rate after either liquid was added ($F_{3,45.1}$ = 0.83, p=0.486), although

lobsters in the reduced/stable pH treatment flicked 17-23 times less per minute than lobsters in other conditions.

Escape response: kinematics

There were no significant differences across treatments in the maximum velocity that lobsters reached on their first or second tail flips (Flip 1, ANOVA: $F_{3,55} = 0.877$, p=0.46; Flip 2, ANOVA: $F_{3,20} = 0.529$, p=0.667; Fig. 3.9A). The second tail flip is typically faster than the first (Paired t-test, df=23, t=-3.64, p=0.001), increasing from 1.39 ± 0.26 m/s to 1.54 ± 0.32 ms^{-1}.

The duration of both the first and second tail flips was also not different among treatments (Flip 1, ANOVA: $F_{3,48} = 0.736$, p=0.536; Flip 2, ANOVA: $F_{3,22} = 3.059$, p=0.050), although the second flip, from the start of abdominal flexion to maximum flexion, was 6-22 ms shorter in lobsters from reduced/high fluctuating pH conditions (Fig. 3.9B). The second tail flip, lasting 94 ± 20 ms, was significantly longer than the first tail flip of 71 ± 15 ms (Paired t-test, df=25, t=5.424, p<0.001).

The distance covered per tail flip also did not differ among treatments (Flip 1, ANOVA: $F_{3,48} = 1.514$, p=0.223; Flip 2, ANOVA: $F_{3,22} = 0.183$, p=0.907; Fig. 3.9C). The distances covered by the first and second tail flips were not different, averaging 8.7 ± 2.0 cm.

Escape response: abdominal muscle mass

The mass of the abdominal muscle was 30.1 ± 6.3 g in ambient/stable conditions, 27.5 ± 6.0 g in the reduced/stable treatment, 30.2 ± 6.6 g in the reduced/low fluctuating treatment, and 32.0 ± 9.0 g in the reduced/high fluctuating pH conditions. Mass significantly increased with carapace length of the lobster (ANCOVA: F=145.00, df=1, p<0.001), but there was no significant effect of treatment on this relationship (F=0.740, df=3, p=0.532; Fig. 3.10A). There was no interaction between carapace length and treatment.

The cross-sectional (CS) area of the middle of the abdominal muscle mass was 473 ± 68 mm^2 in ambient/stable conditions, 455 ± 66 mm^2 in the reduced/stable treatment, and 481 ± 75 mm^2 and 487 ± 90 mm^2 in the reduced/low fluctuating and reduced/high fluctuating pH conditions, respectively. The cross-sectional area significantly increased with carapace length (ANCOVA: F=154.491, df=1, p<0.001). There was no significant effect of treatment on this relationship (F=0.045, df=3, p=0.979; Fig. 3.10B), and there was no interaction between carapace length and treatment.

Discussion

Survival and growth

All lobsters survived the three-month exposure to reduced pH conditions, indicating no pH-induced mortality. This is in contrast to other experiments with juvenile crustaceans, such as post-settlement juvenile *Homarus gammarus*, the European lobster. Within a five-week exposure period a pH reduction of 0.4 units, survival was reduced to approximately 83% of that in ambient conditions (Small et al., 2016). This mortality was linked to frequent

molt-related deaths (Small et al., 2016). In early juvenile American lobsters (*Homarus americanus*), survival also decreased with reduced pH and occurred around molting events (Menu-Courey et al., 2018). In this study, too few spiny lobster juveniles molted (n=1-4/treatment) to ascertain impacts of pH on molt-related deaths, but none of the molts were fatal.

The two metrics of growth studied here, carapace length and mass, reflect different aspects of growth. Carapace length changes only after molting, which is a complex, hormone-induced process that may be performed not only to accommodate growth of new tissue but also to replace lost appendages or facilitate mating. Neither metric of growth increased for lobsters in our study, including those that molted, although we anticipated growth from lobsters in ambient conditions. Early juvenile *H. gammarus*, which were approximately three or four years younger than the spiny lobsters used here, grew ~5% in wet body mass in just five weeks, and this growth was not affected by pH conditions (Small et al., 2016). In juvenile American lobsters, a reduction of 0.6 pH units was associated with lower growth in length and mass, while an intermediate decrease of 0.3 pH units was sufficient to increase the intermolt period significantly (McLean et al., 2018). While squid was provided in excess and eaten readily, the natural diet of California spiny lobsters is more varied. Mussels, a targeted source of food (Robles, 1987), provide more energy for growth over metabolism than squid (Díaz-Iglesias et al., 2011). Nevertheless, we observed no loss in body mass, which suggests that animals were not food limited. Lobsters across all treatments maintained their mass despite the likely metabolic cost of additional acid-base regulation for in high pCO_2 conditions.

PREDATOR DEFENSES

Predation is thought to be the largest source of mortality for juvenile *P. interruptus* until they reach sexual maturity at four to five years of age and are at a size refuge against most predators (Engle, 1979). Despite the need to examine defense functionalities to fully understand the future impact of ocean acidification in the environment, they are rarely studied. Here, juvenile California spiny lobsters survived exposure to high pCO_2 conditions but those in fluctuating pH conditions displayed some negative sublethal effects that may hamper their ability to successfully defend themselves against predators in future oceans. Juvenile California spiny lobster defenses were resilient in some aspects, but were negatively impacted by ocean acidification-like conditions in others. Interestingly, the hardness of the cuticle was affected differently in the two structures studied, highlighting the importance of studying multiple regions of the body to draw overall conclusions.

EXOSKELETAL DEFENSES

While the postmolt stage of the molt cycle is when the most significant impacts would likely occur, as the formation of the new cuticle and mineralization is energetically-costly, intermolt periods are the longest stage. Commonly, individuals in OA experiments are not sampled just after molting, perhaps confounding changes in mineral content that are believed to materialize during cuticle reformation with changes that actually occur through the intermolt period. The 3 month duration of this study, in concurrence with the longer intermolt period of this juvenile lobsters than many other crustaceans studied under OA-like conditions,

allowed a closer examination of potential changes to many aspects of the cuticle between molting events.

Ultrastructure

Thickness of the antennal and carapace exoskeleton was not different among treatments, which is not unexpected for the lobsters that did not molt. Crustaceans typically do not show degradation of the cuticle under OA conditions, except for one study where shrimp antennae were shortened (Kurihara et al., 2008). This is because the bulk of the cuticle is comprised of sugars and proteins in the form of rotating lamellae (Roer and Dillaman, 1984), components that remain intact when cuticle is decalcified in the laboratory for other studies. The small subset of lobsters that did molt had slightly thicker cuticles, but relative thickness was the same across all treatments. Examination of the scaling of cuticle thickness might reveal that juvenile lobsters have relatively thicker exoskeletal armor that would enhance their protection against greater predator threats. California spiny lobsters were able to maintain relative cuticle thickness through the intermolt period despite decreases in pH.

Mineralization

It is generally thought that mineral content during the intermolt period is stable, only added to the newly-formed cuticle after molting and potentially drawn away to be stored in gastroliths prior to molting again (Shechter et al., 2008). Thus, most studies of crustaceans in OA-like conditions have examined mineral content after at least one cycle of molting in

reduced pH conditions. For lobsters exposed to reduced pH conditions over the intermolt period, we did not find differences in Ca and Mg of the carapace, antennae, and horn core using EDX, while ICP-MS analysis revealed a significant decrease in both calcium and magnesium to the carapace of intermolt lobsters in reduced/ high fluctuating pH conditions. There was no similar difference in the abdominal segment. While EDX provides a valuable semi-quantitative and spatial analysis of elements across the cross-sectional surface of the cuticle, ICP-MS provides a precise quantification of elements present in the entire cuticle sample.

Crustaceans use bicarbonate to regulate internal acid-base chemistry under external high pCO_2 conditions and the carbonate minerals in the cuticle can be one source of the ion (Henry et al., 1981). A significant decrease in calcium concentration in the carapace was only found in the reduced/high fluctuating treatment, potentially indicating that the lowest pH values of the experiment reached in that treatment at night (7.57) may have triggered calcium carbonate dissolution from the carapace to use for buffering. Magnesium concentration showed significant decreases from ambient conditions in all three reduced pH treatments. Magnesium is likely in the form of magnesian calcite, a more soluble form of calcite, and may have been drawn out first (Davis et al., 2000).

The decrease in mineralization to the carapace, but not the abdominal segment, may reflect differences in the function and construction of these structures. The abdominal cuticle primarily acts as the skeleton for the muscles that control the rapid tail flip escape response and is generally hidden from predators when lobsters are exhibiting their typical sheltering behavior. In contrast, the carapace acts as armor against crushing predators, such as California

sheephead, and is more heavily mineralized than the abdominal segment. The higher concentration of mineral as calcium carbonate and magnesian calcite in the carapace may have made it more favorable to draw from under reduced pH conditions. Thus, there is evidence that exoskeletal regions are differentially affected by environmental pH conditions and that structures with greater mineral availability, and which benefit the most from the hardness that mineralization provides, may be more vulnerable to losing it in high pCO_2 water conditions.

In other juvenile crustaceans, mineralization is often not affected by exposure to pH conditions expected within the next century. For example, there was no change in either Mg or Ca at moderate (0.25 pH unit) decreases in pH for the early juvenile stage of *H. americanus* after 5 weeks of exposure (Menu-Courey et al., 2018). In juvenile blue swimming crabs and hermit crabs exposed to reduced pH conditions (without fully quantifying the carbonate chemistry, there were no effects on Ca content in either but small increases in Mg in hermit crabs (Glandon et al., 2018; Ragagnin et al., 2018). The above results were all found in animals that had molted during the experiment, but in *Homarus gammarus* that didn't molt there was no change in Mg and Ca after just five weeks of exposure to a 0.4 unit decrease in pH (Small et al., 2016), although longer-term exposure might induce detectable changes.

Material properties

Among mineralized organisms, changes to calcium and magnesium after exposure to high pCO_2 are thought to belie changes to the mechanical function of calcified structures, but this is not often tested. In one study, increases to Mg content in mantis shrimp as a result of

ocean acidification-like conditions did not result in significant changes to the hardness or stiffness of the cuticle (deVries et al., 2016). It is likely that changes to mineralization observed under ocean acidification-like conditions did not reach a threshold sufficient to alter material function. Alternatively, in some studies, material properties are affected, resulting in brittle and less stiff regions of mussel shells (Fitzer et al., 2015) and reduced hardness of blue king crab chelae (Coffey et al., 2017), but these responses were not linked to a specific change in composition or structure. Here, we found that small, yet statistically-significant, decreases in calcium in the carapace under reduced pH with high fluctuations did not result in significant changes to the material properties, although hardness was on average decreased by 28%. A direct relationship between compositional changes under ocean acidification-like conditions and material properties has not been consistently identified, and the perceived implications of observed changes to mineralization should be tested when possible.

The outer layer of the horn is poorly mineralized in comparison to typical crustacean cuticle, and is comprised of just 1.4% Ca and 0.3% Mg. Hardness of the outer horn layer was significantly lower (15%) when lobsters were exposed to reduced/high fluctuating pH conditions. We could not separate the horn layers for precise analysis of their elemental composition with ICP-MS, and it is possible EDX did not detect changes to mineralization that may have occurred. The horns are primarily used to help lock threatened lobsters into tight underhangs, where they function as an anchor against the rock. High amounts of halogens are present in the outer ring (Lowder, unpublished data) and this composition is also found in the dactyl tips of crabs who scrape algae from rocks (Cribb et al., 2009). The replacement of calcium carbonate with halogens provides structures with greater toughness rather than hardness, which is beneficial for avoiding wear and breakage on rocky surfaces

(Cribb et al., 2009; Schofield et al., 2009). This would be functionally important for the rostral horns that must lodge into the rocky underhangs of their shelter. It is interesting though that horn hardness was affected by reduced pH conditions despite its uncalcified state, hinting at a potentially complex interplay of elements under different ocean carbon chemistry parameters.

Flexural stiffness

The antennae are a primary defense against near-range predators, used by lobsters to push away potential threats and maintain their distance (Spanier and Zimmer-Faust, 1988). Sufficient flexural stiffness of the antennae is necessary for lobsters to hold predators at bay, and their resistance to bending was unaffected by reduced pH conditions.

BEHAVIORAL DEFENSES

Chemosensing

Lobsters in all treatments were able to distinguish between the control liquid added to their tanks and the mussel slurry, an expected response as the cue was many orders of magnitude greater than the prey concentration that induces antennule flicking and prey searching behavior in this species (Zimmer-Faust and Case, 1983). Additionally, the mussel slurry slightly clouded the seawater, adding a visual signal that, while not likely linked to the presence of mussels, may have evoked a response from these lobsters that can use vision to locate prey (Lindberg, 1955). There was no difference in the response to the prey cue among

the treatments, as measured by antennule flick rates, indicating that the complex set of pathways for detecting, processing, and acting upon the cue were not affected by the reduced pH conditions used in this study. There are several proposed mechanisms that may, either singly or in tandem, hinder cue reception or response behavior under reduced pH conditions. The chemistry of the cue may be altered via protonation with the increased concentration of hydrogen ions, which has been implicated in reducing the response to cues at pH 7.7 in *Carcinus maenus* crabs (Roggatz et al., 2016). Alternatively, sensing apparatus may be physically damaged. The thin cuticle on spiny lobster aesthetasc sensilla functions only due to limited permeability of molecules (Grünert and Ache, 1988; Derby et al., 1997). There is not enough known about the mineralogical composition of these structures to determine their vulnerability to dissolution, but pH-related changes to the structure may block molecules that are normally received for signaling or allow permeation of unimportant molecules that may overwhelm other cues.

High pCO_2 conditions may also impact the neurochemistry of marine organisms and is becoming an increasingly-documented effect in fish. At pH 7.8, larval clownfish demonstrate the loss of the ability to distinguish between positive homing and parental cues and irrelevant homing and predator cues, spending increased time in the latter cues that are normally avoided (Munday et al., 2009; Dixson et al., 2010). Interestingly, the response is sensitive to different levels of pH reduction; at pH 7.6, larval clownfish fail to respond to any cue presented. In ocean-phase coho salmon, a reduction in this type of beneficial avoidance behavior at reduced pH was linked to disruption of neural signaling in the olfactory bulb (Williams et al., 2019). If any one of these pathways are affected by reduced pH conditions, a decrease in outward recognition of cues may be observed. Impaired chemoreception abilities

have been found in crustaceans ranging from a marine hermit crab and amphipod to a freshwater crayfish, as manifested in a reduction in antennal flicking (Allison et al., 1992; Ben-Horin, 2009; de la Haye et al., 2011; de la Haye et al., 2012; Kim et al., 2015), loss of association with preferred substrate (Smith et al., 2017), increased foraging time (Wu et al., 2017), and latency in successful mate-tracking (Borges et al., 2018). Florida spiny lobsters (*Panulirus argus)* exposed to short term reductions in pH (decrease of 0.45 pH units) showed a nonsignificant but approximately 50% reduction in baseline antennule flicking with no stimulus, and rather than shelter with other healthy individuals, they sheltered more frequently with individuals diseased with PaV1 (Ross and Behringer, 2019).

Here, we have found no evidence of altered chemosensory abilities. Possibly, the concentration of the cue was great enough to overwhelm any small sensitivities of the chemosensory mechanisms. Additionally, the composition of complex cues such as homogenized mussel tissue and the diversity of other prey scents that generalized predators such as spiny lobsters must recognize may allow them to still sense some chemicals, even if part of the cue is altered by a reaction with $[H^+]$. We did observe a small (~20 flicks min^{-1}) and insignificant decrease in flicking rate for lobsters exposed to reduced/stable conditions, which, due to the daytime highs in the fluctuating conditions, was at the lowest pH (7.65) during the time of testing. Additional decreases in pH may illicit significant reductions in responses, but juveniles' chemosensory abilities appear resilient to the decreases in pH expected by the year 2100.

Kinematics

There was no evidence that reduced pH conditions affect the kinematics of the tail-flip escape response. Lobsters exposed to reduced pH conditions reached the same maximum velocities and covered the same distances in the same amount of time as lobsters exposed to ambient conditions. The tail-flip is a complex escape response that requires sufficient abdominal muscle power, the ability of lobster to recognize the threat of the stimulus in front of them, and enough energy available to perform the energy-intensive flexion. An examination of the abdominal muscle mass and cross-sectional area did not reveal any differences across treatments that would contribute to potential changes in power for the tail-flip, confirming that there are no apparent impacts of medium-term reduced pH conditions on the integrity of the abdominal muscle, which is the largest muscular region in the body.

In juvenile lobsters, the tail flip escape response is readily employed when threatened, especially during the postmolt stage even though exoskeletal armor is not fully-functional (Cromarty et al., 1991). The first tail-flip acts as the power-stroke to gain immediate distance from a predator about to strike, but the subsequent tail flips are also important for keeping distance from the predation threat. Here, we primarily studied the power flip and, when possible, the subsequent tail flip. The ability to sustain tail-flipping over a longer duration and distance was not studied here, however. Despite the importance of the escape response and the multiple ways that reduced pH may affect this behavior, it has not been well-studied in crustaceans. Among crustaceans, copepods in reduced pH conditions did not show any differences in swimming activity than those in ambient conditions (Almén et al., 2017), although swimming is a much more frequent activity for this crustacean group. The escape

responses of other marine organisms were negatively affected by reduced pH conditions. For example, reduced pH led to faster fatigue in the king scallop (Schalkhausser et al., 2014) and decreased the number of conch snails initiating an escape response when threatened (Watson et al., 2014). In damselfish. fewer young initiated an escape response under reduced pH and when they did, the duration and velocity were lower (Allan et al., 2013). The reduced responses to predators observed in some of these studies indicates that decision-making is impaired. This neurosensory decline has been implicated in the lack of response to chemical cues these fish and invertebrates, but was not evident in juvenile spiny lobsters in this study.

Effects of fluctuating pH conditions

Our experimental design allowed us to examine how diurnal fluctuations mediate responses of juvenile lobsters to reduced pH. While each treatment had the same mean pH value, fluctuations above this value might provide a short, daily refuge period when processes like calcification can mainly be carried out (Wahl et al., 2018). Indeed, we found distinct differences in exoskeletal defenses between fluctuating and stable conditions, but not between the ambient/stable and reduced/stable conditions. The effects of fluctuating conditions on exoskeletal defense were, however, negative. Carapace Mg concentration was significantly reduced in both fluctuating treatments, and horn hardness was significantly reduced in the reduced/high fluctuating treatment. Notably, there were also significant differences among the reduced/fluctuating and the reduced/stable treatments. Antennae flexural stiffness and carapace Mg concentration were lower in the high fluctuating treatment compared to the stable reduced treatment. These results demonstrate the importance of replicating natural pH

variability from an organism's environment when conducting ocean acidification experiments,

These results indicate that future scenarios of fluctuating pH conditions are not beneficial to *P. interruptus*, despite the current natural fluctuations they experience in kelp forests (Frieder et al., 2012; Kapsenberg and Hofmann, 2016). This is in contrast to the results of some other studies employing pH fluctuations (Ou et al., 2015), including one where reef fish experienced lower pH at night in fluctuating conditions than in stable conditions (Jarrold et al., 2017), as lobsters did here too. Like some organisms, juvenile spiny lobsters may find fluctuating low pH conditions stressful; fluctuating reduced pH conditions raised oxidative stress levels in the mussel *Mytilus edulis* (Mangan et al., 2017). In this study, negative effects tended to be greater under reduced pH with high fluctuations than that with low fluctuations. Potentially, the negative effects may result from the pH dropping below a threshold value at night around 7.55-7.60 pH units, which lobsters do not appear to encounter frequently, if at all, in the kelp forest habitat were they were collected (Frieder et al., 2012).

Conclusions

Juvenile California spiny lobster defenses were resilient in some aspects but were negatively impacted by ocean acidification-like conditions in others. While both behavioral defenses were not affected, there were changes to the calcification and material properties in different areas of the cuticle that are key for fending off kelp forest predators. These results indicate that the crustacean cuticle responds to reduced pH conditions in complex and non-intuitive ways, necessitating careful study across multiple levels of organization (structure,

composition, and material properties) to fully understand how the cuticle responds under OA-like conditions. *P. interruptus* is one of 19 species recognized within its genus distributed worldwide (Ptacek et al., 2001). Other species live in a variety of habitats, such as coral reefs, rocky reefs, and kelp forest habitats, and have similar predator defenses, but they use them to a different degree (Briones-Fourzán et al., 2006). Yet, spiny lobsters have a great deal of conserved traits, such as the morphology that allows for stridulation (Patek, 2003), and pH tolerance might also be shared. While not all possible means of defense were tested here, the wide range of resilience found among a diversity of defenses in *P. interruptus* suggests that this species will likely be able to survive, grow, and defend itself against a variety of predation strategies in the coming century.

Acknowledgements

We deeply appreciate the extensive input, teaching, and labor of Phil Zerofski throughout the experiment, especially with helping to build the experimental system and facilitating lobster collection. Many volunteers were critical for carrying out this work: Cierra Kelly, Jack Shurtz, Duc Tran, Steven Ly, Eric Young, Grace Chan, Kyle Perdue, Zoe Sebright, Alex Hill, and Brian Zhou helped maintain the experimental treatments and collect tail flip escape response video. Cierra Kelly helped collect chemoreception videos and analyzed them with Jack Shurtz. Travis Buck, Kevin Hovel, Brett Pickering, Lyndsay Sutterley, Matt Costa, and Georgie Zelanak either provided traps, helped set them up, or helped recover trapped lobsters. Sebastian Davis, Yaamini Venkataraman, and Summer Webb helped collect water samples from La Jolla seagrass beds. David Cervantes from the Dickson

Laboratory provided the sampling protocol and analyzed water samples. Scripps Coastal & Open Ocean BiogeochemistrY lab members, including Alyssa Griffin, Sam Kekuewa, and Ariel Pezner, provided expertise in helping train and troubleshoot while analyzing experimental water samples. Jack Shurtz, Hengyu Zhou, Zhuoying Lin, and Jan Hsaio helped analyze camcorder videos of lobster tail flip escapes. Brigid McCay, Jan Hsaio, and Chrissy Tustison aided in dissecting abdominal muscles. This work was partially supported through access and utilization of the NanoEngineering Materials Research Center (NE-MRC) and the Nano3 facility at UC San Diego, and we appreciate the training and support from Sabine Faulhaber. This material is based upon work supported by the National Science Foundation Graduate Research Fellowship Program, the UC San Diego Frontiers of Innovation Scholars Program, and the generous support of the PADI Foundation.

Chapter 3, in part, is in preparation for submission for publication. Lowder, K.B., deVries, M.S., Kelly, C.B., Andersson, A.J., Hattingh, R., Day, J.M, and Taylor, J.R.A. The dissertation author was the primary investigator and author of this material.

Tables

Table 3.1. Water parameters during the experimental period as mean ± sd. Values in brackets indicate the sample size. pH is calculated by applying the offset between discrete water samples and portable probe readings to the daily probe readings. Daily ranges of pH are calculated from two Apex probes that were rotated between lobster tanks daily. Temperature is from daily portable probe readings. DIC and TA are directly measured from discrete water samples, while pCO_2, HCO_3^-, and calcite saturation state are all calculated from discrete water samples using CO2Sys.

Treatment	Daytime pH (total)	Daily range of pH	Mean pH (total)	Temperature (°C)	DIC (µmol/kg SW)	TA (µmol/kg SW)	pCO_2 (µatm)	HCO_3^- (µmol/kg SW)	Ω Calcite
Ambient/stable	7.97 ± 0.03 [1329]	0.01 ± 0.01 [49]	7.97	16.5 ± 0.6 [1560]	2030 ± 16 [12]	2219 ± 10 [12]	464 ± 39 [12]	1873 ± 30 [12]	3.37 ± 0.32 [12]
Reduced/stable	7.67 ± 0.04 [1350]	0.01 ± 0.02 [50]	7.67	16.6 ± 0.6 [1569]	2136 ± 11 [12]	2218 ± 9 [12]	978 ± 53 [12]	2023 ± 13 [12]	1.90 ± 0.15 [12]
Reduced/low fluctuating	7.72 ± 0.03 [1317]	0.11 ± 0.02 [54]	7.67	16.4 ± 0.5 [1662]	2124 ± 11 [12]	2219 ± 8 [12]	863 ± 71 [12]	2008 ± 14 [12]	2.06 ± 0.14 [12]
Reduced/high fluctuating	7.77 ± 0.03 [1333]	0.21 ± 0.03 [46]	7.67	16.4 ± 0.7 [1667]	2103 ± 12 [12]	2219 ± 8 [12]	751 ± 52 [12]	1979 ± 17 [12]	2.34 ± 0.20 [12]

Figures

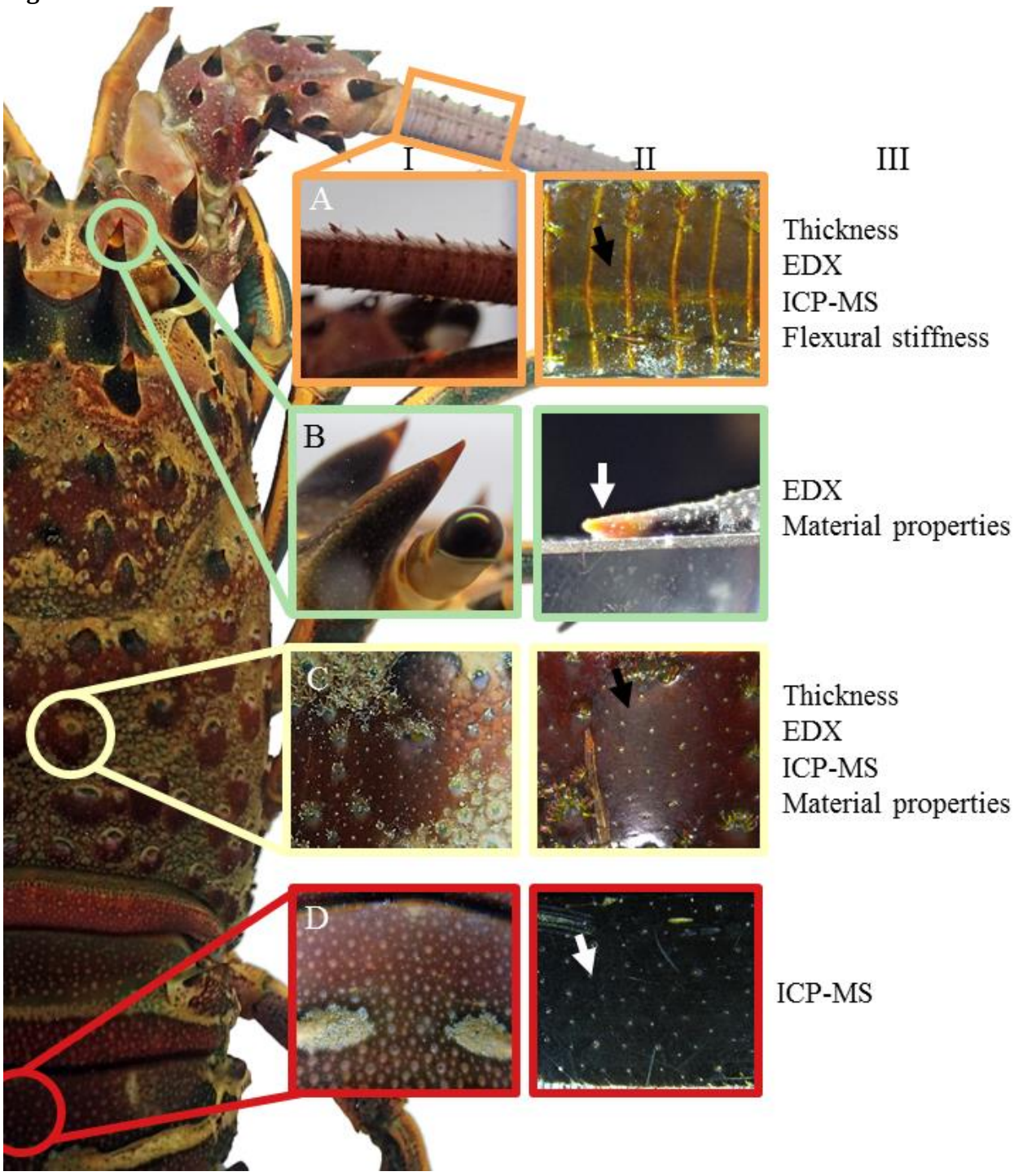

Figure 3.1. Exoskeletal defense structures of *Panulirus interruptus*. A) antenna, B) horn tip, C) carapace spine, D) abdominal segment in image columns I and II. The analyses performed for each structure are listed in column III. Arrows indicate areas where nanoindentation was performed normal to the surface.

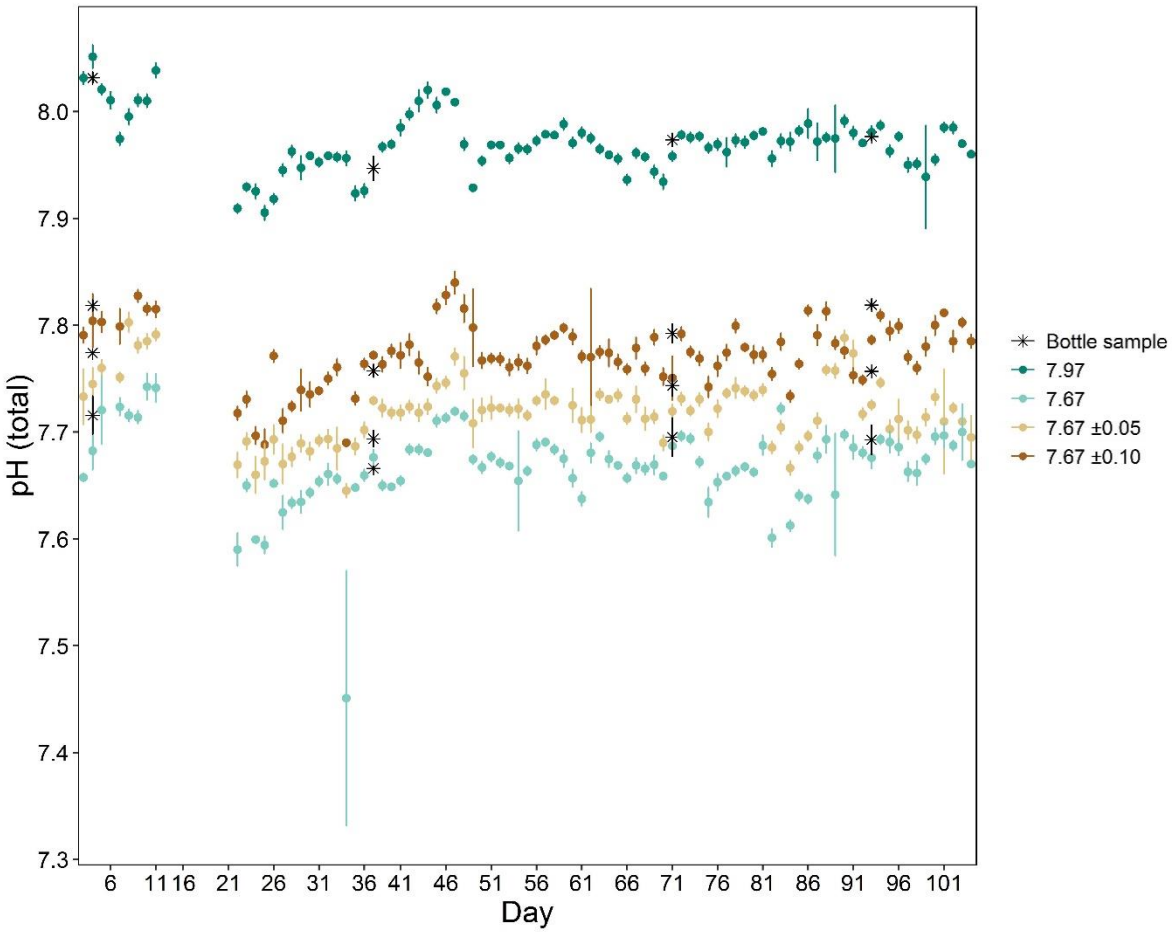

Figure 3.2. Daytime pH of each treatment across the experimental duration. pH_{NBS}, shown as mean ± sd, in each replicate was measured daily with a portable pH electrode and corrected to pH_{total} via four sets of bottle samples. Electrical failures in the system disrupted pH control for short periods of time in seven instances, and one probe used to measure days 12-21 was not functioning correctly and was excluded.

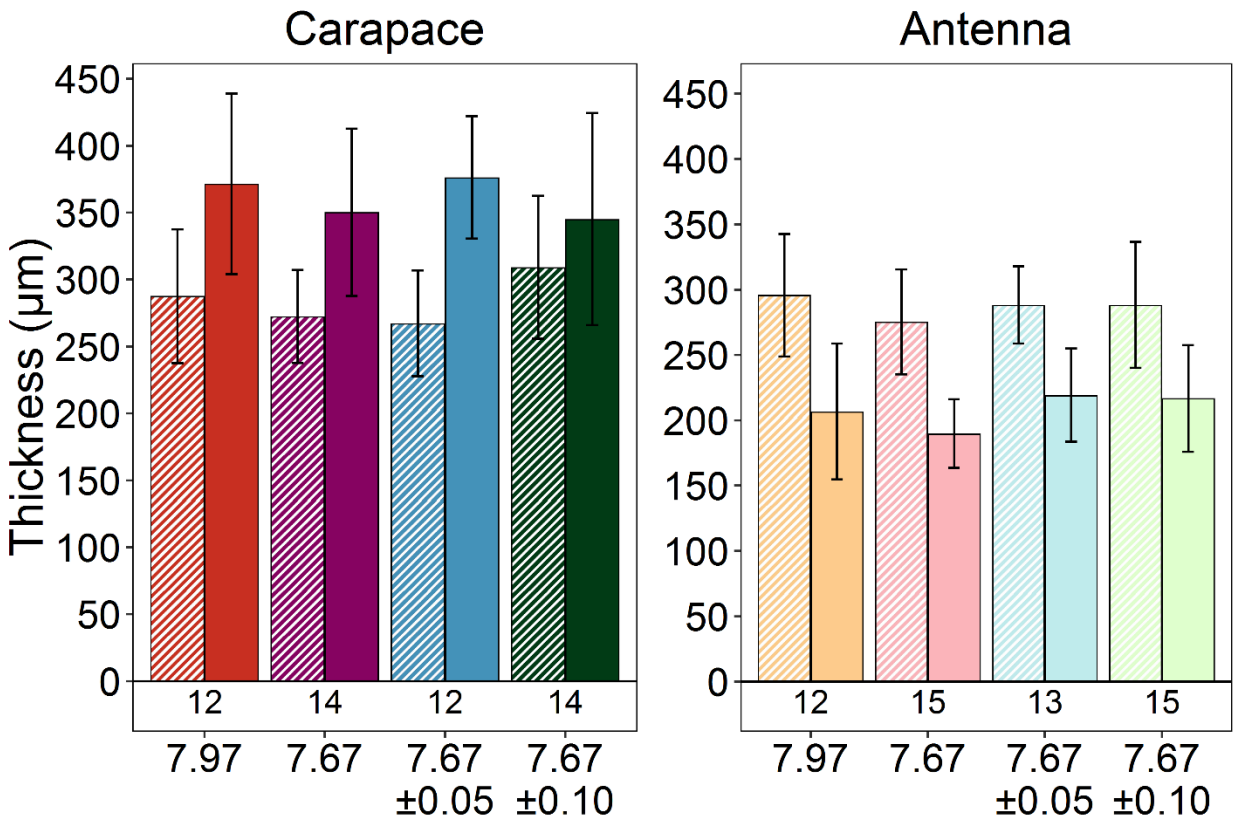

Figure 3.3. Thickness of the two layers that comprise the majority of the cuticle. There were no differences in the thickness of epi- and exocuticle layers in either the carapace or antennae. Hashed bars represent the endocuticle layer, while solid bars represent the exocuticle layer. Values on the bottom denote sample size.

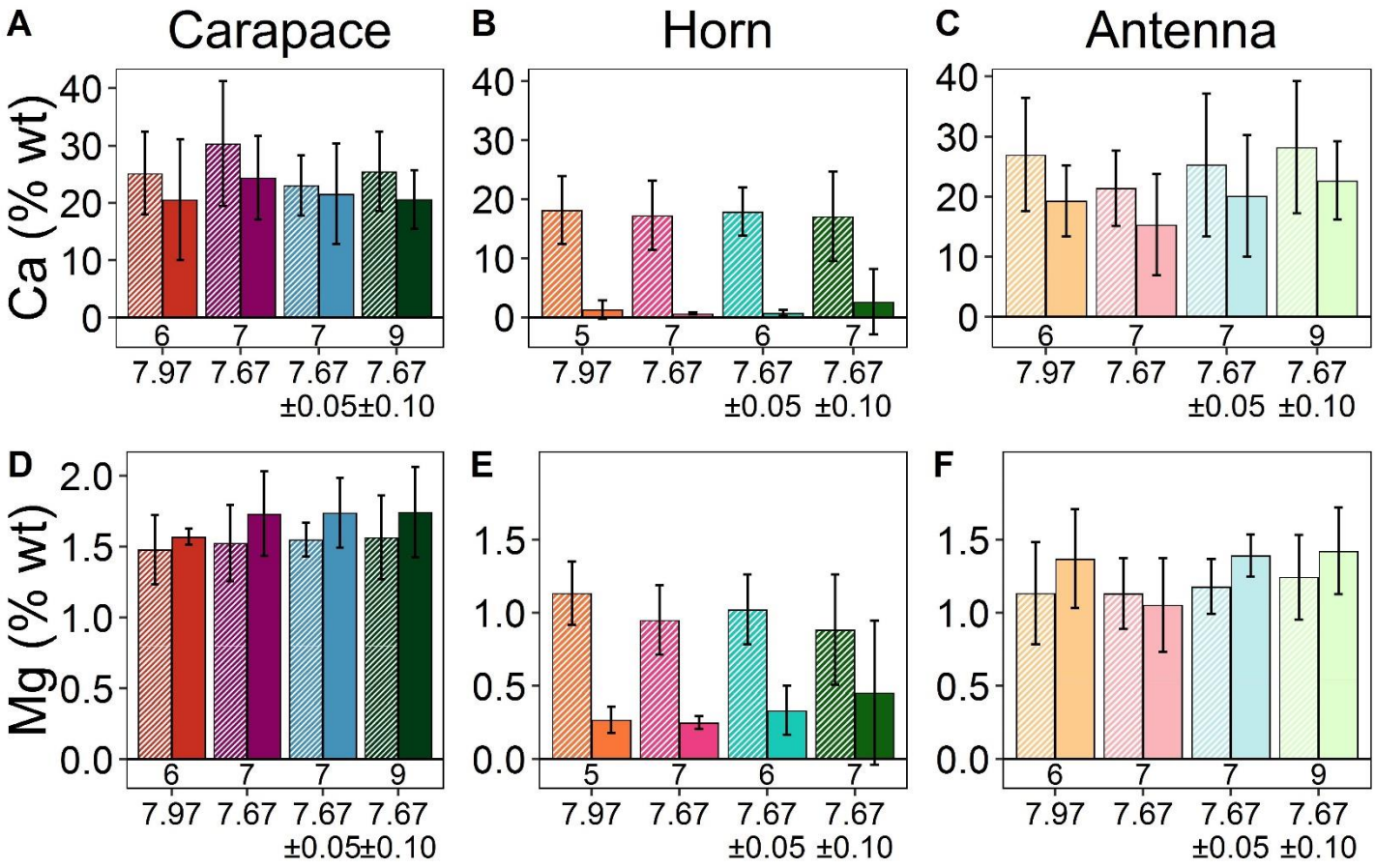

Figure 3.4. Ca and Mg % wt of three exoskeletal structures. The endocuticle layer/horn core are represented by striped bars and the exocuticle layer/horn outer ring are solid. There were no significant differences in either element across treatment conditions.

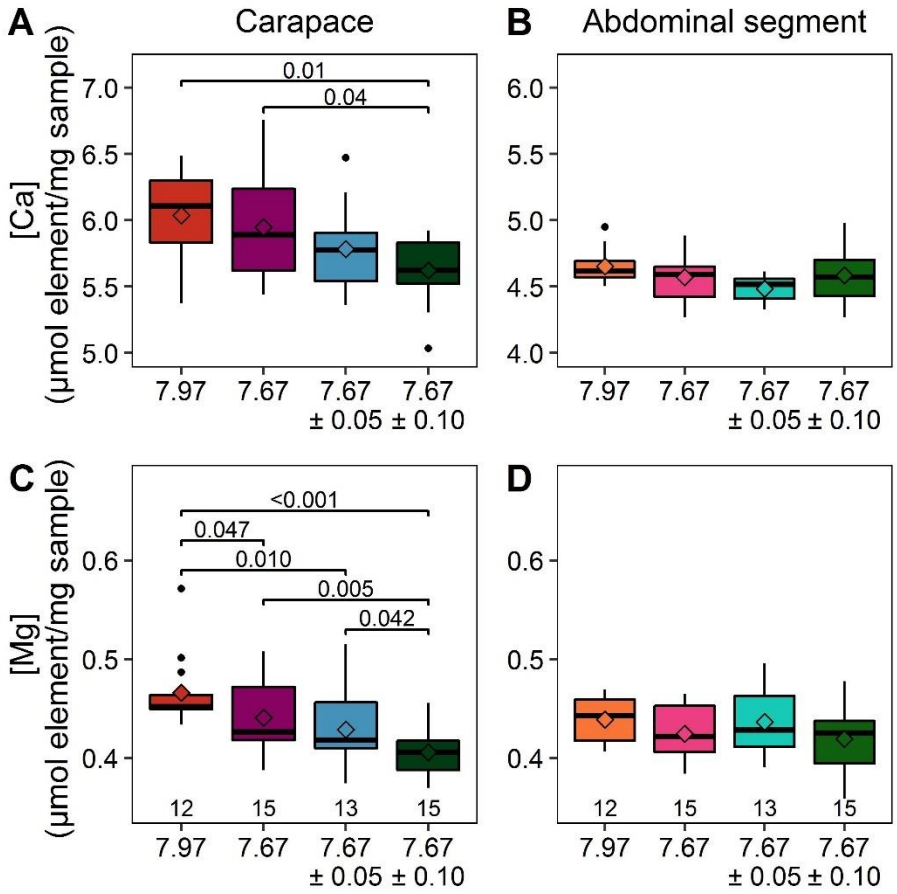

Figure 3.5. Calcium and magnesium concentrations measured with ICP-MS. In the carapace of lobsters in the reduced/high fluctuating treatment, there was significantly less calcium (A) present than in lobsters in ambient/stable conditions. Lobsters in both fluctuating treatments had significantly less magnesium than those in ambient/stable treatments. There were no differences found in the cuticle of the abdominal segment, which had lower and less variable amounts of calcium but similar amounts of Mg to the carapace. Note different axes for panels A and B. α=0.025 after a Bonferroni correction. Sample size is at the bottom of each bar. Diamonds represent the mean. Horizontal lines represent the median.

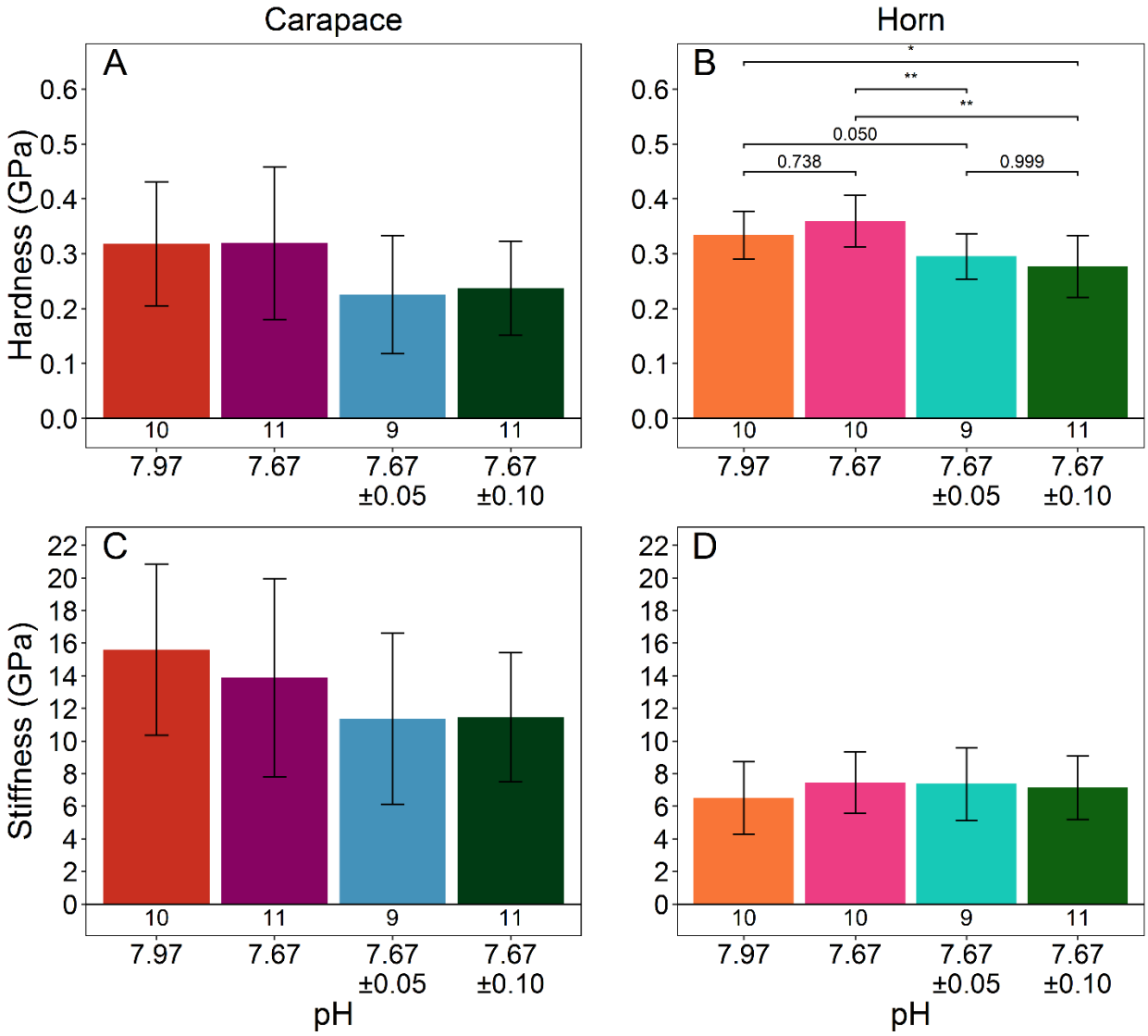

Figure 3.6. Material properties of the carapace spine (A and C) and rostral horn (B and D). The carapace spine did not show any differences in material properties among treatments. The horn significantly differed in hardness. Lobsters exposed to stable pH conditions (both ambient and reduced pH) were harder than lobsters exposed to reduced/high fluctuating pH conditions. Values under bars are the sample size, and * represents $p < 0.05$ while ** represents $p < 0.01$.

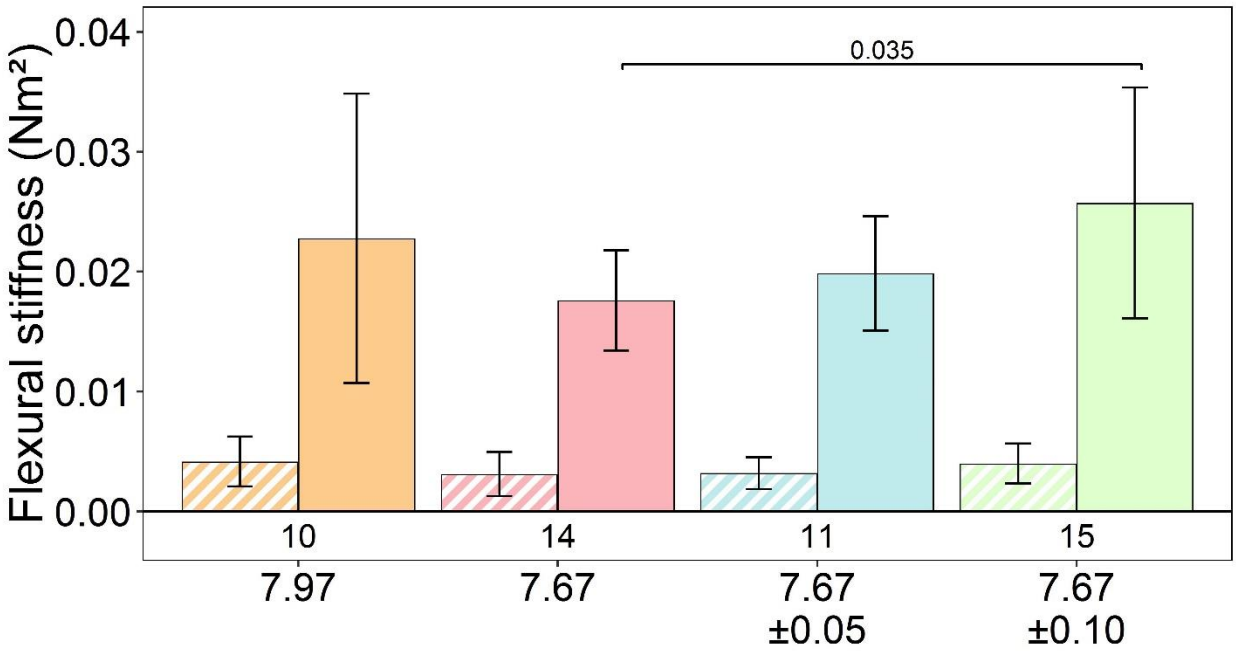

Figure 3.7. Flexural stiffness of the antennae at proximal (solid) and distal (hashed) locations. The low stiffness at the distal location was similar across all treatments. While antennae from the reduced/high fluctuating treatment were stiffer at the proximal base than lobsters in the reduced/stable pH treatment, there were no significant differences in flexural stiffness from the ambient/stable treatment.

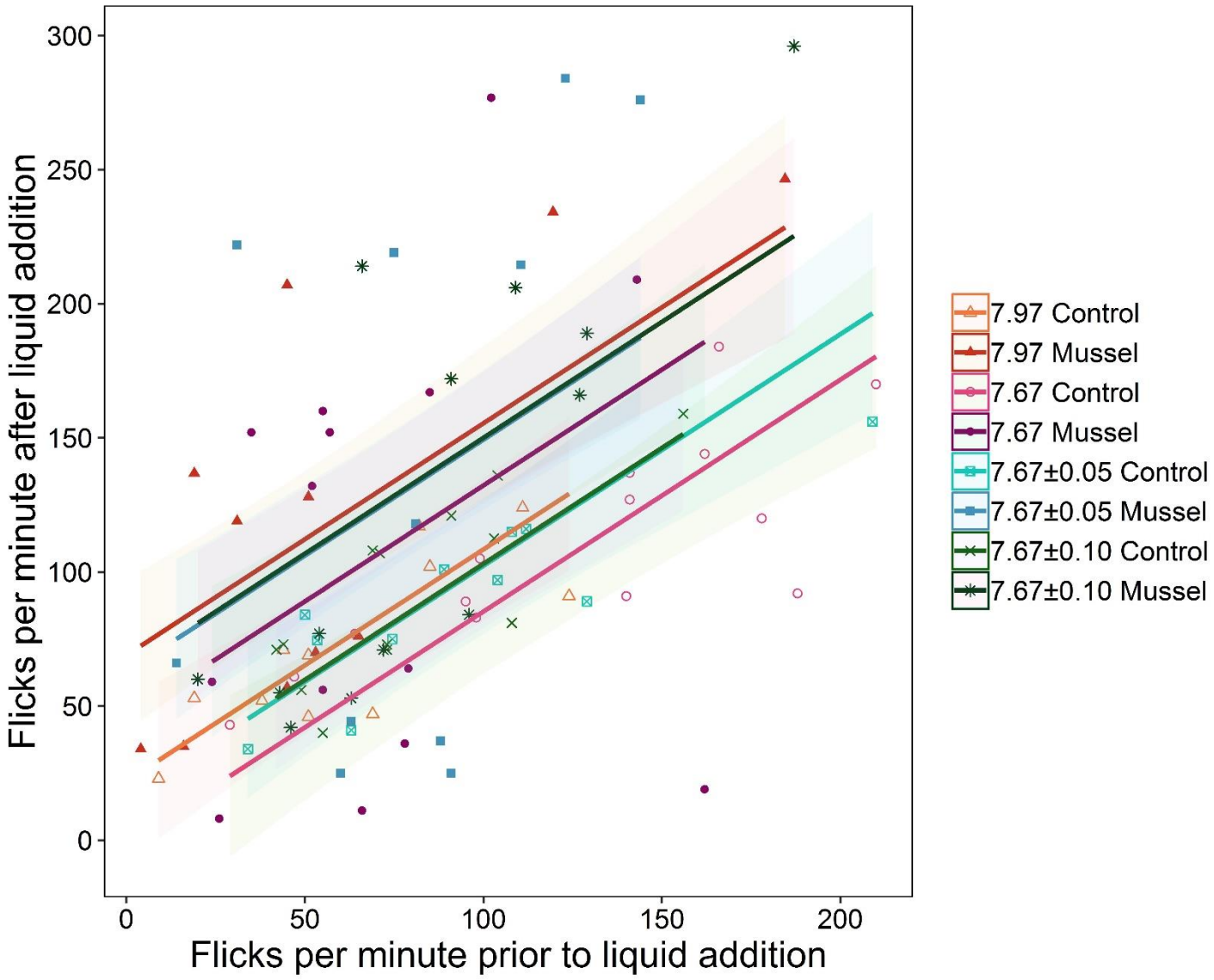

Figure 3.8. Juvenile spiny lobster antennule flick rates following the addition of either control liquid (treatment water) or prey cue (mussel slurry) as a function of baseline flick rate. Individual lobsters have variable resting flick rates and response to the addition of chemical cue, but these responses are not different among treatments. Shading represents 95% confidence intervals.

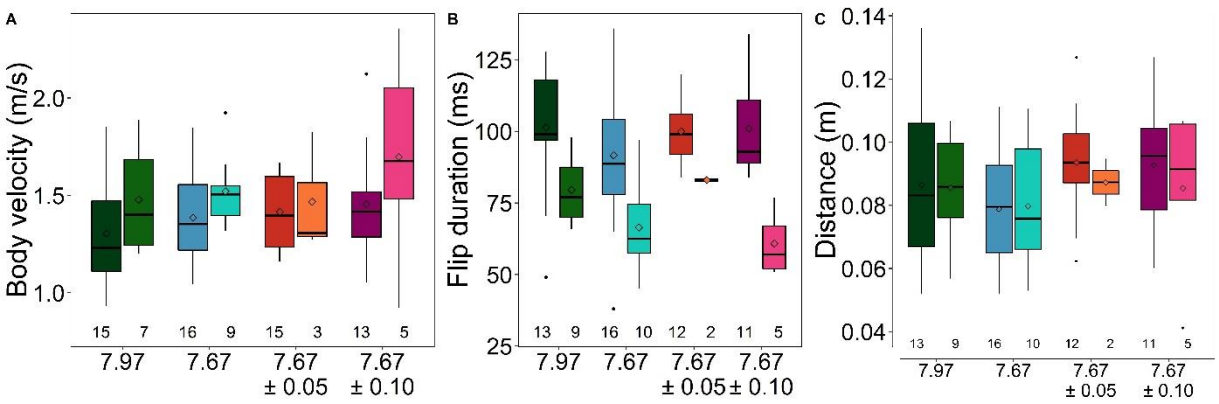

Figure 3.9. Kinematics of lobster tail flips. The velocity of the lobster (A), the duration of each tail-flip (B), and the distance covered by each flip (C) were not different among treatments. The first flip from each start is the left bar for each treatment, while the second flip,is the right bar denoted by a lighter shade. Values on the bottom denote sample size.

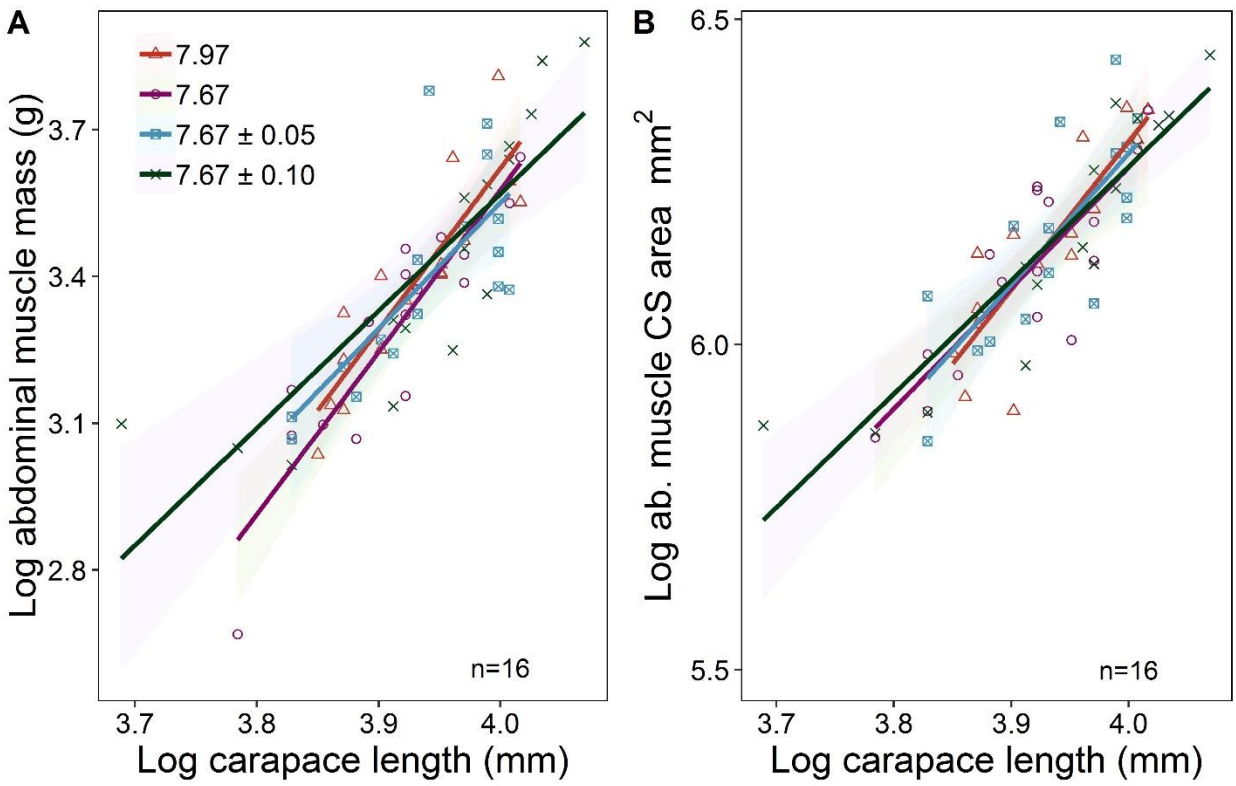

Figure 3.10. Abdominal muscle mass (A) and the cross-sectional area of the muscle (B) both significantly increase with carapace length, but did not differ among treatments.

References

Aggio, J. F., and Derby, C. D. 2008. Hydrogen peroxide and other components in the ink of sea hares are chemical defenses against predatory spiny lobsters acting through non-antennular chemoreceptors. Journal of Experimental Marine Biology and Ecology, 363: 28-34.

Alenius, B., and Munguia, P. 2012. Effects of pH variability on the intertidal isopod, *Paradella dianae.* Marine and Freshwater Behaviour and Physiology, 45: 245-259.

Allan, B. J., Domenici, P., McCormick, M. I., Watson, S.-A., and Munday, P. L. 2013. Elevated CO_2 affects predator-prey interactions through altered performance. PLoS ONE, 8: e58520.

Allison, V., Dunham, D. W., and Harvey, H. H. 1992. Low pH alters response to food in the crayfish *Cambarus bartoni*. Canadian Journal of Zoology, 70: 2416-2420.

Almén, A.-K., Brutemark, A., Jutfelt, F., Riebesell, U., and Engström-Öst, J. 2017. Ocean acidification causes no detectable effect on swimming activity and body size in a common copepod. Hydrobiologia, 802: 235-243.

Andersson, A., and Mackenzie, F. 2012. Revisiting four scientific debates in ocean acidification research. Biogeosciences, 9: 893-905.

Andersson, A. J., Kline, D. I., Edmunds, P. J., Archer, S. D., Bednaršek, N., Carpenter, R. C., Chadsey, M., Goldstein, P., Grottoli, A.G., Hurst, T.P. 2015. Understanding ocean acidification impacts on organismal to ecological scales. Oceanography, 28: 16-27.

Auguie, B. 2016. gridExtra: Miscellaneous functions for "grid" graphics. R package version 2.2. 1.

Bates, D., Sarkar, D., Bates, M. D., and Matrix, L. 2007. The lme4 package. R package version, 2: 74.

Ben-Horin, T., Iacchei, M., Selkoe, K., Mai, T. T., and Toonen, R. J. 2009. Characterization of eight polymorphic microsatellite loci for the California spiny lobster, *Panulirus*

interruptus and cross-amplification in other achelate lobsters. Conservation Genetics Resources, 1: 193-197.

Borges, F. O., Sampaio, E., Figueiredo, C., Rosa, R., and Grilo, T. F. 2018. Hypercapnia-induced disruption of long-distance mate-detection and reduction of energy expenditure in a coastal keystone crustacean. Physiology & behavior, 195: 69-75.

Briones-Fourzán, P., Pérez-Ortiz, M., and Lozano-Álvarez, E. 2006. Defense mechanisms and antipredator behavior in two sympatric species of spiny lobsters, *Panulirus argus* and *P. guttatus*. Marine Biology, 149: 227-239.

Challener, R. C., Robbins, L. L., and McClintock, J. B. 2015. Variability of the carbonate chemistry in a shallow, seagrass-dominated ecosystem: implications for ocean acidification experiments. Marine and Freshwater Research, 67: 163-172.

Chen, P.-Y., Lin, A. Y.-M., McKittrick, J., and Meyers, M. A. 2008. Structure and mechanical properties of crab exoskeletons. Acta Biomaterialia, 4: 587-596.

Clark, H. R., and Gobler, C. J. 2016. Diurnal fluctuations in CO2 and dissolved oxygen concentrations do not provide a refuge from hypoxia and acidification for early-life-stage bivalves. Marine Ecology Progress Series, 558: 1-14.

Coffey, W. D., Nardone, J. A., Yarram, A., Long, W. C., Swiney, K. M., Foy, R. J., and Dickinson, G. H. 2017. Ocean acidification leads to altered micromechanical properties of the mineralized cuticle in juvenile red and blue king crabs. Journal of Experimental Marine Biology and Ecology, 495: 1-12.

Cribb, B. W., Rathmell, A., Charters, R., Rasch, R., Huang, H., and Tibbetts, I. R. 2009. Structure, composition and properties of naturally occurring non-calcified crustacean cuticle. Arthropod Structure & Development, 38: 173-178.

Cromarty, S., Cobb, J. S., and Kass-Simon, G. 1991. Behavioral analysis of the escape response in the juvenile lobster *Homarus americanus* over the molt cycle. Journal of Experimental Biology, 158: 565-581.

Davis, K. J., Dove, P. M., and De Yoreo, J. J. 2000. The role of Mg2+ as an impurity in calcite growth. Science, 290: 1134-1137.

de la Haye, K., Spicer, J., Widdicombe, S., and Briffa, M. 2011. Reduced sea water pH disrupts resource assessment and decision making in the hermit crab *Pagurus bernhardus*. Animal Behaviour, 82: 495-501.

de la Haye, K. L., Spicer, J. I., Widdicombe, S., and Briffa, M. 2012. Reduced pH sea water disrupts chemo-responsive behaviour in an intertidal crustacean. Journal of Experimental Marine Biology and Ecology, 412: 134-140.

Derby, C. D., Cate, H. S., and Gentilcore, L. R. 1997. Perireception in olfaction: molecular mass sieving by aesthetasc sensillar cuticle determines odorant access to receptor sites in the Caribbean spiny lobster *Panulirus argus*. Journal of experimental biology, 200: 2073-2081.

deVries, M. S., Webb, S. J., Tu, J., Cory, E., Morgan, V., Sah, R. L., Deheyn, D.D., Taylor, J.R.A. 2016. Stress physiology and weapon integrity of intertidal mantis shrimp under future ocean conditions. Scientific Reports, 6: 38637.

Dickson, A., and Millero, F. J. 1987. A comparison of the equilibrium constants for the dissociation of carbonic acid in seawater media. Deep Sea Research Part A. Oceanographic Research Papers, 34: 1733-1743.

Dickson, A. G. 1990. Standard potential of the reaction: AgCl (s) + $12H_2$ (g)= Ag (s) + HCl (aq), and and the standard acidity constant of the ion HSO_4^- in synthetic sea water from 273.15 to 318.15 K. The Journal of Chemical Thermodynamics, 22: 113-127.

Dickson, A. G., Sabine, C. L., and Christian, J. R. 2007. Guide to best practices for ocean CO_2 measurements, North Pacific Marine Science Organization, Sidney, BC. 191 pp.

Dillaman, R., Hequembourg, S., and Gay, M. 2005. Early pattern of calcification in the dorsal carapace of the blue crab, *Callinectes sapidus*. Journal of Morphology, 263: 356-374.

Dixson, D. L., Munday, P. L., and Jones, G. P. 2010. Ocean acidification disrupts the innate ability of fish to detect predator olfactory cues. Ecology Letters, 13: 68-75.

Duquette, A., McClintock, J. B., Amsler, C. D., Pérez-Huerta, A., Milazzo, M., and Hall-Spencer, J. M. 2017. Effects of ocean acidification on the shells of four Mediterranean gastropod species near a CO_2 seep. Marine pollution bulletin, 124: 917-928.

Díaz-Iglesias, E., Robles-Murillo, A. K., Buesa, R. J., Báez-Hidalgo, M., and López-Zenteno, M. 2011. Bioenergetics of red spiny lobster *Panulirus interruptus* (Randall, 1840) juveniles fed with mollusc. Aquaculture, 318: 207-212.

Engle, J. M. 1979. Ecology and growth of juvenile California spiny lobster, *Panulirus interruptus* (Randall). p. 298. Unpublished doctoral thesis, University of Southern California, Los Angeles, California, United States.

Findlay, H. S., Kendall, M. A., Spicer, J. I., and Widdicombe, S. 2010. Post-larval development of two intertidal barnacles at elevated CO_2 and temperature. Marine Biology, 157: 725-735.

Fitzer, S. C., Zhu, W., Tanner, K. E., Phoenix, V. R., Kamenos, N. A., and Cusack, M. 2015. Ocean acidification alters the material properties of *Mytilus edulis* shells. Journal of the Royal Society Interface, 12: 20141227.

Frieder, C., Nam, S., Martz, T., and Levin, L. 2012. High temporal and spatial variability of dissolved oxygen and pH in a nearshore California kelp forest. Biogeosciences, 9: 3917-3930.

Glandon, H. L., Kilbourne, K. H., Schijf, J., and Miller, T. J. 2018. Counteractive effects of increased temperature and pCO2 on the thickness and chemistry of the carapace of juvenile blue crab, *Callinectes sapidus*, from the Patuxent River, Chesapeake Bay. Journal of Experimental Marine Biology and Ecology, 498: 39 - 45.

Graves, S., Piepho, H.-P., Selzer, L., and Dorai-Raj, S. 2012. multcompView: visualizations of paired comparisons. R package version 0.1-5, URL http://CRAN.R-project.org/package=multcompView.

Grünert, U., and Ache, B. W. 1988. Ultrastructure of the aesthetasc (olfactory) sensilla of the spiny lobster, *Panulirus argus*. Cell and Tissue Research, 251: 95-103.

Henry, R., Kormanik, G., Smatresk, N., and Cameron, J. 1981. The role of $CaCO_3$ dissolution as a source of HCO_3^- for the buffering of hypercapnic acidosis in aquatic and terrestrial decapod crustaceans. Journal of Experimental Biology, 94: 269-274.

Hofmann, G. E., Smith, J. E., Johnson, K. S., Send, U., Levin, L., Micheli, F., Paytan, A., Price, N.N., Peterson, B., Takeshita, Y., Matson, P.G., Crook, E.D., Kroeker, K.J., Gambi, M.C., Rivest, E.B., Frieder, C., Yu, P.C., Martz, T.R.. 2011. High-frequency dynamics of ocean pH: a multi-ecosystem comparison. PloS ONE, 6.

Jarrold, M. D., Humphrey, C., McCormick, M. I., and Munday, P. L. 2017. Diel CO_2 cycles reduce severity of behavioural abnormalities in coral reef fish under ocean acidification. Scientific reports, 7: 10153.

Johnson, M. D., Rodriguez, L. M., O'Connor, S. E., Varley, N. F., and Altieri, A. H. 2019. pH variability exacerbates effects of ocean acidification on a Caribbean crustose coralline alga. Frontiers in Marine Science, 6: 150.

Johnson, Z. I., Wheeler, B. J., Blinebry, S. K., Carlson, C. M., Ward, C. S., and Hunt, D. E. 2013. Dramatic variability of the carbonate system at a temperate coastal ocean site (Beaufort, North Carolina, USA) is regulated by physical and biogeochemical processes on multiple timescales. PLoS One, 8: e85117.

Kapsenberg, L., and Hofmann, G. E. 2016. Ocean pH time-series and drivers of variability along the northern Channel Islands, California, USA. Limnology and Oceanography, 61: 953-968.

Kassambara, A. 2018. ggpubr:'ggplot2'Based Publication Ready Plots. R package version 0.1. 8.

Kim, T. W., Taylor, J., Lovera, C., and Barry, J. P. 2015. CO2-driven decrease in pH disrupts olfactory behaviour and increases individual variation in deep-sea hermit crabs. ICES Journal of Marine Science, 73: 613-619.

Knapp, J. L., Bridges, C. R., Krohn, J., Hoffman, L. C., and Auerswald, L. 2015. Acid–base balance and changes in haemolymph properties of the South African rock lobsters, *Jasus lalandii*, a palinurid decapod, during chronic hypercapnia. Biochemical and biophysical research communications, 461: 475-480.

Kurihara, H., Masaaki, M., Hiroko, F., Masahiro, H., and Atsushi, I. 2008. Long-term effects of predicted future seawater CO_2 conditions on the survival and growth of the marine shrimp *Palaemon pacificus*. Journal of Experimental Marine Biology and Ecology, 367: 41-46.

Leduc, A. O., Kelly, J. M., and Brown, G. E. 2004. Detection of conspecific alarm cues by juvenile salmonids under neutral and weakly acidic conditions: laboratory and field tests. Oecologia, 139: 318-324.

Lenth, R. 2018. Emmeans: Estimated marginal means, aka least-squares means. R package version, 1.

Lindberg, R. G. 1955. Growth, population dynamics, and field behavior in the spiny lobster, *Panulirus interruptus* (Randall), University of California Press.

Mangan, S., Urbina, M. A., Findlay, H. S., Wilson, R. W., and Lewis, C. 2017. Fluctuating seawater pH/pCO_2 regimes are more energetically expensive than static pH/pCO_2 levels in the mussel *Mytilus edulis*. Proc. R. Soc. B, 284: 20171642.

McClintock, J. B., Angus, R. A., Mcdonald, M. R., Amsler, C. D., Catledge, S. A., and Vohra, Y. K. 2009. Rapid dissolution of shells of weakly calcified Antarctic benthic macroorganisms indicates high vulnerability to ocean acidification. Antarctic Science, 21: 449-456.

McDonald, M. R., McClintock, J. B., Amsler, C. D., Rittschof, D., Angus, R. A., Orihuela, B., and Lutostanski, K. 2009. Effects of ocean acidification over the life history of the barnacle *Amphibalanus amphitrite*. Marine Ecology Progress Series, 385: 179-187.

McElhany, P., and Busch, D. S. 2013. Appropriate pCO2 treatments in ocean acidification experiments. Marine biology, 160: 1807-1812.

McLean, E. L., Katenka, N. V., and Seibel, B. A. 2018. Decreased growth and increased shell disease in early benthic phase *Homarus americanus* in response to elevated CO_2. Marine Ecology Progress Series, 596: 113-126.

Mehrbach, C., Culberson, C. H., Hawley, J. E., and Pytkowicz, R. M. 1973. Measurement of the apparent dissociation constants of carbonic acid in seawater at atmospheric pressure. Limnology and Oceanography, 18: 897-907.

Menu-Courey, K., Noisette, F., Piedalue, S., Daoud, D., Blair, T., Blier, P. U., Azetsu-Scott, K., and Calosi, P. 2018. Energy metabolism and survival of the juvenile recruits of the American lobster (*Homarus americanus*) exposed to a gradient of elevated seawater pCO_2. Marine Environmental Research.

Munday, P. L., Dixson, D. L., Donelson, J. M., Jones, G. P., Pratchett, M. S., Devitsina, G. V., and Døving, K. B. 2009. Ocean acidification impairs olfactory discrimination and homing ability of a marine fish. Proceedings of the National Academy of Sciences, 106: 1848-1852.

Munday, P. L., Welch, M. J., Allan, B. J., Watson, S.-A., McMahon, S. J., and McCormick, M. I. 2016. Effects of elevated CO2 on predator avoidance behaviour by reef fishes is not altered by experimental test water. PeerJ, 4: e2501.

Newcomb, L. A., Milazzo, M., Hall-Spencer, J. M., and Carrington, E. 2015. Ocean acidification bends the mermaid's wineglass. Biology letters, 11: 20141075.

Onitsuka, T., Takami, H., Muraoka, D., Matsumoto, Y., Nakatsubo, A., Kimura, R., Ono, T., Nojiri, Y. 2017. Effects of ocean acidification with pCO 2 diurnal fluctuations on survival and larval shell formation of Ezo abalone, *Haliotis discus hannai*. Marine environmental research.

Ou, M., Hamilton, T. J., Eom, J., Lyall, E. M., Gallup, J., Jiang, A., Lee, J., Close, D.A., Yun, S.-S., Brauner, C.J. 2015. Responses of pink salmon to CO2-induced aquatic acidification. Nature Climate Change, 5: 950-955.

Page, H. N., Andersson, A. J., Jokiel, P. L., Ku'ulei, S. R., Lebrato, M., Yeakel, K., Davidson, C., D'Angelo, S., Bahr, K.D. 2016. Differential modification of seawater carbonate chemistry by major coral reef benthic communities. Coral Reefs, 35: 1311-1325.

Pane, E. F., and Barry, J. P. 2007. Extracellular acid-base regulation during short-term hypercapnia is effective in a shallow-water crab, but ineffective in a deep-sea crab. Marine Ecology Progress Series, 334: 1-9.

Patek, S. N., Oakley, T.H. 2003. Comparative tests of evolutionary trade-offs in a palinurid lobster acoustic system. Evolution; international journal of organic evolution, 57: 2082--2100.

Pierrot, D., Lewis, E., and Wallace, D. 2006. MS Excel Program Developed for CO2 System Calculations.

Ptacek, M. B., Sarver, S. K., Childress, M. J., and Herrnkind, W. F. 2001. Molecular phylogeny of the spiny lobster genus *Panulirus* (Decapoda: Palinuridae). Marine and Freshwater Research, 52: 1037-1047.

R Core Team 2018. R: A Language and Environment for Statistical Computing. R Foundation for Statistical Computing, Vienna, Austria.

Raabe, D., Sachs, C., and Romano, P. 2005. The crustacean exoskeleton as an example of a structurally and mechanically graded biological nanocomposite material. Acta Materialia, 53: 4281--4292.

Ragagnin, M. N., McCarthy, I. D., Fernandez, W. S., Tschiptschin, A. P., and Turra, A. 2018. Vulnerability of juvenile hermit crabs to reduced seawater pH and shading. Marine Environmental Research.

Rankin, A., Seo, K., Graeve, O. A., and Taylor, J. R. 2019. No compromise between metabolism and behavior of decorator crabs in reduced pH conditions. Scientific reports, 9: 6262.

Robles, C. 1987. Predator foraging characteristics and prey population structure on a sheltered shore. Ecology, 68: 1502-1514.

Roer, R., and Dillaman, R. 1984. The Structure and Calcification of the Crustacean Cuticle. Integrative and Comparative Biology, 24: 893--909.

Roggatz, C. C., Lorch, M., Hardege, J. D., and Benoit, D. M. 2016. Ocean acidification affects marine chemical communication by changing structure and function of peptide signalling molecules. Global change biology, 22: 3914-3926.

Ross, E., and Behringer, D. 2019. Changes in temperature, pH, and salinity affect the sheltering responses of Caribbean spiny lobsters to chemosensory cues. Scientific Reports, 9: 4375.

Schalkhausser, B., Bock, C., Pörtner, H.-O., and Lannig, G. 2014. Escape performance of temperate king scallop, *Pecten maximus*, under ocean warming and acidification. Marine biology, 161: 2819-2829.

Schalkhausser, B., Bock, C., Stemmer, K., Brey, T., Pörtner, H.-O., and Lannig, G. 2013. Impact of ocean acidification on escape performance of the king scallop, *Pecten maximus*, from Norway. Marine Biology, 160: 1995-2006.

Schofield, R. M. S., Niedbala, J. C., Nesson, M. H., Tao, Y., Shokes, J. E., Scott, R. A., and Latimer, M. J. 2009. Br-rich tips of calcified crab claws are less hard but more fracture resistant: a comparison of biomineralized and heavy-element biomaterials. Journal of Structural Biology, 166: 272-287.

Semesi, I. S., Beer, S., and Björk, M. 2009. Seagrass photosynthesis controls rates of calcification and photosynthesis of calcareous macroalgae in a tropical seagrass meadow. Marine Ecology Progress Series, 382: 41-47.

Shabani, S., Kamio, M., and Derby, C. D. 2008. Spiny lobsters detect conspecific blood-borne alarm cues exclusively through olfactory sensilla. Journal of Experimental Biology, 211: 2600-2608.

Shechter, A., Berman, A., Singer, A., Freiman, A., Grinstein, M., Erez, J., Aflalo, E. D., Sagi, A. 2008. Reciprocal changes in calcification of the gastrolith and cuticle during the molt cycle of the red claw crayfish *Cherax quadricarinatus*. The Biological Bulletin, 214: 122-134.

Silbiger, N. J., and Sorte, C. J. 2018. Biophysical feedbacks mediate carbonate chemistry in coastal ecosystems across spatiotemporal gradients. Scientific reports, 8: 796.

Small, D. P., Calosi, P., Boothroyd, D., Widdicombe, S., and Spicer, J. I. 2016. The sensitivity of the early benthic juvenile stage of the European lobster *Homarus gammarus* (L.) to elevated pCO_2 and temperature. Marine Biology, 163: 1-12.

Smith, J. N., Richter, C., Fabricius, K. E., and Cornils, A. 2017. Pontellid copepods, *Labidocera* spp., affected by ocean acidification: A field study at natural CO_2 seeps. PloS one, 12: e0175663.

Spanier, E., and Zimmer-Faust, R. K. 1988. Some physical properties of shelter that influence den preference in spiny lobsters. Journal of Experimental Marine Biology and Ecology, 121: 137-149.

Spicer, J. I., Raffo, A., and Widdicombe, S. 2007. Influence of CO_2-related seawater acidification on extracellular acid–base balance in the velvet swimming crab Necora puber. Marine Biology, 151: 1117-1125.

Swiney, K. M., Long, W. C., and Foy, R. J. 2015. Effects of high pCO_2 on Tanner crab reproduction and early life history—Part I: long-term exposure reduces hatching success and female calcification, and alters embryonic development. ICES Journal of Marine Science: Journal du Conseil, 73: fsv201.

Taylor, J. R. A., Gilleard, J. M., Allen, M. C., and Deheyn, D. D. 2015. Effects of CO2-induced pH reduction on the exoskeleton structure and biophotonic properties of the shrimp *Lysmata californica*. Scientific Reports, 5: 10608.

Truchot, J. P. 1979. Mechanisms of the compensation of blood respiratory acid-base disturbances in the shore crab, *Carcinus maenas* (L.). Journal of Experimental Zoology, 210: 407-416.

Tukey, J. W. 1977. Exploratory Data Analysis, Addison-Wesley Publishing Company, Reading, Mass. 688 pp.

Uppström, L. R. 1974. The boron/chlorinity ratio of deep-sea water from the Pacific Ocean. *In* Deep Sea Research and Oceanographic Abstracts, pp. 161-162. Elsevier.

Wahl, M., Schneider Covachã, S., Saderne, V., Hiebenthal, C., Müller, J., Pansch, C., and Sawall, Y. 2018. Macroalgae may mitigate ocean acidification effects on mussel calcification by increasing pH and its fluctuations. Limnology and Oceanography, 63: 3-21.

Watson, S.-A., Lefevre, S., McCormick, M. I., Domenici, P., Nilsson, G. E., and Munday, P. L. 2014. Marine mollusc predator-escape behaviour altered by near-future carbon dioxide levels. Proceedings of the Royal Society B: Biological Sciences, 281: 20132377.

Whiteley, N. M., Suckling, C. C., Ciotti, B. J., Brown, J., McCarthy, I. D., Gimenez, L., and Hauton, C. 2018. Sensitivity to near-future CO_2 conditions in marine crabs depends on their compensatory capacities for salinity change. Scientific Reports, 8: 15639.

Wickham, H. 2007. Reshaping data with the reshape package. Journal of Statistical Software, 21: 1-20.

Wickham, H. 2016. ggplot2: elegant graphics for data analysis, Springer.

Wickham, H. 2017. Forcats: Tools for working with categorical variables (factors). R package version 0.2. 0. URL: https://CRAN.R-project.org/package=forcats.

Wickham, H., Francois, R., Henry, L., and Müller, K. 2016. dplyr: A Grammar of Data Manipulation. R package version 0.5. 0. R Core Development Team Vienna.

Williams, C. R., Dittman, A. H., McElhany, P., Busch, D. S., Maher, M. T., Bammler, T. K., MacDonald, J. W., and Gallagher, E.P. 2019. Elevated CO_2 impairs olfactory-mediated neural and behavioral responses and gene expression in ocean-phase coho salmon (*Oncorhynchus kisutch*). Global Change Biology, 25: 963-977.

Wu, F., Wang, T., Cui, S., Xie, Z., Dupont, S., Zeng, J., Gu, H., Kong, H., Hu, M., and Lu, W. 2017. Effects of seawater pH and temperature on foraging behavior of the Japanese stone crab *Charybdis japonica*. Marine Pollution Bulletin, 120: 99-108.

Yao, H., Dao, M., Imholt, T., Huang, J., Wheeler, K., Bonilla, A., Suresh, S., Ortiz, C. 2010. Protection mechanisms of the iron-plated armor of a deep-sea hydrothermal vent gastropod. Proceedings of the National Academy of Sciences, 107: 987-992.

Zeebe, R. E., and Wolf-Gladrow, D. 2001. CO2 in seawater: equilibrium, kinetics, isotopes, Gulf Professional Publishing.

Zimmer-Faust, R. K., and Case, J. F. 1983. A proposed dual role of odor in foraging by the California spiny lobster, *Panulirus interruptus* (Randall). The Biological Bulletin, 164: 341-353.

Zimmer-Faust, R. K., Tyre, J. E., and Case, J. F. 1985. Chemical attraction causing aggregation in the spiny lobster, *Panulirus interruptus* (Randall), and its probable ecological significance. The Biological Bulletin, 169: 106-118.

Zylinski, S., and Johnsen, S. 2011. Mesopelagic cephalopods switch between transparency and pigmentation to optimize camouflage in the deep. Current Biology, 21: 1937-1941.

CHAPTER 4: Assessment of ocean acidification and warming on the growth, calcification, and biophotonics of a California grass shrimp

Kaitlyn B. Lowder, Michael C. Allen, James M. D. Day, Dimitri D. Deheyn, Jennifer R. A. Taylor

ICES Journal of Marine Science

ICES Journal of Marine Science (2017), 74(4), 1150–1158. doi:10.1093/icesjms/fsw246

Contribution to Special Issue: 'Towards a Broader Perspective on Ocean Acidification Research Part 2'

Original Article

Assessment of ocean acidification and warming on the growth, calcification, and biophotonics of a California grass shrimp

Kaitlyn B. Lowder,[1,*] Michael C. Allen,[1] James M. D. Day,[2] Dimitri D. Deheyn,[1] and Jennifer R. A. Taylor[1]

[1]*Marine Biology Research Division, Scripps Institution of Oceanography, University of California, San Diego, La Jolla, CA 92093, USA*
[2]*Geosciences Research Division, Scripps Institution of Oceanography, University of California, San Diego, La Jolla, CA 92093, USA*

**Corresponding author: tel: (858) 822-4712; fax: (858) 534-7313; e-mail:*kblowder@ucsd.edu

Lowder, K. B., Allen, M. C., Day, J. M. D., Deheyn, D. D., and Taylor, J. R. A. Assessment of ocean acidification and warming on the growth, calcification, and biophotonics of a California grass shrimp. – ICES Journal of Marine Science, 74: 1150–1158.

Received 24 June 2016; revised 7 November 2016; accepted 11 December 2016; advance access publication 18 January 2017.

Cryptic colouration in crustaceans, important for both camouflage and visual communication, is achieved through physiological and morphological mechanisms that are sensitive to changes in environmental conditions. Consequently, ocean warming and ocean acidification can affect crustaceans' biophotonic appearance and exoskeleton composition in ways that might disrupt colouration and transparency. In the present study, we measured growth, mineralization, transparency, and spectral reflectance (colouration) of the caridean grass shrimp *Hippolyte californiensis* in response to pH and temperature stressors. Shrimp were exposed to ambient pH and temperature (pH 8.0, 17 °C), decreased pH (pH 7.5, 17 °C), and decreased pH/increased temperature (pH 7.5, 19 °C) conditions for 7 weeks. There were no differences in either Mg or Ca content in the exoskeleton across treatments nor in the transparency and spectral reflectance. There was a small but significant increase in percent growth in the carapace length of shrimp exposed to decreased pH/increased temperature. Overall, these findings suggest that growth, calcification, and colour of *H. californiensis* are unaffected by decreases of 0.5 pH units. This tolerance might stem from adaptation to the highly variable pH environment that these grass shrimp inhabit, highlighting the multifarious responses to ocean acidification, within the Crustacea.

Keywords: biophotonics, calcification, colouration, crypsis, ocean acidification, shrimp.

Introduction

Rife among marine invertebrates and fish are examples of vibrant colouration used for diverse purposes such as advertising mutualistic services [cleaner fish (Cheney *et al.*, 2009)], provoking territorial aggression [Garibaldi damselfish (Caron and Rainboth, 1992)], and crypsis [octopus (Zylinski and Johnsen, 2011)] (see also Cott, 1940; Stevens and Merilaita, 2011). For cryptic colouration to be effective in variable environments, and to be responsive to specific cues, some species change their colouration over a range of time scales, from seconds to months. Octopuses and cuttlefish are some of the most well-known examples of marine invertebrates that are capable of rapid colour changes, sensing the ambient light of their surrounding environment to quickly react to changes in background colours, enabling them to match the colouration of nearby structures and even mimic shapes of other species (Hanlon, 2007; Hanlon *et al.*, 2010).

Dynamic cryptic colouration is relatively common in arthropods, including crustaceans (Umbers *et al.*, 2014). Fiddler crabs in the genus *Uca* are particularly colourful and can adjust chromatophores within a relatively short period (minutes, hours) when under stress (Detto *et al.*, 2008) or in response to illumination and background colour (Brown and Sandeen, 1948; Rao and Nagabhushanam, 1967). Chromatophores of different colours can respond disparately, enabling fine control of animal colour to better camouflage against changing backgrounds, as observed for the shore crab *Hemigrapsus oregonensis* (Jensen and Egnotovich, 2015) and the grass shrimp *Hippolyte varians* (Keeble and Gamble, 1899). The isopod *Idothea montereyensis* can match

either red algae clumps or green surfgrass meadows as they get swept between them, with complete colour shift taking place over one moult cycle (Lee, 1966).

Although colouration may be well-controlled under favorable environmental conditions, changes in parameters such as temperature and salinity may induce stress-related and unfavorable changes to colouration mechanisms. Both increased and decreased temperatures enact chromatophore contraction in some crustaceans (Smith, 1930; Fingerman and Tinkle, 1956; Powell, 1962; Silbiger and Munguia, 2008), perhaps as a thermoregulation mechanism (Brown and Sandeen, 1948), but this results in exposing the visually contrasting gut to predators. Changes in temperature or salinity can also lead to pooled extracellular fluid between muscle fibers, thereby increasing opacity, as shown in the grass shrimp *Palaemonetes pugio* (Bhandiwad and Johnsen, 2011). When acclimating to new salinities, the shrimp *Farfantepenaeus paulensis* acquires a reddish colour, which is believed to be a sign of stress (Perazzolo *et al.*, 2002). Crustacean colouration is thus, in part, a function of environmental parameters for some species.

This environmental component of colouration may make some marine invertebrates susceptible to changes in global ocean carbonate chemistry and temperature, a result of anthropogenic carbon emissions that have increased since the Industrial Revolution (IPCC, 2013). Although research focused on the potential effects of ocean acidification (OA) and ocean warming has demonstrated largely negative effects among calcifying mollusks and echinoderms in response to increased pCO_2 (Kroeker *et al.*, 2013; Busch and McElhany, 2016), crustaceans exhibit responses that vary amongst taxonomic groups and life stages. For example, under increased pCO_2, Tanner crabs experience no effect on hatching duration, but have smaller embryos (Swiney *et al.*, 2015) and experience lower survival in juveniles and ovigerous females (Long *et al.*, 2013; Swiney *et al.*, 2015). American lobster (*Homarus americanus*) larvae exposed to high pCO_2 displayed increased growth, but no effects on survival (Waller *et al.*, 2017), demonstrating the need to better understand the diversity of crustacean responses.

Changes in cuticle calcium content in response to increased pCO_2, as observed in many marine calcifiers, have implications for the biophotonics of crypsis and camouflage, but this response is also variable among species. Tanner crabs displayed decreased calcium content in larvae, juveniles, and ovigerous females (Long *et al.*, 2013, 2017; Swiney *et al.*, 2015) whereas two species of penaeid prawns demonstrated increased exoskeleton calcium levels in response to increased pCO_2 (Wickins, 1984), and exoskeleton calcium content was doubled in the adult red rock shrimp *Lysmata californica* (Taylor *et al.*, 2015). The increased mineralization observed in these shrimp can change the refractive index of the cuticle and scatter light (Johnsen, 2001), potentially resulting in a more opaque cuticle that limits visibility of the chromatophores underneath. Increased light scattering will also disrupt body transparency, a strategy associated with crypsis and camouflage. Indeed, reduced body transparency was observed in the red rock shrimp, though the red coloured stripes were not affected (Taylor *et al.*, 2015), suggesting complex interactions between the exoskeleton and the underlying chromatophores. It is therefore possible that the decreased pH associated with OA affects both animal transparency and colour, with potential effects on their visual ecology.

When co-occurring with ocean acidification, ocean warming may present itself either as a stressor or as a mitigator. Already, warmer water off the southern New England coast has coincided with declines in American lobster populations (Wahle *et al.*, 2015) and laboratory experiments implementing both increased pCO_2 and temperature have yielded sometimes synergistic and sometimes antagonistic results. In a calcareous tubeworm, increased temperatures mitigated the negative effects of increased pCO_2 alone (Li *et al.*, 2016). In juvenile *Homarus gammarus*, increased pCO_2 elicited different responses depending on temperature; both calcium and magnesium in the exoskeleton decreased only when high pCO_2 was coupled with higher temperature (Small *et al.*, 2016). Combined stressors may thus produce different responses than expected from single stressors alone and so must be considered together when studying potential changes on calcification, colouration, and transparency.

Given the likely ecological importance of cryptic colouration in crustaceans and its susceptibility to environmental conditions, we examined the growth, biophotonics, and exoskeleton mineral composition of a caridean grass shrimp, *Hippolyte californiensis*. These shrimp show vivid shades of green or brown, which enables them to blend in with the eelgrass and substrate of their habitat. Here, we considered ocean acidification and warming conditions as both are occurring together in many marine ecosystems where they can act antagonistically or synergistically (McDonald *et al.*, 2009; Harvey *et al.*, 2013; Paganini *et al.*, 2014). We exposed shrimp to decreased pH and decreased pH/increased temperature conditions for 7 weeks, and measured growth and exoskeleton mineral composition as well as shrimp transmittance and spectral reflectance. We hypothesized that changes in exoskeleton calcification would affect the biophotonics of shrimp, thus hindering the ability of grass shrimp to blend in with their eelgrass habitat and remain cryptic to predators.

Material and methods

Animal acquisition and care

Grass shrimp, *H. californiensis*, (Crustacea: Decapoda: Caridea) were collected with seine nets from eelgrass beds at Mission Point, Mission Bay, CA (32°45′N and 117°14′W) from January to February 2015. Shrimp were transported to the Scripps Institution of Oceanography (SIO), University of California, San Diego, where they were held in communal tanks (1.89 l) in an experimental aquarium for up to 32 days prior to the start of the experiment. Tanks received flow-through seawater pumped from the SIO pier at ambient conditions (see experimental design and maintenance below). Prior to and throughout the 7-week experiment, shrimp were fed an ad libitum diet of crushed sinking pellets (Tetra Cichlid Sticks, Blacksbury, VA, USA) 5 days a week. Excess food was removed each day ∼5 h after feeding.

Experimental design and maintenance

The experimental OA system consisted of three large header tanks (150 l) that each received filtered seawater pumped in from the SIO pier (3–4 m depth, 300 m offshore) at ambient pH_{SWS} (7.98 ± 0.04), pCO_2 (465 ± 64 µatm), temperature (17.1 ± 0.8 °C), and salinity (33.40 ± 0.11 PSU) (mean ± s.d. during the experimental period). One header tank was maintained at ambient pH and temperature conditions, a second tank was adjusted for decreased pH and ambient temperature (pH_{SWS} = 7.53 ± 0.07; pCO_2 = 1452 ± 260 µatm; temperature = 17.0 ± 0.5 °C) and a

Table 1. Temperature and carbonate chemistry parameters [mean (s.d.)] throughout the experiment.

Treatment	pCO_2 (μatm)	pHsws	Temperature* (°C)	Salinity* (PSU)	TA* (μmol/kgSW)	HCO_3 (μmol kg^{-1})	CO_3 (μmol kg^{-1})	Ω Ca	Ω Ar
Decreased pH	1452 (260)	7.53 (0.07)	16.8 (0.5)	33.39 (0.09)	2227 (8)	2087 (15)	57 (8.2)	1.37 (0.20)	0.881 (0.13)
Decreased pH/ Increased T	1620 (486)	7.48 (0.10)	19.1 (0.5)	33.39 (0.13)	2220 (15)	2074 (25)	59 (15)	1.43 (0.37)	0.928 (0.25)
Ambient	465 (64)	7.98 (0.04)	16.9 (0.8)	33.40 (0.11)	2223 (12)	1870 (26)	143 (13)	3.44 (0.32)	2.21 (0.21)

Measured parameters ($n = 12$ per treatment) are indicated by asterisk.

third tank was adjusted for decreased pH and increased temperature ($pH_{SWS} = 7.48 \pm 0.10$; $pCO_2 = 1620 \pm 486$ μatm; 20.2 ± 0.4 °C). Experimental values were selected to approach current predictions for temperature increases of 3 °C by the year 2100 and decreases in ocean surface pH values of 0.3 pH units, although experimental pH values were considerably lower (IPCC, 2014).

Decreased pH conditions were accomplished by bubbling 100% CO_2 into the two treatment-header tanks, which was controlled by an Apex Lite aquarium controller (pH accuracy 0.01; temperature accuracy 0.1 °C, Neptune Systems, Morgan Hill, CA, USA). For the decreased pH/increased temperature treatment, ambient seawater was mixed with heated ambient seawater fed into the header tank. Both pH and temperature in the header tanks were continuously monitored with the Apex controller (data logged every 20 min.). One aquarium pump (Hydor Koralia pump, 425 gph, Bassano del Grappa, Italy) was placed in each header tank to provide adequate mixing. Each header tank supplied flow-through seawater to 16 experimental tanks (1.89 L, Lee's Kritter Keeper, CA, USA) that contained single shrimp, for a combined total of 48 individuals.

Prior to the start of the experiment, individuals were assigned to each treatment so that body size and colour morph (brown or green) were evenly distributed across treatments. Some shrimp initially had eggs and were thus divided equally among the treatments ($n = 7$ or 8 egg-carrying specimens per treatment). Experimental water parameters were gradually altered over the course of 3 days in an effort to minimize abrupt transitions of conditions and potential stress. Once the targeted water parameters were reached, the experiment was run for 7 weeks. Animals were checked daily for moulting, with the shed exoskeleton (exuviae) promptly removed.

Water chemistry

Daily readings of pH and temperature were taken for 7 weeks from each tank (header and experimental) using a portable probe (HQ40d, probe PHC201, accuracy 0.01 pH, 0.1 temperature, Hach, Loveland, CO, USA). All pH probes were calibrated weekly with NBS buffer solutions (Fisher Scientific, Fair Lawn, NJ, USA). In addition, water samples were collected from each header tank and a subset of experimental tanks (two random tanks from each treatment) at the start of the experiment and every 3 weeks (four samplings total) in accordance with standard operating procedures (Dickson *et al.*, 2007). All water samples were submitted to the Dickson laboratory at SIO for analysis of pH_{SWS}, density-based salinity, and total alkalinity (A_T) at 25 °C (Table 1). Carbonate and aragonite saturation states, concentrations of carbonate and bicarbonate, and pCO_2 were calculated using CO_2Sys 2.01 (Table 1) (Pierrot *et al.*, 2006). For calculations, dissociation constants of K_1, K_2 were from Mehrbach *et al.* (1973), refit by Dickson and Millero (1987). The HSO_4 constant was from Dickson (1990), the $[B]_T$ value was from Uppstrom (1974), and the seawater pH scale was used. Water samples were used to calculate the average difference between Hach pH probe readings and spectrophotometric pH values per sampling set. Corrected daily measures of pH from the Hach probe were then averaged for the experimental tanks in each treatment (Table 1).

Growth

At both the start and end of the experiment, and before further analyses, each shrimp was photographed dorsally and laterally with an HD digital camera (Leica DFC290, Buffalo Grove, IL, USA) attached to a stereomicroscope (Leica M165 C, Buffalo Grove, IL, USA). From the dorsal images, carapace length was measured from both the left and right eye orbits to the centre of the posterior edge of the carapace using the microscope software (LAS 4, Leica Microsystems, Buffalo Grove, IL, USA). Animals were then consistently blotted dry and weighed with an analytical balance. Initial carapace length ranged from 7.15 to 9.99 mm and initial body mass ranged from 0.027 to 0.062 g. Shrimp were assigned to treatments such that each had similar means and ranges of body size. All animals appeared healthy and intact.

Mineralization

After shrimp were photographed and weighed at the end of the experiment ($n = 13$ for ambient, $n = 14$ for decreased pH, $n = 8$ for decreased pH/increased temperature), they were euthanized by quickly separating the carapace from the abdomen with a razor blade (except for those used for biophotonic analysis; see below). The carapace section was immediately placed in a −20 °C freezer until elemental trace analysis was performed using inductively coupled plasma mass spectrometry (ICP-MS). Cleaned carapace cuticle samples were placed in a freeze dryer for 24 h before being weighed and placed in Teflon vials for digestion with 0.5 ml of concentrated Teflon-distilled (TD) nitric acid (HNO_3) on a hotplate at 120 °C for >24 h. Samples were dried down and diluted by a factor of 4000 with 2% TD HNO_3 before being transferred to pre-cleaned centrifuge tubes for analysis. Samples were doped with an indium solution at this time to monitor instrumental drift. Measurements were done using a *ThermoScientific iCAPq* c ICP-MS (Thermo Fisher Scientific GmbH, Bremen, Germany), in standard mode. Masses of Mg and Ca were sequentially measured for 30 ratios, resulting in internal precision of <2% (2 s.d.). Elements were corrected for total mole fraction ($n = 13$, 7, 13; two less samples due to missed runs). Total procedural blanks represented <0.3% of the measurement for Mg and Ca. Raw data were corrected off line for instrument background and drift. Samples were bracketed by internal standards of crab carapace ($n = 3$) and two artificial fish otolith solutions,

which allowed for calculation of absolute values. The standards yielded external precision of better than 1% for Mg and Ca (2 s.d.).

Biophotonics: spectral reflectance and transmittance measurements

Three shrimp from each treatment were randomly selected and euthanized in a −20 °C freezer before being analysed for biophotonic properties as described earlier in Taylor *et al.* (2015). Briefly, transmission (transparency) and bright field spectral reflectance (here considered colour for simplification) were quantified using PARISS® hyperspectral imaging from the same general area of each shrimp, for consistency. This area was reached by moving the electronically controlled stage 500 µm anteriorly from the centre of the posterior edge of the carapace. Analyses were performed on a Nikon 80i microscope at the 4× objective, which was calibrated for spectral accuracy before each day of analyses. Acquisition parameters and identification and mapping of common spectra were performed as previously described in Taylor *et al.* (2015). Analyses of transmittance and spectral reflectance were both collected from the dorsal and lateral view of the shrimp; as the data were similar for both angles of the body, only the dorsal data were considered further.

Statistical analyses

All water parameters, growth, mineralization, and colouration data were tested for normality using Shapiro-Wilk tests and for homogeneity of variances using Bartlett's test. ANOVA or Kruskal-Wallis tests were used to compare data across treatments, with *post-hoc* tests (Tukey HSD, Dunn's test) used when warranted. ANCOVAs were used to examine how initial shrimp size (mass or length) related to percent change in growth across treatments. All statistical analyses were performed using R version 3.2.0 (R Core Team, 2015). All data are presented as mean ± s.d.

Results

Water chemistry

pH was relatively stable throughout the experiment, although there was an unexpected drop of pH conditions midway through the experiment. Indeed, for the first two water sampling periods, the ambient pH was stable (adjusted Hach pH readings; 8.03 ± 0.02, $n = 270$) but then dropped by 0.07 pH units for the last two periods (pH = 7.95 ± 0.01, $n = 447$). The drop was found in all treatments. In the decreased pH treatment, the pH values were 7.61 ± 0.03 ($n = 280$) and 7.48 ± 0.04 ($n = 438$) (a drop of 0.13 pH units), and in the decreased pH/increased temperature treatment, these values were 7.59 ± 0.06 ($n = 273$) and 7.42 ± 0.05 ($n = 438$) (a drop of 0.17 pH units). Thus, animals experienced relatively steady pH during each of the two periods, but had to accommodate a drop in pH treatments midway through the experiment. This drop could not be correlated with any specific changes in environmental conditions of seawater offshore and might be due to the replacement of a broken Hach pH probe, which occurred at that time.

The pH of the decreased pH treatment and the decreased pH/increased temperature treatment was not significantly different during the first half of the experiment (Dunn, df = 5, $n = 280$, 273 $p = 0.065$). However, the pH of these treatments was significantly different from one another during the second half of the experiment by about 0.06 pH units (Dunn, df = 5, $n = 438$, 438, $p = 0.0001$). Temperatures in the ambient and decreased pH treatments were not significantly different from one another (Dunn, df = 2, $n = 695, 691$, $p = 0.13$) (Table 1).

Nevertheless, calculated pCO_2 was not significantly different between the decreased pH (1452 ± 260 µatm) and decreased pH/increased temperature (1620 ± 486 µatm) treatments over the course of the experiment (ANOVA: $F_{2,33} = 45.49$, $n = 12$, $p < 0.001$; Tukey test, $n = 12$, df = 2, $p = 0.41$) (Table 1). However, these treatments were both significantly different from the ambient pCO_2 (465 ± 64 µatm) (ANOVA: $F_{2,33} = 45.49$, $n = 12$, $p < 0.001$; Tukey, $n = 12$, df = 2, $p < 0.001$) (Table 1).

Survival and growth

There was no mortality during the experiment, but several individuals escaped their tanks through small gaps in the mesh lids and were discounted from further analysis (escapees: ambient: $n = 3$; decreased pH: $n = 2$; decreased pH/increased temperature: $n = 8$). All animals moulted at least twice, with an average of 3.9 ± 1.2 moults in ambient, 3.9 ± 0.9 moults in decreased pH, and 4.4 ± 0.9 moults in decreased pH/increased temperature treatments. There were no significant differences in the number of moults among treatments (Kruskal-Wallis, df = 2, $n = 13, 14, 8$, $p = 0.66$).

All shrimp showed increases in growth parameters of carapace length and body mass. Percent growth in carapace length was not significantly different among treatments: 11.4 ± 6.4, 14.8 ± 10.6, and 17.1 ± 7.8%, in the ambient, decreased pH, and decreased pH/increased temperature treatments, respectively (Kruskal-Wallis, df = 2, $n = 13, 14, 8$, $p = 0.27$). However, shrimp in all treatments showed typical logarithmic growth; smaller animals had a greater growth increment (carapace length) than larger animals (ANCOVA: $F_{3,31} = 7.51$, slope = −6.22, $R^2 = 0.421$, $p = 0.0002$, Figure 1a). Percent growth data were log-transformed prior to linear regression analysis. When initial length is included as a covariate, shrimp from the decreased pH/increased temperature treatment grew slightly more (0.09–0.24 mm larger, on average) than those in the other two treatments (ANCOVA: $F_{3,31} = 7.51$, $n = 13, 14, 8$, slope = −6.22, $R^2 = 0.421$, $p = 0.03$, Figure 1a).

Percent growth in body mass was 24.2 ± 10.0% in ambient, 34.7 ± 35.3% in decreased pH, and 33.3 ± 17.7% in decreased pH/increased temperature treatments, respectively, and were not signficantly different from one another (Kruskal-Wallis, df = 2, $n = 13, 14, 8$, $p = 0.58$). Shrimp also showed logarithmic growth in body mass, when initial mass was included as a covariate (ANCOVA: $F_{3,31} = 3.005$, slope = −2.113, $R^2 = 0.2253$, $n = 13, 14, 8$, $p = 0.008$, Figure 1b). There were no significant differences in the relationship between percent change in body mass to initial mass among treatments (ANCOVA: $F_{3,31} = 3.005$, slope = −2.113, $R^2 = 0.2253$, $n = 13, 14, 8$, $p = 0.22, 0.82$, Figure 1b).

Mineralization

ICP-MS analysis revealed that the mean concentration (µmol element (mg cuticle)$^{-1}$) of Ca in the carapace cuticle samples was not different among treatments (ANOVA, $F_{2,30} = 0.063$, $n = 13, 7, 13$, $p = 0.94$) (Figure 2). The mean concentration of Mg also did not differ among treatments (ANOVA, $F_{2,30} = 0.115$, $n = 13, 7, 13$, $p = 0.89$) (Figure 2).

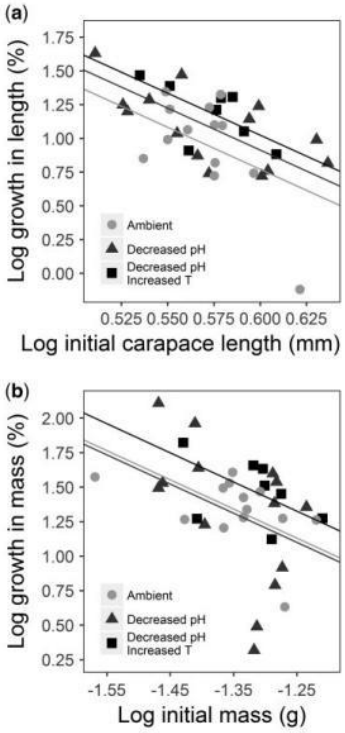

Figure 1. Shrimp growth. (a) Percent growth in carapace length for shrimp in ambient, decreased pH, and decreased pH/increased temperature treatments. Slopes for the log-transformed data did not differ among treatments. The y-intercepts were significantly different, revealing that shrimp in decreased pH/increased temperature grew significantly more at a given initial size compared with those in ambient and decreased pH treatments. (b) All shrimp of a given initial mass increased in mass similarly, with no effect of treatment.

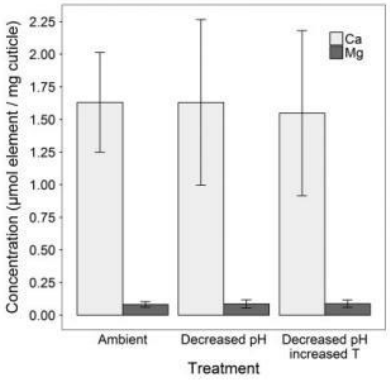

Figure 2. Mean concentrations of Mg and Ca across treatments. Shrimp did not exhibit changes in mineralization under decreased pH and decreased pH/increased temperature conditions.

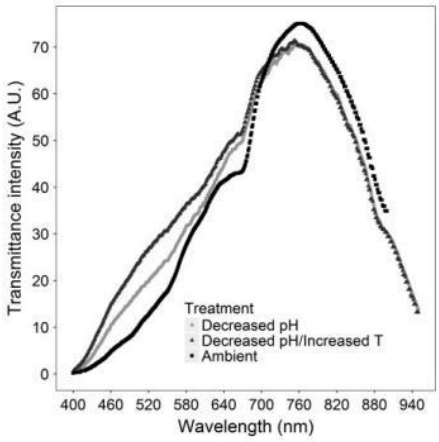

Figure 3. Representative transmittance spectra for shrimp from ambient, decreased pH and decreased pH/increased temperature treatments in arbitrary units (AU). There were no differences in spectral profile or intensity among treatments.

Biophotonics: spectral reflectance and transmittance

Neither shrimp transmittance nor spectral reflectance were affected by decreased pH and decreased pH/increased temperature treatments, both in terms of intensity and spectral profile (Figures 3 and 4). Transmittance peaked at 750–760 nm (red/near infrared) for shrimp from all treatments (Figure 3). Spectral reflectance for all shrimp peaked at multiple wavelengths, although it was highest at 715–720 nm (red) and steeply dropped off at longer wavelengths. Additional peaks occurred at 614–618 nm (orange/red) and 470–476 (blue) in all shrimp, while most light was absorbed at 530–535 nm (green) (Figure 4).

Discussion

Colouration of shrimp is a critical aspect of their ecology that may be susceptible to ocean acidification and warming as a result of induced physiological stress and changes to exoskeleton calcification. We studied the grass shrimp *H. californiensis* and found that it is robust to both decreased pH and decreased pH/increased temperature in terms of growth (moult frequency, moult increment), exoskeleton mineralization (Ca and Mg content), and biophotonics (transmittance and spectral reflectance).

Shrimp tolerance to pH and temperature stressors

Different responses of caridean shrimp to similar stressors demonstrate the important role that experimental conditions, specific

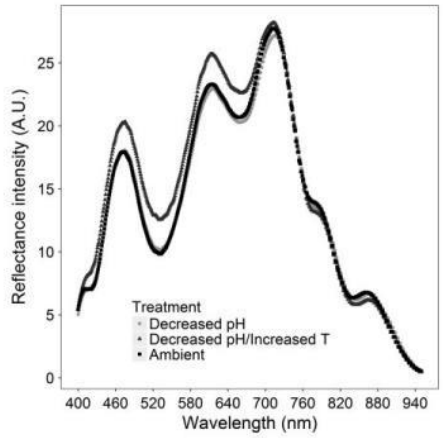

Figure 4. Representative reflectance spectra for shrimp from ambient, decreased pH and decreased pH/increased temperature treatments in AUs There were no differences in spectral profile or intensity among treatments.

habitats, and evolutionary history play. The tolerance demonstrated by *H. californiensis* in our study could be a result of the duration of our experiment, which lasted 7 weeks. A similar study on the red rock shrimp, *L. californica*, showed significant changes in calcification and transparency under comparable pH conditions within a shorter time frame of 3 weeks (Taylor *et al.*, 2015). It is possible that the longer duration of this experiment provided more time for grass shrimp to adjust to decreased pH conditions. Indeed, individual species show responses to OA conditions on different time scales (Long *et al.*, 2013), indicating the importance of evaluating responses over broader temporal regimes.

Grass shrimp may also exhibit tolerance to our experimental conditions due to their adaptation to habitat-specific pH and temperature variability. While the red rock shrimp *L. californica* lives in rocky habitats in the same geographic area, *H. californiensis* inhabits shallow eelgrass meadows in quiet bays; the latter can experience relatively large seasonal changes in temperature (15–25 °C) (Elliott and Kaufmann, 2007) and likely experiences daily and seasonal pH fluctuations due to its location in the bay, where water circulation is low and dissolved inorganic carbon is taken up in conjunction with photosynthesis (Larkum *et al.*, 2007). Our experiment did not replicate the natural daily fluctuations of pH and temperature in the eelgrass habitat, but it did reveal that *H. californiensis* tolerates large but stable reductions in pH. It is not yet understood how fluctuating versus stable reductions in pH affect animal responses, but exposure to broadened fluctuations of pH may change the response of animals already near their limits of physiological tolerance. Our decreased pH treatments were 0.2 pH units lower than our target of 7.7, but they were within present-day pH ranges experienced by some seagrass habitats (Hendriks *et al.*, 2014; Challener *et al.*, 2015). Though the pH range in the eelgrass habitat of *H. californiensis* was not measured for this study, it is likely that our low experimental pH may already be reached for brief periods in this fluctuating environment and thus be within the expected physiological tolerance of this grass shrimp.

Survival and growth largely unaffected

Crustacean moult frequency and increment are susceptible to environmental conditions such as temperature (Fowler *et al.*, 1971), but responses to decreased pH are mixed among species and life stages (Kurihara *et al.*, 2008). Here, neither decreased pH nor decreased pH/increased temperature affected the moult frequency of *H. californiensis*. Shrimp moulted an average of three times, or approximately every 16 days, which is comparable to the grass shrimps *P. pugio* and *Hippolyte williamsi* that moulted every 10 and 36 days, respectively, under ambient laboratory conditions (Oberdörster *et al.*, 2000; Espinoza-Fuenzalida *et al.*, 2008).

Although decreased pH altered the growth increment in some species of crustaceans, such as juvenile tanner crabs and juvenile marine shrimp *Palaemon pacificus* (Kurihara, 2008; Long *et al.*, 2013), it did not affect *H. californiensis*. Shrimp exhibited the same logarithmic growth curves across treatments; smaller shrimp showed greater increases in both mass and carapace length than larger shrimp, as expected. Thus, decreased pH alone (pH 7.5) did not affect the growth of *H. californiensis* under our experimental settings.

The combined stressors of decreased pH/increased temperature did not affect moulting frequency either, despite increases typically observed at higher temperatures (Travis, 1954; Fowler *et al.*, 1971; Breteler, 1975; Iguchi and Ikeda, 1995). These combined stressors, however, did affect linear growth; shrimp in the decreased pH/increased temperature treatment showed a greater percent growth in carapace length at all sizes than shrimp in ambient and decreased pH treatments. Thus, shrimp experienced increased growth of the exoskeleton when reduced pH was combined with the higher temperature. Though the direct effect of temperature was not tested, moderate increases of temperature alone are well-documented to increase growth in crustaceans (Ponce-Palafox *et al.*, 1997; Crear *et al.*, 2000; Stoner *et al.*, 2010). These results highlight the importance of studying multiple stressors together.

Cuticle mineralization remains unaffected

We hypothesized that shrimp cuticle would exhibit increased calcification under decreased pH, as observed in the red rock shrimp under similar pH conditions (Taylor *et al.*, 2015) and other species of crustaceans, including barnacles and prawns (Wickins, 1984; McDonald *et al.*, 2009; Findlay *et al.*, 2010). Other crustaceans, such as the mantis shrimp *Neogonodactylus bredini*, may show changes in one calcifying element (Mg) but not another (Ca) (deVries *et al.*, 2016), suggesting preferential building of calcite, magnesian calcite, or amorphous calcium carbonate. In *H. californiensis*, there was no difference in the concentration of magnesium and calcium in the cuticle, the two elements typically used for mineralization. Thus, *H. californiensis* experienced no net changes in calcification under our experimental conditions, in alignment with some species of barnacle and crab (Findlay *et al.*, 2010; Small *et al.*, 2010; Long *et al.*, 2013). In contrast, other taxa, such as corals and mollusks, experience mostly decreases in calcification, as revealed via meta-analysis (Kroeker *et al.*, 2013)

Active crustaceans are believed to have strong acid-base regulation abilities, as bicarbonate taken up from the seawater through

the gills may be able to partially or fully compensate for hemolymph acidosis (Melzner *et al.*, 2009). However, it is plausible that this bicarbonate can be used as a precursor to calcium carbonate (Small *et al.*, 2010), which may allow some species to maintain calcification in undersaturated conditions. The specific mechanism(s) driving the mixed effects of OA on calcification in crustacean species is in need of more targeted study.

Transparency and colour are robust to environmental change

Neither decreased pH nor decreased pH/increased temperature affected the transmittance and reflectance of the shrimp. Because transparency was measured through both the exoskeleton and tissue, these results indicate that there are no additional light-scattering discontinuities in the ultrastructure of cuticle formed under these conditions, and either that shrimp tissue did not become more opaque, as can occur when animals are stressed by abiotic conditions (Bhandiwad and Johnsen, 2011), or that the effects of the rest of the body overwhelmed any effect on the cuticle. In contrast, transparency decreased significantly in the shrimp *L. californica* under similar decreased pH conditions (Taylor *et al.*, 2015). Unlike *H. californiensis*, however, *L. californica* experienced concomitant increases in cuticle calcification, which may have been the main contributing factor to the observed change in transparency.

Spectral reflectance (colour) of shrimp was also unaffected by pH and temperature stressors. All shrimp demonstrated peaks in blue, yellow, and especially red/infrared wavelengths, although reflectance overall was relatively low, around 27% for these shrimp compared with the 80% of red stripes for *L. californica* (Taylor *et al.*, 2015). Spectral reflectance of *H. californiensis* is comparable to that of blue fiddler crabs, *Uca panacea*, which was <15% (Darnell, 2012). Green wavelengths, however, were particularly absorbed in dull-coloured experimental shrimp, a contrast to what most newly caught, vibrant green shrimp must be primarily reflecting. Thus, while spectral reflectance of experimental shrimp measured here may not represent wild shrimp, the attrition of colour in the laboratory setting was similar across treatments. Our results, however, show that neither decreased pH alone nor decreased pH in tandem with increased temperature affects the biophotonics of these grass shrimp, suggesting that their crypsis will likely be unaffected by future ocean acidification and warming.

Conclusions

In contrast to other studied shrimp, reduced pH conditions did not appear to affect the growth, mineralization, and biophotonic properties of grass shrimp in our study, which emphasizes the variable responses of closely related species and the importance of exposure duration and habitat conditions. Combined pH and temperature stressors had a slight effect on animal growth, demonstrating the importance of using a multi-stressor approach in studies of potential organismal responses to OA. Overall, this study encourages further OA research focused on crustaceans and aspects of ecological importance.

Acknowledgements

We are especially grateful to Zerofski for aid in animal collection and help with the experimental tank system set-up, Maya deVries for her input throughout this experiment, Jenny Tu for her aid in the analysis of colouration, and David Cervantes, Guy Emanuele, and Andrew Dickson from SIO's Dickson Laboratory for analyzing water chemistry samples. Janell Kosmatka, Brenda Groom, Jasmine Lin, and Kaiin Wong provided help with experimental care and colouration analysis. We also thank S. Johnsen for feedback on preparation of the article.

Funding

The hyperspectral imager was funded by Air Force Office of Scientific Research (AFOSR) grant no. MURI BIOPAINTS FA9550-10-1-0555 to D.D.D. Research was funded by the Marine Biology Research Division at Scripps Institution of Oceanography to J.R.A.T.

References

Bhandiwad, A., and Johnsen, S. 2011. The effects of salinity and temperature on the transparency of the grass shrimp *Palaemonetes pugio*. The Journal of Experimental Biology, 214: 709–716.

Breteler, W. K. 1975. Laboratory experiments on the influence of environmental factors on the frequency of moulting and the increase in size at moulting of juvenile shore crabs, *Carcinus maenas*. Netherlands Journal of Sea Research, 9: 100–120.

Brown, F. A., and Sandeen, M. I. 1948. Responses of the chromatophores of the fiddler crab, Uca, to light and temperature. Physiological Zoology, 21: 361–371.

Busch, D. S., and McElhany, P. 2016. Estimates of the direct effect of seawater pH on the survival rate of species groups in the California current ecosystem. PloS One, 11: e0160669.

Caron, S., and Rainboth, W. J. 1992. Field analysis of color cues that elicit territorial behavior in the Garibaldi, *Hypsypops rubicundus* (Pomacentridae). Copeia, 1992: 1080–1084.

Challener, R. C., Robbins, L. L., and McClintock, J. B. 2015. Variability of the carbonate chemistry in a shallow, seagrass-dominated ecosystem: implications for ocean acidification experiments. Marine and Freshwater Research, 67: 163–172.

Cheney, K. L., Grutter, A. S., Blomberg, S. P., and Marshall, N. J. 2009. Blue and yellow signal cleaning behavior in coral reef fishes. Current Biology, 19: 1283–1287.

Cott, H. B. 1940. Adaptive coloration in animals, Methuen & Co. Ltd., London. 508 pp.

Crear, B., Thomas, C., Hart, P., and Carter, C. 2000. Growth of juvenile southern rock lobsters, *Jasus edwardsii*, is influenced by diet and temperature, whilst survival is influenced by diet and tank environment. Aquaculture, 190: 169–182.

Darnell, M. Z. 2012. Ecological physiology of the circadian pigmentation rhythm in the fiddler crab *Uca panacea*. Journal of Experimental Marine Biology and Ecology, 426: 39–47.

Detto, T., Hemmi, J. M., and Backwell, P. R. Y. 2008. Colouration and Colour Changes of the Fiddler Crab, *Uca capricornis*: A Descriptive Study. PLoS One, 3: e1629.

deVries, M. S., deVries, M. S., Webb, S. J., Tu, J., Cory, E., Morgan, V., Sah, R. L., et al. 2016. Stress physiology and weapon integrity of intertidal mantis shrimp under future ocean conditions. Scientific Reports, 6: 38637.

Dickson, A. G. 1990. Standard potential of the reaction: AgCl (s) + $^{12}H_2$ (g) = Ag (s) + HCl (aq), and the standard acidity constant of the ion HSO_4^- in synthetic sea water from 273.15 to 318.15 K. The Journal of Chemical Thermodynamics, 22: 113–127.

Dickson, A., and Millero, F. J. 1987. A comparison of the equilibrium constants for the dissociation of carbonic acid in seawater media. Deep Sea Research Part A. Oceanographic Research Papers, 34: 1733–1743.

Dickson, A. G., Sabine, C. L., and Christian, J. R. 2007. Guide to Best Practices for Ocean CO_2 Measurements. North Pacific Marine Science Organization, Sidney, BC. 191 pp.

Elliott, D. T., and Kaufmann, R. S. 2007. Spatial and temporal variability of mesozooplankton and tintinnid ciliates in a seasonally hypersaline estuary. Estuaries and Coasts, 30: 418–430.

Espinoza-Fuenzalida, N. L., Thiel, M., Dupre, E., and Baeza, J. A. 2008. Is *Hippolyte williamsi* gonochoric or hermaphroditic? A multi-approach study and a review of sexual systems in Hippolyte shrimps. Marine Biology, 155: 623–635.

Findlay, H. S., Kendall, M. A., Spicer, J. I., and Widdicombe, S. 2010. Post-larval development of two intertidal barnacles at elevated CO_2 and temperature. Marine Biology, 157: 725–735.

Fingerman, M., and Tinkle, D. W. 1956. Responses of the white chromatophores of two species of prawns (*Palaemonetes*) to light and temperature. Biological Bulletin, 110: 144–152.

Fowler, S., Small, L., and Kečkeš, S. 1971. Effects of temperature and size on molting of euphausiid crustaceans. Marine Biology, 11: 45–51.

Hanlon, R. 2007. Cephalopod dynamic camouflage. Current Biology, 17: R400–R404.

Hanlon, R. T., Watson, A. C., and Barbosa, A. 2010. A "mimic octopus" in the Atlantic: flatfish mimicry and camouflage by *Macrotritopus defilippi*. The Biological Bulletin, 218: 15–24.

Harvey, B. P., Gwynn, -Jones, D., and Moore, P. J. 2013. Meta-analysis reveals complex marine biological responses to the interactive effects of ocean acidification and warming. Ecology and Evolution, 3: 1016–1030.

Hendriks, I. E., Olsen, Y. S., Ramajo, L., Basso, L., Steckbauer, A., Moore, T. S., Howard, J., et al. 2014. Photosynthetic activity buffers ocean acidification in seagrass meadows. Biogeosciences, 11: 333–346.

Iguchi, N., and Ikeda, T. 1995. Growth, metabolism and growth efficiency of a euphausiid crustacean *Euphausia pacifica* in the southern Japan Sea, as influenced by temperature. Journal of Plankton Research, 17: 1757–1769.

IPCC. 2013. Climate Change 2013: The Physical Science Basis. Contribution of Working Group I to the Fifth Assessment Report of the Intergovernmental Panel on Climate Change. Ed. by Stocker, T. F., Qin D., Plattner G.-K., Tignor M., Allen S. K., Boschung J., Nauels A., Xia Y., Bex V. and Midgley P. M. Cambridge University Press, Cambridge, UK and New York, NY, USA, 1535 pp.

IPCC. 2014. Climate Change 2014: Synthesis Report. Contribution of Working Groups I, II and III to the Fifth Assessment Report of the Intergovernmental Panel on Climate Change. Eds. by Core Writing Team, R. K. Pachauri and L. A. Meyer. IPCC, Geneva, Switzerland, 151 pp.

Jensen, G. C., and Egnotovich, M. S. 2015. A whiter shade of male: Color background matching as a function of size and sex in the yellow shore crab *Hemigrapsus oregonensis* (Dana, 1851). Current Zoology, 61: 729–738.

Johnsen, S. 2001. Hidden in plain sight: the ecology and physiology of organismal transparency. The Biological Bulletin, 201: 301–318.

Keeble, F. W., and Gamble, F. W. 1899. The colour-physiology of *Hippolyte varians*. Proceedings of the Royal Society of London, 65: 461–468.

Kroeker, K. J., Kordas, R. L., Crim, R., Hendriks, I. E., Ramajo, L., Singh, G. S., Duarte, C. M., et al. 2013. Impacts of ocean acidification on marine organisms: quantifying sensitivities and interaction with warming. Global Change Biology, 19: 1884–1896.

Kurihara, H. 2008. Effects of CO_2-driven ocean acidification on the early developmental stages of invertebrates. Marine Ecology Progress Series, 373: 275–284.

Kurihara, H., Masaaki, M., Hiroko, F., Masahiro, H., and Atsushi, I. 2008. Long-term effects of predicted future seawater CO_2 conditions on the survival and growth of the marine shrimp *Palaemon pacificus*. Journal of Experimental Marine Biology and Ecology, 367: 41–46.

Larkum, A. W., Drew, E. A., and Ralph, P. J. 2007. Photosynthesis and metabolism in seagrasses at the cellular level. *In* Seagrasses: Biology, Ecology, and Conservation, pp. 323–345. Springer, Netherlands.

Lee, W. L. 1966. Color change and the ecology of the marine isopod *Idothea (Pentidothea) montereyensis* Maloney, 1933. Ecology, 47: 930–941.

Li, C., Meng, Y., He, C., Chan, V. B., Yao, H., and Thiyagarajan, V. 2016. Mechanical robustness of the calcareous tubeworm *Hydroides elegans*: warming mitigates the adverse effects of ocean acidification. Biofouling, 32: 191–204.

Long, W. C., Swiney, K. M., and Foy, R. J. 2017. Effects of high pCO_2 on Tanner crab reproduction and early life history, Part II: carryover effects on larvae from oogenesis and embryogenesis are stronger than direct effects. ICES Journal of Marine Science, 74: 1191–1200.

Long, W. C., Swiney, K. M., Harris, C., Page, H. N., and Foy, R. J. 2013. Effects of ocean acidification on juvenile red king crab *(Paralithodes camtschaticus)* and Tanner crab *(Chionoecetes bairdi)* growth, condition, calcification, and survival. Plos One, 8: e60959.

McDonald, M. R., McClintock, J. B., Amsler, C. D., Rittschof, D., Angus, R. A., Orihuela, B., and Lutostanski, K. 2009. Effects of ocean acidification over the life history of the barnacle *Amphibalanus amphitrite*. Marine Ecology Progress Series, 385: 179–187.

Mehrbach, C., Culberson, C. H., Hawley, J. E., and Pytkowicz, R. M. 1973. Measurement of the apparent dissociation constants of carbonic acid in seawater at atmospheric pressure. Limnology and Oceanography, 18: 897–907.

Melzner, F., Gutowska, M., Langenbuch, M., Dupont, S., Lucassen, M., Thorndyke, M. C., Bleich, M., Pörtner, H.-O. 2009. Physiological basis for high CO_2 tolerance in marine ectothermic animals: pre-adaptation through lifestyle and ontogeny? Biogeosciences, 6: 2313–2331.

Oberdörster, E., Brouwer, M., Hoexum-Brouwer, T., Manning, S., and McLachlan, J. A. 2000. Long-term pyrene exposure of grass shrimp, *Palaemonetes pugio*, affects molting and reproduction of exposed males and offspring of exposed females. Environmental Health Perspectives, 108: 641.

Paganini, A. W., Miller, N. A., and Stillman, J. H. 2014. Temperature and acidification variability reduce physiological performance in the intertidal zone porcelain crab *Petrolisthes cinctipes*. Journal of Experimental Biology, 217: 3974–3980.

Perazzolo, L. M., Gargioni, R., Ogliari, P., and Barracco, M. A. 2002. Evaluation of some hemato-immunological parameters in the shrimp *Farfantepenaeus paulensis* submitted to environmental and physiological stress. Aquaculture, 214: 19–33.

Pierrot, D., Lewis, E., and Wallace, D. W. R. 2006. MS Excel Program Developed for CO_2 System Calculations. ORNL/CDIAC-105a. Department of Energy, Oak Ridge, Tennessee. Carbon Dioxide Information Analysis Center, Oak Ridge National Laboratory, USA.

Ponce-Palafox, J., Martinez-Palacios, C. A., and Ross, L. G. 1997. The effects of salinity and temperature on the growth and survival rates of juvenile white shrimp, *Penaeus vannamei*, Boone, 1931. Aquaculture, 157: 107–115.

Powell, B. 1962. The responses of the chromatophores of *Carcinus maenas* (L., 1758) to light and temperature. Crustaceana, 4: 93–102.

R Core Team 2015. R: A Language and Environment for Statistical Computing. R Foundation for Statistical Computing, Vienna, Austria.

Rao, K. R., and Nagabhushanam, R. 1967. The responses of the white chromatophores of the crab *Uca annulipes* (H. Milne Edwards) to light and temperature. Crustaceana, 13: 155–160.

Silbiger, N., and Munguia, P. 2008. Carapace color change in *Uca pugilator* as a response to temperature. Journal of Experimental Marine Biology and Ecology, 355: 41–46.

Small, D., Calosi, P., White, D., Spicer, J. I., and Widdicombe, S. 2010. Impact of medium-term exposure to CO_2 enriched seawater on the physiological functions of the velvet swimming crab, *Necora puber*. Aquatic Biology, 10: 11–21.

Small, D. P., Calosi, P., Boothroyd, D., Widdicombe, S., and Spicer, J. I. 2016. The sensitivity of the early benthic juvenile stage of the European lobster *Homarus gammarus* (L.) to elevated pCO_2 and temperature. Marine Biology, 163: 1–12.

Smith, D. C. 1930. The effects of temperature changes upon the chromatophores of crustaceans. The Biological Bulletin, 58: 193–202.

Stevens, M., and Merilaita, S. 2011. Animal camouflage: mechanisms and function, Cambridge University Press, New York, USA.

Stoner, A. W., Ottmar, M. L., and Copeman, L. A. 2010. Temperature effects on the molting, growth, and lipid composition of newly-settled red king crab. Journal of Experimental Marine Biology and Ecology, 393: 138–147.

Swiney, K. M., Long, W. C., and Foy, R. J. 2015. Effects of high pCO_2 on Tanner crab reproduction and early life history—Part I: long-term exposure reduces hatching success and female calcification, and alters embryonic development. ICES Journal of Marine Science. DOI: 10.1093/icesjms/fsv201.

Taylor, J. R. A., Gilleard, J. M., Allen, M. C., and Deheyn, D. D. 2015. Effects of CO_2-induced pH reduction on the exoskeleton structure and biophotonic properties of the shrimp *Lysmata californica*. Scientific Reports, 5: 10608.

Travis, D. F. 1954. The molting cycle of the spiny lobster, *Panulirus argus* Latreille. I. Molting and growth in laboratory-maintained individuals. The Biological Bulletin, 107: 433–450.

Umbers, K. D., Fabricant, S. A., Gawryszewski, F. M., Seago, A. E., and Herberstein, M. E. 2014. Reversible colour change in Arthropoda. Biological Reviews, 89: 820–848.

Uppstrom, L. R. 1974. The boron/chloronity ratio of deep-sea water from the Pacific Ocean. Deep-Sea Research, 21: 161–162.

Wahle, R. A., Dellinger, L., Olszewski, S., and Jekielek, P. 2015. American lobster nurseries of southern New England receding in the face of climate change. ICES Journal of Marine Science, 72: i69–i78.

Waller, J. D., Wahle, R. A., McVeigh, H., and Fields, D. M. 2017. Linking rising pCO2 and temperature to the larval development and physiology of the American lobster (Homarus americanus). ICES Journal of Marine Science, 74: 1210–1219.

Wickins, J. 1984. The effect of hypercapnic sea water on growth and mineralization in penaied prawns. Aquaculture, 41: 37– 48.

Zylinski, S., and Johnsen, S. 2011. Mesopelagic cephalopods switch between transparency and pigmentation to optimize camouflage in the deep. Current Biology, 21: 1937–1941.

Handling editor: Brock Woodson

Acknowledgements

Chapter 4, in full, is a reprint of the material as it appears in **Lowder, K.B.,** Allen, M.C., Day, J.M., Deheyn, D.D. and Taylor, J.R.A., 2017. Assessment of ocean acidification and warming on the growth, calcification, and biophotonics of a California grass shrimp. *ICES Journal of Marine Science*, *74*(4), pp.1150-1158. The dissertation author was the primary investigator and author of this material. The material is used by permission of Oxford University Press.

Conclusions

Both southern California crustaceans were quite tolerant of ocean acidification and ocean warming-like conditions predicted for the region in the next century. California spiny lobster larvae and juveniles exposed to stable reduced pH maintained their survival, growth, and a suite of predator defenses relative to lobsters in control conditions (Chapters 2 and 3). When exposed to fluctuating, reduced pH conditions, however, juveniles showed different, often negative responses, indicating how important it is to incorporate natural variability into OA experiments to best predict future responses of all marine organisms. While juveniles in reduced pH conditions were able to detect the chemical cues of predators and tail-flip away to avoid threats, we found differences in how the various regions of the exoskeleton armor responded to these conditions, stemming from their differences in construction (Chapter 1). This underlines the importance of studying multiple body structures when exposing organisms to changes in abiotic conditions, as focusing on a single region and its response, whether it is negatively, positively, or neutrally affected, can drastically skew the overall prognosis for the species. Grass shrimp, despite the differences in habitat and defense strategies, responded just as the spiny lobsters did to pH decreases, without any discernable changes (Chapter 4). There have been a variety of crustacean responses to stable OA-like conditions described in the literature, and very few species have exhibited tolerance across all studied responses, especially considering the breadth of measures performed in these experiments. There is still much to learn about the mechanisms behind both species' tolerance, but it might stem from their mutual "weed-haunting habit," as Keeble and Gamble describe the habitat preference of *Hippolyte* shrimp in their 1904 paper, "The Colour-Physiology of Higher Crustacea." The variable conditions found within autotroph-dominated environments, especially in the

dynamic upwelling region of the California Current, may have driven adaptations to cope with variable, sometimes low, pH conditions. For both of these species, increasing temperature is likely to be important. In both experiments that incorporated warming, the animals responded only with increases in growth, suggesting that even these increases in temperature are still within their range of thermal tolerance. Now, the OA field is rapidly incorporating multiple stressors such as temperature and oxygen into experiments, which is critical for better understanding the complex effects of these stressors together. To fully understand the prognosis for a species, however, requires not just studying the sometimes-obvious responses of survival and growth, but recognizing and studying the additional aspects of the biology of the animal that impacts its fitness, such as prey capture ability, reproduction, and the integrity of a wide diversity of predator defenses.

There has been some interest in the OA field of identifying suitable model organisms to study in-depth with more standardized approaches to pH levels, multiple stressors, and experimental duration than are employed now. The crustaceans, however, are an excellent example of the challenges associated with this effort. The literature on larval responses demonstrates that there is a wide range of tolerance amongst young crustaceans, and the field is likely to benefit from exploring and better understanding the reasons behind these differences, whether they are derived from the experimental methodology, the exposure of parents to OA-like conditions beforehand, the variability of the animal's natural environment, or the carbonate chemistry parameters in the animal's habitat compared to global means. In the California spiny lobster, we found another challenge to focusing on a model species: that of specialized exoskeletal regions, each of which is only present in a very small portion of crustaceans. Only by focusing on the horn in Chapter 3 did we learn that poorly-mineralized

structures may still be vulnerable to the impacts of OA. Across the broad diversity of crustaceans, there are likely many such surprising responses that we have yet to discover. While it is important for the field to identify patterns of responses among organisms, there is still much to be learned from studying a broad range of species.